BENEFITS AND LIMITATIONS OF GENETICALLY ENCODED BIOSENSORS USE IN PLANTS: USE CASE OF WOUNDING RESPONSE IN POTATO

Valentina Levak

Doctoral Dissertation
Jožef Stefan International Postgraduate School
Ljubljana, Slovenia

Supervisor: Prof. Dr. Kristina Gruden, National Institute of Biology, Ljubljana, Slovenia
Co-Supervisor: Assist. Prof. Dr. Tjaša Lukan, National Institute of Biology, Ljubljana, Slovenia

Evaluation Board:
Assist. Prof. Dr. Špela Baebler, Chair, National Institute of Biology, Ljubljana, Slovenia & Jožef Stefan International Postgraduate School, Ljubljana, Slovenia
Assist. Prof. Dr. Anže Županič, Member, National Institute of Biology, Ljubljana, Slovenia
Prof. Dr. Saskia van Wees, Member, Utrecht University, Utrecht, The Netherlands

MEDNARODNA PODIPLOMSKA ŠOLA JOŽEFA STEFANA
JOŽEF STEFAN INTERNATIONAL POSTGRADUATE SCHOOL



Valentina Levak

BENEFITS AND LIMITATIONS OF GENETICALLY ENCODED BIOSENSORS USE IN PLANTS: USE CASE OF WOUNDING RESPONSE IN POTATO

Doctoral Dissertation

KORISTI IN OMEJITVE UPORABE GENETSKO ZAPISANIH BIOSENZORJEV V RASTLINAH: PRIMER ODZIVA NA RANJENJE PRI KROMPIRJU

Doktorska disertacija

Supervisor: Prof. Dr. Kristina Gruden

Co-Supervisor: Assist. Prof. Dr. Tjaša Lukan

Ljubljana, Slovenia, June 2026

To my family, who patiently watered the roots of my interest in plants.

Acknowledgments

This research took part at National Institute of Biology, in the labs of Department for Biotechnology and Systems Biology. I would like to thank my mentor, Prof. Dr. Kristina Gruden, and co-mentor, Assist. Prof. Dr. Tjaša Lukan, for their patient supervision and insightful guidance. I would also like to thank Assist. Prof. Dr. Špela Baebler, Prof. Dr. Saskia Van Wees and Assist. Prof. Dr. Anže Županič for reviewing this work and providing valuable feedback for its improvement. I would also like to thank all my colleagues who made the difficult days bearable and the good days even more enjoyable. Thank you also to my family and friends for their inexhaustible support and encouragement.

This work was funded by the Slovenian Research and Innovation Agency, research core funding No. P4-0165 and No. P4-0463, project J4-1777, and program for young researchers.

Abstract

Genetically encoded biosensors are powerful tools for studying plant immune response, as they enable real-time, *in vivo* monitoring of defence-related signals with high spatial and temporal resolution. By shifting the focus from static endpoint measurements to dynamic analyses of signal timing, intensity, and localization, biosensors reveal important features that are critical for effective immune responses.

This work provides a critical review of biosensor applications in plant immunity and crops, together with original experimental research. We investigated jasmonic acid (JA) and salicylic acid (SA) signalling in potato (*Solanum tuberosum* L.) response to herbivory by the Colorado potato beetle (CPB, *Leptinotarsa decemlineata* [Say]) and to mechanical wounding. Three complementary biosensors were employed: a transcriptional reporter of JA-dependent gene expression (*MC::EYFP*), a direct reporter of JA-Ile signalling based on JAZ degron degradation (AtJas9-Venus-N7), and a bacterial bioluminescent reporter for SA (Acinetobacter ADPWH_*lux*). Imaging intact plants was essential, as tissue excision or leaf detachment abolished detectable JA-dependent responses, highlighting the importance of *in vivo* approaches. Together, these sensors enabled visualization of distinct stages of the JA signalling cascade and their spatial relationship with SA accumulation.

Our results revealed a previously undescribed spatial organization of wound-induced hormone signalling. JA-dependent gene expression was consistently suppressed in cells immediately adjacent to wound sites, despite active JA-Ile signalling in the same region. In contrast, JA responses propagated into some millimetres of surrounding tissue, while SA accumulated preferentially near the wound edge. Depletion of SA and treatments with SA analogue INA and JA demonstrated that local SA signalling suppresses JA-dependent transcription in wound-proximal cells. This spatial antagonism between SA and JA was observed following both mechanical damage and herbivory, although the suppressed zone was broader after insect feeding. Cells at the wound margin showing persistent JA suppression later exhibited physiological features consistent with secondary cell wall formation, suggesting a role for localized hormone crosstalk in wound healing and barrier formation.

To enable following more analytes simultaneously, we systematically assessed strategies for multiplexing fluorescent biosensors in living plant tissues. Multiple fluorescent proteins were characterized for brightness and spectral properties, and methods for separating overlapping signals were evaluated. Channel dye separation using standard multichannel imaging provided reliable signal discrimination while minimizing acquisition time, photobleaching, and motion artifacts, and an objective segmentation pipeline enabled quantitative analysis of compartment-specific signals.

Overall, this work demonstrates how genetically encoded biosensors can resolve the spatiotemporal dynamics of plant defence signalling. Particularly, it identifies spatially confined SA–JA antagonism as a key regulatory feature of wound responses. These approaches complement omics-based analyses and advance mechanistic understanding of plant immunity directly in crop species.

Povzetek

Genetsko zapisani biosenzorji so zmogljiva orodja za raziskovanje rastlinskega imunskega odziva, saj omogočajo sprotno spremljanje obrambnih signalov *in vivo* z visoko prostorsko in časovno ločljivostjo. S preusmeritvijo s statičnih meritev na dinamične analize časovne dinamike, intenzitete in lokalizacije signalov biosenzorji razkrivajo pomembne značilnosti, ki so ključne za učinkovit imunski odziv.

To delo podaja pregled uporabe biosenzorjev v raziskavah rastlinske imunosti in pri kulturnih rastlinah ter vključuje izvirne eksperimentalne raziskave. Preučevali smo signalizacijo, povezano z jasmonsko kislino (JA) in salicilno kislino (SA) v krompirju (*S. tuberosum* L.) pri odzivu na napad koloradskega hrošča (*L. decemlineata* [Say]) in na mehansko ranjenje. Uporabili smo tri dopolnjujoče se biosenzorje: transkripcijski reporter od JA-odvisnega izražanja genov (*MC::EYFP*), biosenzor prisotnosti JA-Ile, ki temelji na razgradnji JAZ degrona (AtJas9-Venus-N7), ter bakterijski bioluminiscenčni biosenzor za SA (Acinetobacter ADPWH_*lux*). Biosenzorja JA smo spremljali na intaktnih rastlinah, saj je ločitev lista od rastline onemogočila zaznavo od JA-odvisnih odzivov, kar poudarja pomen *in vivo* pristopov. Uporabljeni biosenzorji so skupaj omogočili vizualizacijo različnih stopenj signalne kaskade JA ter njihove prostorske povezanosti s kopičenjem SA.

Rezultati uporabe navedenih biosenzorjev so razkrili doslej neopisano prostorsko organizacijo hormonske signalizacije, sprožene z ranjenjem lista. Od JA-odvisno izražanje genov je bilo v celicah neposredno ob mestu poškodbe zavrto, kljub prisotnosti JA-Ile v istem območju. Odziv z JA se je razširil nekaj milimetrov stran od rane v okoliško tkivo, medtem ko se je SA prednostno kopičila ob robu rane. Preprečitev kopičenja SA ter tretiranje z 2,6-dikloroizonikotinsko kislino (INA), ki je analog SA, in z JA so pokazali, da SA zavira od JA-odvisno transkripcijo v celicah v neposredni bližini rane. Ta prostorski antagonizem med SA in JA je bil opažen tako po mehanski poškodbi kot po napadu koloradskega hrošča, pri čemer je bil zavrti pas širši po napadu koloradskega hrošča. V celicah ob robu rane, kjer je bilo od JA odvisno izražanje genov trajno zavrto, je kasneje prišlo do nastanka sekundarne celične stene, kar nakazuje vlogo lokalnega hormonskega antagonističnega delovanja pri celjenju ran in tvorbi zaščitne pregrade pred škodljivci.

Da bi omogočili spremljanje več analitov hkrati, smo sistematično ovrednotili strategije za uporabo več fluorescentnih biosenzorjev v živem rastlinskem tkivu. Izbrano paleto fluorescentnih proteinov smo okarakterizirali glede na svetlost in spektralne lastnosti ter ovrednotili metode za ločevanje prekrivajočih se signalov. Ločitev fluorescentnih proteinov po standardnem večkanalnem slikanju je omogočilo zanesljivo razločitev signalov, pri tem pa tudi skrajšan časa zajema, zmanjšano bledenje in zmanjšan nastanek artefaktov zaradi gibanja. Razviti pristop za segmentacijo pa je omogočil kvantitativno analizo signalov v različnih celičnih razdelkih.

To delo prikazuje, kako genetsko zapisani biosenzorji omogočajo razumevanje prostorsko-časovne dinamike obrambnega odziva pri rastlinah. Opredeljuje zlasti prostorski antagonizem med SA in JA pri odzivu na ranjenje listov. Tovrstni pristopi z genetsko zapisanimi biosenzorji dopolnjujejo omične analize in prispevajo k poglobljenemu mehanističnemu razumevanju rastlinske imunosti, tudi neposredno pri kulturnih rastlinah.

Contents

List of Figures **xv**

1 Introduction **1**
1.1 Plant Defence Response ... 1
1.1.1 More than gene-for-gene resistance: Plant immunity as a quantitative feature ... 2
1.1.2 Immune response is spatially coordinated ... 3
1.1.3 Stressful event: Herbivore attack ... 4
1.1.4 Wounding-triggered signalling cascade ... 4
1.1.5 Wounding response predominantly relies on jasmonic acid signalling pathway ... 4
1.1.6 Involvement of other signalling pathways ... 7
1.1.7 At the wound edge: Localized response ... 7
1.1.8 At the wound edge: Induced resistance ... 7
1.1.9 At the wound edge: Cell death and healing ... 7
1.2 Employing Systems Biology Approaches to Follow and Understand Plant Defence Response ... 8
1.2.1 Biosensors as tools in systems biology approach ... 8
1.2.1.1 Genetically encoded biosensors ... 9
1.2.1.2 Towards biosensors multiplexing: Discrimination of the fluorophores ... 9
1.3 Scientific Problems and Aims of the Thesis ... 10
1.4 Research Hypotheses ... 11
1.5 Publications Included and Candidate's Contributions ... 11

2 Scientific Publications **13**
2.1 Biosensors: A Sneak Peek into Plant Cell's Immunity ... 13
2.2 Jasmonic Acid and Salicylic Acid Interact to Determine Spatial Regulation of Gene Expression Responses in Potato Leaf to Herbivory by Colorado Potato Beetle and Mechanical Wounding ... 32
2.3 Robust Quantification of Multiplexed Fluorescent Protein-Based Biosensors in Plant Tissues ... 46

3 Discussion **79**

4 Conclusions **85**

Appendix A Supplementary Material of Included Publications **87**
A.1 Supplementary Material for Publication 2.2 ... 87
A.2 Supplementary Material for Publication 2.3 ... 87

Appendix B Permission for Reproduction of Included Publications **88**
B.1 Permission for Reproduction of Publication 2.1 88
B.2 Permission for Reproduction of Publication 2.2 89
B.3 Permission for Reproduction of Publication 2.3 90

References **91**

Bibliography **103**

Biography **105**

List of Figures

Figure 1: Spatial antagonism of salicylic acid (SA) and jasmonic acid (JA) in response to *Pseudomonas syringae* infection. 3
Figure 2: JA biosynthesis. 5
Figure 3: JA-dependent transcriptional regulation. 6

Abbreviations

13-LOX	...	13-lipoxygenase
ABA	...	abscisic acid
AOC	...	allene oxide cyclase
AOS	...	allene oxide synthase
Aux	...	auxin
Avr factor	...	avirulence factor
BIK1	...	Botrytis-induced kinase 1
BR	...	brassinosteroid
CK	...	cytokinin
CPB	...	Colorado potato beetle
CycB1	...	cyclin B1
DAMP	...	damage associated molecular pattern
EDS1-PAD4-ADR1	...	complex of proteins: enhanced disease susceptibility 1, phytoalexin deficient 4 and activated disease resistance 1
ERF	...	ethylene responsive factor
ET	...	ethylene
ETI	...	effector triggered immunity
ETS	...	effector triggered susceptibility
EYFP	...	enhanced yellow fluorescent protein
GA	...	gibberellic acid
GUS	...	beta-glucosidase synthase
HAMP	...	herbivore associated molecular pattern
HDA	...	histone deacetylase
hpt	...	hours post treatment
HR	...	hypersensitive response
Ile	...	isoleucine
INA	...	2,6-dichloroisonicotinic acid
IPS	...	International Postgraduate School
JA	...	jasmonic acid
JAR1	...	jasmonate resistant 1 protein
JAZ	...	jasmonate ZIM-domain protein
MAPK, MPK	...	mitogen-activated protein kinase
MC	...	multicystatin
MeJA	...	methyl jasmonate
MKK	...	MAPK kinase
MYB TF	...	myeloblastosis transcription factor
NahG	...	salicylate hydroxylase, gene/protein G of naphthalene degradation operon
NIB	...	National Institute of Biology

NLR	... nucleotide binding domain and leucine rich repeat receptor
NPR1	... non-expressor of pathogenesis-related genes 1 protein
OPDA	... oxylipin 12-oxo-phytodienoic acid
OPR3	... 12-oxophytodienoate reductase 3
PAMP	... pathogen associated molecular pattern
PCD	... programmed cell death
PMT	... photomultiplier tube
PR1	... pathogenesis related protein 1
PRR	... pattern recognition receptor
PSII	... photosystem II
PTI	... pattern triggered immunity
R-protein	... resistance protein
RbohD	... respiratory burst oxidase homologue D
REF1	... regeneration factor 1 peptide
ROS	... reactive oxygen species
SA	... salicylic acid
SCF^{COI1}	... protein complex of Skp1-Cullin1-F-box protein and coronatine insensitive protein
SNR	... signal-to-noise ratio
T3SS	... type 3 secretion system
TF	... transcription factor
TPL	... topless protein
VSP1	... vegetative storage protein 1

Chapter 1

Introduction

1.1 Plant Defence Response

Plants respond to environmental stress by activating signalling cascades that lead to the synthesis of protective molecules and the formation of physical barriers, such as secondary metabolites and reinforced cell walls (Doughari, 2015). Plant hormones are central regulators of these cascades, coordinating efficient local and systemic responses and enabling crosstalk between distinct signalling modules. Classical growth regulators, including auxins (Aux), cytokinins (CK), gibberellins (GA), brassinosteroids (BR), and abscisic acid (ABA), are key drivers of plant growth and development and have been most extensively studied in this context. However, they also contribute to stress responses, for example, ABA in drought tolerance.

In contrast, defence responses to biotic stressors such as microbes and herbivores are primarily governed by salicylic acid (SA), jasmonic acid (JA), and ethylene (ET) signalling pathways (Bari & Jones, 2009). Plant defence against biotic stress is generally divided into two categories: (i) responses to biotrophs, which require living host tissue, and (ii) responses to herbivores and necrotrophs, the latter feeding on and proliferating in dead tissue. Defence against biotrophs is predominantly SA-dependent, whereas resistance to herbivores and necrotrophs relies mainly on JA and ET signalling. This distinction is referred to as trophic divergence (Huang et al., 2020).

Plant immune responses rely on both the innate immunity of individual cells and systemic signalling that spreads from infection sites. This multilayered defence was conceptualized by the 'zigzag model' proposed by Jones and Dangl in 2006. According to this model, plants recognize pathogen-associated molecular patterns (PAMPs) such as bacterial flagellin or fungal chitin via cell-surface pattern-recognition receptors (PRRs), leading to the activation of pattern-triggered immunity (PTI). Pathogens can suppress PTI via effector proteins that interfere with host immune signalling, resulting in effector-triggered susceptibility (ETS). Through coevolution, some of these effectors, termed avirulence (Avr) proteins, which are frequently species or strain-specific, have become recognizable by plant resistance (R) proteins, either directly or indirectly (for example, via perception of pathogen-induced modifications of host proteins). These R-proteins, often cytoplasmic nucleotide-binding domain leucine-rich repeat receptors (NLRs), mediate effector-triggered immunity (ETI), restoring plant defence capacity (Jones & Dangl, 2006).

Increasing evidence shows that PTI and ETI terms were limited in their definition considering apoplastic and general (preserved e.g. among kingdoms) molecular patterns (PAMPs) and T3SS-secreted and more specific (e.g. species or strain-specific) effectors (Jones & Dangl, 2006, vs. Thomma et al., 2011). For example, considering their specificity,

some PAMPs were shown to be narrowly conserved while some effectors are widespread across species. Additionally, considering their involvement in pathogen fitness (PAMPs) or virulence (effectors), some PAMPs and effectors can have a role in both (Thomma et al., 2011). The zigzag model related PTI and ETI terms are therefore nowadays replaced by other classifications, such as based on the structure of receptors (PRR- and NLR-mediated immunity) or, preferably, based on localization of detection of molecular patterns or effectors (extracellularly and intracellularly triggered immunity or surface-receptor and intracellular-receptor mediated immunity) (Ngou et al., 2022). Besides novel insights into the nature of perceived molecular patterns, research of signalling components also showed that extracellularly and intracellularly triggered immunity are highly intertwined and activate convergent downstream responses, including Ca^{2+} influx, reactive oxygen species (ROS) bursts, mitogen-activated protein kinase (MAPK) activation, induction of defence-related genes, and phytohormone production (Lu & Tsuda, 2021; Tsuda & Katagiri, 2010). While extracellularly and intracellularly triggered immunity share broadly similar transcriptional signatures, intracellularly triggered immunity responses are typically stronger and more sustained (Bernoux et al., 2022). Intracellularly triggered immunity frequently, though not always, culminates in a hypersensitive response (HR)—a form of localized cell death that restricts pathogen spread (Morel & Dangl, 1997). In some cases, intracellularly triggered immunity can result instead in extreme resistance, where infection is effectively blocked without visible cell death, often when R-proteins are expressed at high levels (Ross et al., 2021). Extracellularly and intracellularly triggered immunity are mutually potentiated. For example, pathogen effectors can increase the abundance of proteins that contribute to extracellularly triggered immunity (Jones et al., 2024). Conversely, loss of extracellularly triggered immunity results in reduced cell death compared to the combined activation of extracellularly and intracellularly triggered immunity (Jones et al., 2024). Furthermore, several surface-receptor mediated immunity coreceptors have been shown to be essential for full intracellularly triggered immunity activation (Ngou et al., 2021; Yuan, Jiang, et al., 2021). On the other hand, signalling via intracellularly triggered immunity components EDS1-PAD4-ADR1 is required for extracellularly triggered immunity (Pruitt et al., 2021; Tian et al., 2021). The combined response of extracellularly and intracellularly triggered immunity exceeds the sum of the individual responses, both qualitatively, such as through phosphorylation of RbohD and MAPKs and generation of apoplastic ROS, and quantitatively, reflected in higher abundance of BIK1, RbohD, and MPK3 proteins. These synergistic effects occur at both transcriptional and post-transcriptional levels (Ngou et al., 2021; Yuan, Jiang, et al., 2021). Interestingly, during extracellularly triggered immunity, transcriptional and translational responses are less tightly correlated than during intracellularly triggered immunity (Yuan, Jiang, et al., 2021; Yuan, Ngou, et al., 2021). Extracellularly triggered immunity also amplifies the HR triggered by several effectors, involving MAPK and Rboh activity (Ngou et al., 2021).

1.1.1 More than gene-for-gene resistance: Plant immunity as a quantitative feature

The zigzag model involving PTI and ETI (or extracellularly and intracellularly triggered immunity, respectively) primarily describe immune responses based on pathogen perception. In this framework, ETS and ETI correspond to qualitative features of sensitivity or resistance to a specific pathogen genotype and typically involve a small number of genes with large effects (e.g. Avr paired with their recognizing *R*-genes, either by direct binding, through guarding or guardee-mimicking decoy [Dangl & Jones, 2001; Van Der Hoorn & Kamoun, 2008]). In contrast, quantitative resistance is governed by

numerous genes, often encompassing 10% or more of the genome, each contributing small to moderate effects on immunity. Many of these genes perform functions not traditionally associated with disease resistance. Despite their modest individual impacts, collectively they shape the outcome of most host–pathogen interactions. Quantitative resistance is generally more stable and durable and can confer protection against a broader spectrum (e.g. kingdom-wise) of pathogens, although certain pathogen genotypes may still overcome it (Bartoli & Roux, 2017; Corwin & Kliebenstein, 2017; Delplace et al., 2020).

Another aspect of quantitative resistance lies in the abundance of immune receptors, kinases, and enzymes such as RbohD, where higher protein levels correlate with stronger defence activation (Jones et al., 2024; Lu & Tsuda, 2021; Yuan, Jiang, et al., 2021).

1.1.2 Immune response is spatially coordinated

Studies with high spatial resolution have revealed that immune responses are not uniformly distributed across the affected tissue (Betsuyaku et al., 2018; Calabria et al., 2025; Delannoy et al., 2023; Ghareeb et al., 2020; Hander et al., 2019; Jacob et al., 2023; Lukan et al., 2020, 2023; Salguero-Linares et al., 2022; Zhou et al., 2020). Instead, the energetically costly immune response is confined to specific subsets of cells, with the intensity and type of response depending on the distance from the infection site. For instance, during effector-triggered immunity (ETI) in Arabidopsis infected with *Pseudomonas syringae* (Figure 1) or *Fusarium oxysporum*, spatial separation of the antagonistic hormones JA and SA has been observed (Betsuyaku et al., 2018; Calabria et al., 2025). SA signalling predominates at the boundary of the HR zone, whereas JA signalling is activated in cells located further away. This spatial organization allows for localized defence activation, ensuring that (i) defence does not spread unnecessarily and cause susceptibility to pathogens or pests of differing trophic strategies, and (ii) the interplay of distinct hormonal pathways fine-tunes the balance between defence, growth, and development (S. Huang et al., 2020).

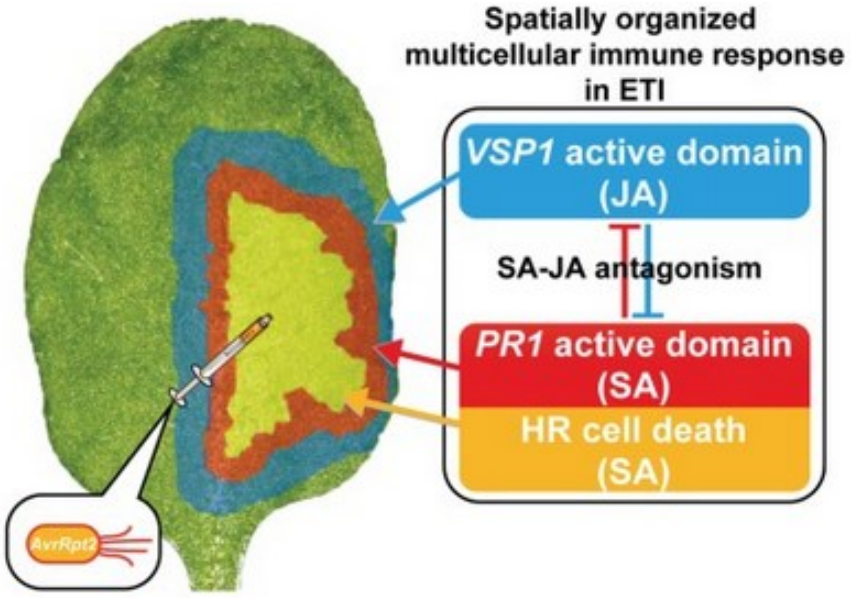


Figure 1: Spatial antagonism of salicylic acid (SA) and jasmonic acid (JA) in response to *P. syringae* infection. SA-depended *PR1* gene expression and JA-depended *VSP1* gene expression occur at mutually exclusive sites of Arabidopsis leaf. SA, which is involved in hypersensitive response (HR) cell death, is active in the region directly surrounding the

infected region while JA is active outwards of SA region. Republished from Betsuyaku et al., 2018, Plant and Cell Physiology, 59, 439 (CC-BY-NC).

1.1.3 Stressful event: Herbivore attack

Wounding is a common stress event in a plant's life, caused by adverse weather conditions or herbivory. It often precedes pathogen invasion or occurs during the early stages of infection. Wound healing is essential to prevent water and nutrient loss and to restore tissue integrity, thereby limiting microbial entry. In certain organs, such as the roots, lost tissue must also be regenerated (Marhava et al., 2019). To mitigate the potentially harmful consequences of wounding and herbivory, plants have evolved complex responses that involve transcriptional reprogramming, enabling tissue repair and the production of protective compounds against herbivores, including secondary metabolites and antinutritive molecules such as proteinase inhibitors (e.g., multicystatin, MC) (Howe & Schaller, 2008).

1.1.4 Wounding-triggered signalling cascade

Wound response is initiated by DAMPs and HAMPs (damage- and herbivore-associated molecular patterns, respectively; reviewed in Hou et al. 2019), which trigger a cascade of cellular events. These include membrane depolarization (reviewed in Farmer et al., 2020), increase in Ca^{2+} levels in the cytosol and nucleus (Bellandi et al., 2022; Toyota et al., 2018) as well as the endoplasmic reticulum (Resentini et al., 2021), generation of ROS (Beneloujaephajri et al., 2013; L'Haridon et al., 2011), and the processing and release of signalling peptides—for example, Pep1, which spreads locally in Arabidopsis (Hander et al., 2019), or REF1 in tomato (Yang et al., 2024). In addition, wounding activates kinase cascades (Tang et al., 2017; Tena et al., 2011), such as two MAPK modules in Arabidopsis: MKK3–MPK1/2/7/14, which is JA-dependent, and MKK4/5–MPK3/6, which is JA-independent (Sözen et al., 2020). Finally, wound responses involve the production and release of bioactive hormone derivatives (Vega-Muñoz et al., 2020).

1.1.5 Wounding response predominantly relies on jasmonic acid signalling pathway

The response to wounding predominantly relies on the JA signalling pathway. JA biosynthesis (Figure 2) is initiated within minutes of wounding (Chauvin et al., 2013; Glauser et al., 2008) and occurs independently of *de novo* transcription or translation (Chung et al., 2008; Kimberlin et al., 2022). The process begins with the oxidation of plastid fatty acids by 13-lipoxygenase (13-LOX), followed by a series of enzymatic reactions leading to the formation of 12-oxo-phytodienoic acid (OPDA). OPDA is then transported to the peroxisome, where it is further converted into JA. Subsequently, JA is translocated to the cytoplasm, where it is conjugated with isoleucine (Ile) by JAR1, forming the bioactive JA-Ile conjugate. This conjugate facilitates the interaction between the SCF^{COI1} complex and the transcriptional repressor JAZ, resulting in JAZ degradation via the 26S proteasome within minutes of JA exposure (Chini et al., 2007; Larrieu et al., 2015). The degradation of JAZ releases transcriptional activators, such as MYC2/3/4, which recruit RNA polymerase II through the multisubunit Mediator complex to drive JA-dependent gene expression (Figure 3) (Zhai et al., 2020).

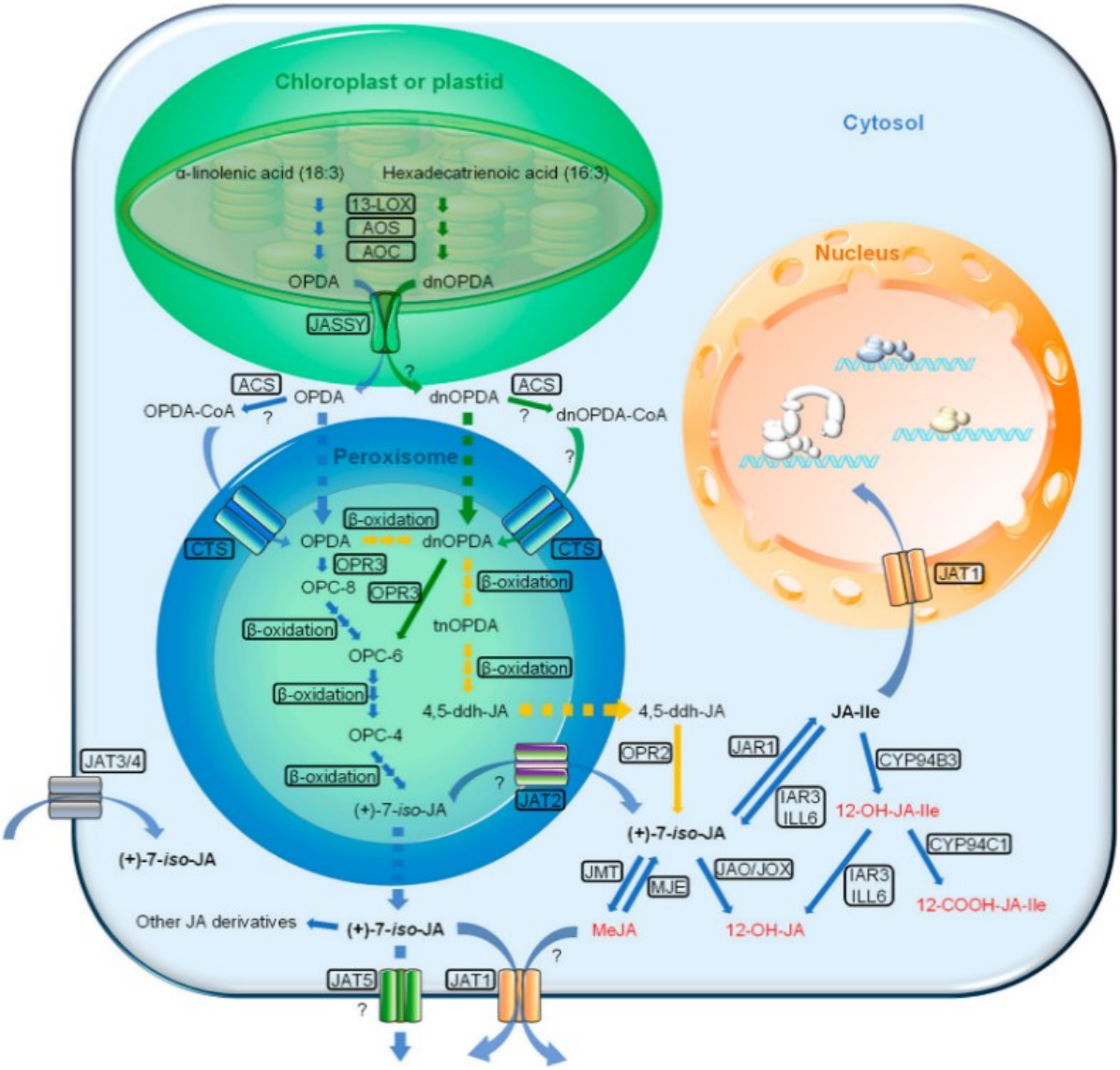


Figure 2: Jasmonic acid (JA) biosynthesis. JA biosynthesis starts from fatty acids in chloroplast, where 13-LOX, AOS and AOC gradually convert them to OPDA. The latter is transported into peroxisome where it is oxidized by OPR3 to form JA. JA is then transported into cytosol, where it is conjugated with isoleucine by JAR1 to form the most bioactive JA derivative, JA-Ile. The latter is transported into nucleus. Republished from Liu & Timko, 2021, International Journal of Molecular Sciences, 22, 2914 (CC-BY).

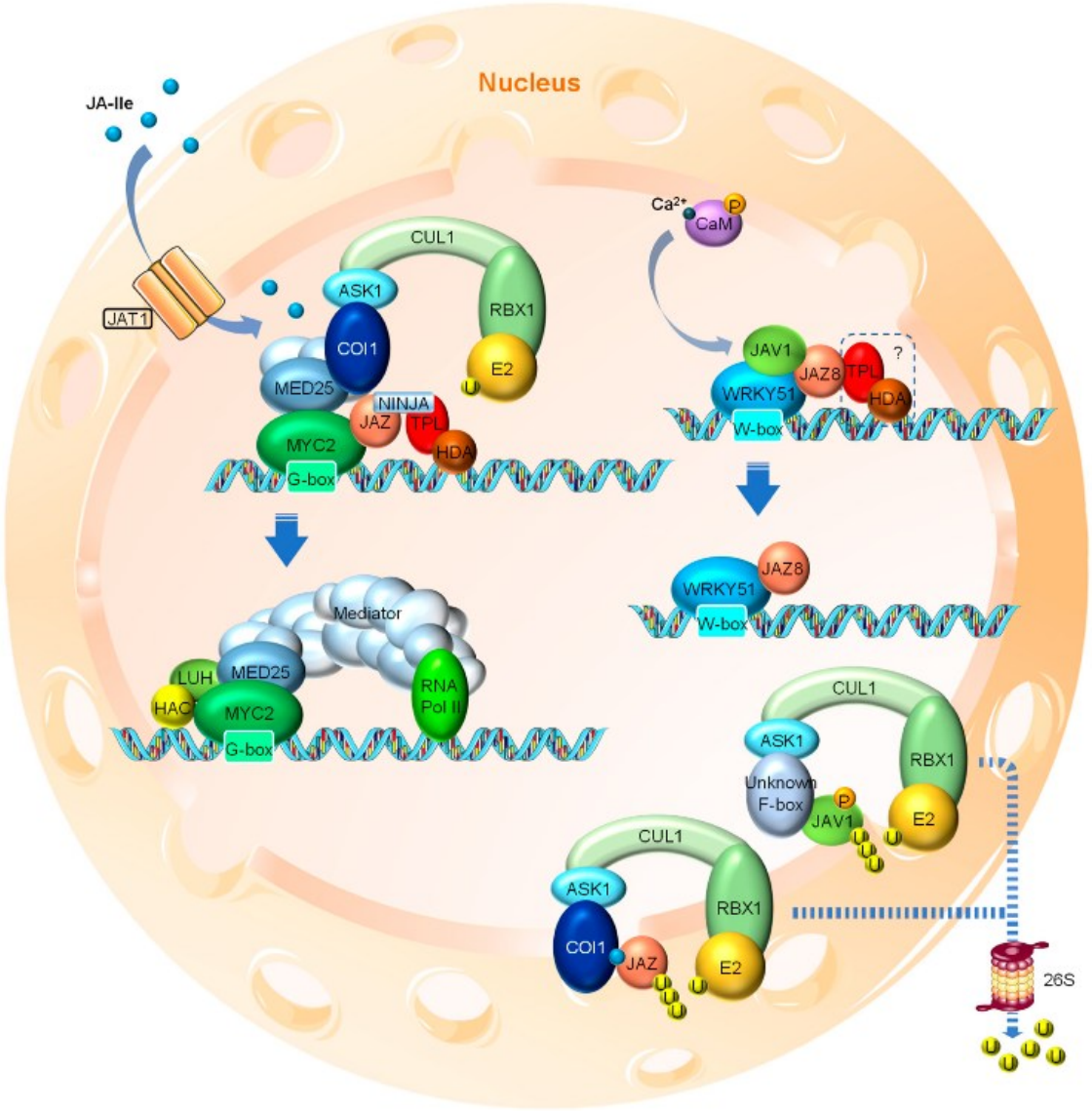


Figure 3: Jasmonic acid (JA)-dependent transcriptional regulation. After transportation to nucleus, JA-Ile bridges SCF^{COI1} E3 ubiquitin ligase complex with a complex of transcriptional repressor JAZ and corepressors NINJA, TPL and HDA. JAZ then undergoes ubiquitination and degradation via 26S proteasome. After repressor complex is released from transcriptional activator MYC2, which binds to G-box in promoters of JA-responsive genes, the transcription is activated. Republished from Liu & Timko, 2021, International Journal of Molecular Sciences, 22, 2914 (CC-BY).

The JA-dependent response is tightly regulated in time. Transcriptional repressors of the JAZ family are degraded within 15 minutes after wounding (Larrieu et al., 2015; Van der Does et al., 2013). Degradation of JAZs is coinciding with the transcriptional activation of JA biosynthesis genes, such as 13-LOX, AOS, AOC and OPR3, and JA biosynthesis regulators, either positive, such as transcriptional activator MYC2, or negative, such as transcriptional repressors JAZs (Hickman et al., 2017), suggesting the onset of both, positive and negative feedback loop. For several of these biosynthesis genes and regulators of their expression, basal and inducible expression occurs independently of *de novo* protein synthesis, meaning that their activity is regulated on the protein level, allowing them to

act immediately upon JA perception (Chung et al., 2008). This early response phase is followed by the downregulation of primary metabolism, along with the upregulation of JA biosynthetic genes and defence-related proteins such as 13-LOX, AOC, AOS, JAR1, and VSP1/2—a timeline that closely mirrors the wound-induced response (Koo et al., 2009). Approximately two hours after wounding, genes involved in regulatory functions and secondary metabolism become prominently upregulated (Hickman et al., 2017).

1.1.6 Involvement of other signalling pathways

JA-dependent regulation is not the only mechanism coordinating an appropriate response to wounding; other signalling pathways are also activated, either independently or through crosstalk at different stages of the response (Vega-Muñoz et al., 2020). In addition to JA, ET, ABA, and Aux have been shown to participate in wound responses (Vega-Muñoz et al., 2020). There is also limited evidence for a role of SA, such as its transient increase following wounding (Ogawa et al., 2010). This orchestrated signalling helps prevent spread of the cell death (Cui et al., 2013, 2019) and hypersensitivity to damage (Zhang et al., 2019).

Importantly, wound responses are tissue specific. In roots, for example, ET rather than JA plays a central role in mediating the response (Marhavý et al., 2019). Wounding of roots or stems can also trigger cell division in meristematic tissues via activation of the Aux signalling pathway; cells surrounding the wound re-enter the cell cycle to facilitate repair (Hoermayer et al., 2020). In contrast, leaves are composed mainly of differentiated cells, so the response focuses on limiting the spread of the wound and preventing cell decay rather than replacing damaged cells.

1.1.7 At the wound edge: Localized response

Local responses to mild wounding, which trigger concentric and confluent distributions of various molecules, have been observed using genetically encoded biosensors. These includes redox responses (Prasad et al., 2020) and Ca^{2+} signals following mechanical wounding (Bellandi et al., 2022; Toyota et al., 2018) or during insect feeding (Vincent et al., 2017), and Pep1 release, which is restricted to cells immediately adjacent to the wound site (Hander et al., 2019). Wound responses have been shown to depend on the intensity of damage, remaining locally confined in the case of mild wounding, but spreading systemically when larger veins are affected (Salvador-Recatalà et al., 2014).

1.1.8 At the wound edge: Induced resistance

Wounding induces resistance to herbivores and necrotrophic pathogens by activating the JA signalling pathway. This activation upregulates genes involved in secondary metabolism, including anthocyanin, tryptophan, and–in Arabidopsis–glucosinolate biosynthesis, as well as the ABA-mediated signalling pathway. At the same time, it downregulates regulators of primary metabolism, innate immune responses, SA biosynthesis, developmental processes, and Aux polar transport (Hickman et al., 2017). Consequently, resources are reallocated from primary metabolism, growth, and development toward defence and resistance.

1.1.9 At the wound edge: Cell death and healing

Cells adjacent to the wound edge enter programmed cell death (PCD) (Cui et al., 2013), while the surrounding ones need to restore the tissue at the wound site, to prevent pathogen entry, and water and nutrient loss. Wound healing response includes ABA, as it induces

formation of suberin, a constituent of secondary cell wall (Serra & Geldner, 2022), and controls JA-dependent wound-induced wax formation in leaves through MYB96 transcription factor (TF), which is involved in upregulation of wax biosynthesis enzymes (Lewandowska et al., 2024). On the other hand, JA-induced MYB108 TF is a negative regulator of ABA-induced cell death upon wounding (Cui et al., 2013).

1.2 Employing Systems Biology Approaches to Follow and Understand Plant Defence Response

In cases described by the zigzag model, the recognition of a single pathogen Avr factor by a corresponding plant R-protein can be sufficient to halt pathogen spread (Van Der Biezen & Jones, 1998). However, this model does not account for the broader molecular networks that underpin such responses (Tsuda et al., 2009) or that contribute to quantitative resistance. Considering these complex regulatory layers becomes particularly important when examining multifactorial stress scenarios, where plants must simultaneously respond to diverse challenges—such as combined heat and drought stress with herbivore attack, or waterlogging accompanied by fungal infection.

Systems biology takes a holistic view of biological research, recognizing that biological systems are more than just the sum of their individual components. It focuses on three key principles: emergence, robustness, and modularity. Emergence refers to new properties that arise from interactions within the system and cannot be predicted from individual components alone. Robustness describes the ability of biological systems to maintain their function despite environmental changes, random fluctuations, or genetic variation, often through feedback regulation. Modularity means that biological systems are organized into interconnected modules that can function relatively independently, allowing damage to remain localized and enabling evolutionary adaptation through rewiring of these modules (Aderem, 2005).

Accordingly, systems biology studies both biological networks and mathematical models of biological processes. Biological networks consist of entities such as genes, RNAs, proteins, and metabolites, connected through their interactions. Mathematical modelling is used to describe and predict biological behaviour by integrating information about network structure, time-series and omics data, spatial organization, and experimental perturbations, together with measurable outputs such as gene expression patterns and molecular distributions (Yue & Dutta, 2022). The field aims to generate large-scale datasets and apply an iterative cycle in which biological networks are constructed, modelled, experimentally tested, and continuously refined based on the obtained results (Aderem, 2005).

1.2.1 Biosensors as tools in systems biology approach

Biosensors are tools that detect specific analytes and report their presence or concentration through a measurable signal (Walia, Waadt & Jones, 2018). They can provide quantitative information on parameters such as the kinetics and duration of molecule production or their interactions, which can be used in mathematical modelling of organismal responses. By monitoring nodes of crosstalk or end products, biosensors allow tracking of interactions between different pathways as well as the activity of individual modules. Additionally, they can guide the design of high-throughput experiments by informing the optimal spatial and temporal resolution for sampling in genomics, transcriptomics, proteomics, and metabolomics studies. Comparing biosensor data across different organisms further enables

assessment of the spatiotemporal range of biological variability, which can be accounted for in sample collection strategies.

1.2.1.1 Genetically encoded biosensors

Genetically encoded biosensors are biomolecular tools expressed within the studied organism, composed of a detector module and a reporter module. The detector module may consist of a protein domain that binds a specific biomolecular analyte, or a gene promoter that is activated in response to the analyte. The reporter module typically contains a reporter protein, such as luciferase, β-glucuronidase, or a fluorescent protein. Luciferase and β-glucuronidase are enzymes that require a substrate to generate a measurable signal, either as luminescence or coloration, whereas most fluorescent proteins emit a signal without any additional substrate. Fluorescent proteins also provide the highest spatial resolution, reaching the subcellular level (Sadanandom & Napier, 2010).

In plants, most genetically encoded biosensors are designed to track plant hormones, particularly those associated with growth and development, such as ABA, Aux, GA and CK (Andres et al., 2024; Brunoud et al., 2012; Griffiths et al., 2024; Herud-Sikimić et al., 2021; Jedličková et al., 2022; Jones et al., 2014; Khakhar et al., 2018; Rowe et al., 2023; Sabatini et al., 1999; Shi et al., 2024; Steiner et al., 2020; Vernoux et al., 2011; Waadt et al., 2014; Zürcher et al., 2013). For these biosensors, at least one strategy of analyte detection was used. Direct biosensors generate a response when an analyte binds to a specific protein domain, whereas indirect biosensors produce a response through activation of a gene promoter or cis-regulatory element fused to a minimal promoter (Sadanandom & Napier, 2010).

1.2.1.2 Towards biosensors multiplexing: Discrimination of the fluorophores

The complexity of plant responses, e.g. achieving balances between opposing processes through crosstalk between different hormonal pathways, highlights the need to monitor multiple processes simultaneously. Such parallel monitoring can be achieved by introducing multiple genetically encoded biosensors that employ distinguishable fluorescent proteins as reporter modules. For instance, the simultaneous use of SA and JA reporters in the same plant could reveal their spatiotemporal interplay at the cellular level, providing more precise insights than comparing reporter activity in separate plants. For successful multiplexing, fluorescent proteins should differ in their localization, excitation, emission, or fluorescence lifetime spectra. However, spectral overlap between fluorophores leads to signal crosstalk, compromising accurate distinction of biological targets (Zimmermann, 2005). Multiplexing in plants faces another challenge that does not exist while working with cell lines (Leiwe et al., 2022): autofluorescence produced by chlorophyll and secondary metabolites (Donaldson, 2020).

These challenges have been addressed through several approaches, one of the most widely used being linear unmixing, which assumes that the total detected signal in each channel can be expressed as a linear combination of the contributing fluorophores (Leiwe et al., 2022; Zimmermann, 2005). This method enables not only visualization but also quantitative analysis of imaging data and is conveniently implemented in confocal microscope software such as Leica LAS X and Zeiss ZEN. Nonetheless, accurate fluorophore separation requires precise reference spectra, which may differ from those available in databases (e.g., FPbase.org; Lambert, 2019) due to instrument-specific limitations, such as filter configurations (Mylle et al., 2013). Importantly, the number of spectral detection channels must be at least equal to the number of fluorophores present in the sample, and all contributing fluorophores must be included in the unmixing calculation (Zimmermann, 2005).

1.3 Scientific Problems and Aims of the Thesis

Genetically encoded biosensors have been predominantly developed for the model plant *Arabidopsis thaliana* (Inzé & Nelissen, 2022; Uauy et al., 2025), while only a limited number have been applied to crop species such as potato (Hipsch et al., 2021; Joshi et al., 2016; Lukan et al., 2023; Moroz & Tanaka, 2020). Transferring biosensors from Arabidopsis to crop species presents several challenges, including difficulties in plant transformation and regeneration (Altpeter et al., 2016), gene silencing and mosaicism (Reddy et al., 2003), and increased autofluorescence caused by higher concentrations of secondary metabolites (Donaldson, 2020). In addition, the larger overall size of crop plants further complicates imaging. Moreover, in the case of transcriptional reporters, gene regulation may differ substantially between crops and Arabidopsis (Wiesel et al., 2015). The biosensors in Arabidopsis were mainly developed for studies of plant growth and development, with comparatively fewer applications in the investigation of stress responses. Yet, analysing stress responses directly in crops is essential for understanding underlying processes and ultimately ensuring food security. Our first aim was to compile existing knowledge on biosensors applicable for studying plant immune responses, their implementation in crop species, and strategies to overcome associated limitations. The second aim was to establish a protocol for monitoring genetically encoded biosensors in intact, soil-grown plants, in a manner suitable for the biosensors of choice, enabling us to follow entire processes *in situ* while minimizing sample size, monitoring biological variability such as spatial, temporal or response strength differences, and limiting artifacts introduced by sampling. This was exemplified using two genetically encoded biosensors implemented in potato that respond to JA. The first is a direct reporter of JAZ degradation AtJas9-Venus-N7, originally developed in Arabidopsis and transferred to potato (Larrieu et al., 2015; Mahkovec Povalej, 2020). Apart from the first report, this sensor had so far not been used for following JA response *in vivo*. The second biosensor is a transcriptional reporter based on a potato native gene promoter, *MC::EYFP* (Lukan, 2018). Both sensors utilize fluorescent proteins as reporters and can be monitored using confocal imaging. Using these sensors, we aimed to identify (i) key timepoints and tissue regions for sampling in other analyses and (ii) parameters for mathematical modelling of the dynamic processes underlying plant stress responses. As a case study, our work focused on JA signalling, which is activated in response to mechanical damage and herbivory attack. Beyond developing an acquisition protocol, this work provided insights into the spatiotemporal dynamics of potato responses to CPB feeding, in comparison to purely mechanical wounding, which does not elicit response to herbivore saliva or regurgitant (Chung et al., 2013; Verhage et al., 2011). Our third aim was to investigate the potential and limitations of multiplexing genetically encoded biosensors. Such an approach would allow simultaneous tracking and integration of different processes. Specifically, we evaluated the potential of Leica's LAS X Dye Separation for linear unmixing of co-expressed fluorescent proteins or of fluorescent proteins and autofluorescence with overlapping excitation, emission, and fluorescence lifetime spectra.

In summary, this dissertation aims to: (i) review the available genetically encoded biosensors in plants used to study plant immune response, and revise their implementation in crop species such as potato, (ii) develop a strategy to follow genetically encoded biosensors in spatiotemporal manner in intact potato plants *in vivo*, (iii) use available genetically encoded biosensors in potato to explore spatiotemporal characteristics of JA signalling in response to mechanical and herbivore wounding, (iv) explore the possibilities to use more than one genetically encoded biosensor based on fluorescent proteins in the

same plant by employing linear unmixing of the signals acquired with laser scanning confocal microscopy.

1.4 Research Hypotheses

1. Genetically encoded biosensors can be used to follow spatiotemporal responses in potato plants.
2. JA signalling is differently spatiotemporally regulated in herbivore and mechanical wounding.
3. Reliable multiplexing of genetically encoded biosensors based on fluorescent proteins as reporters in plants is feasible using linear unmixing.

1.5 Publications Included and Candidate's Contributions

Our first publication (Biosensors: A Sneak Peek into Plant Cell's Immunity) is a review of the existing literature on biosensors that can be used to follow plant immune responses. It highlights the potential of using multiple biosensors within a single plant, a strategy still rarely applied, and reviews existing tools applied in crop species. Key challenges, including autofluorescence, low signal-to-noise ratio, and quantification issues are also discussed alongside possible solutions.

Our second publication (Jasmonic Acid and Salicylic Acid Interact to Determine Spatial Regulation of Gene Expression Responses in Potato Leaf to Herbivory by Colorado Potato Beetle and Mechanical Wounding) investigates JA and SA signalling dynamics in potato leaves following CPB herbivory and mechanical wounding. Using fluorescent biosensors, we show that JA dependent gene expression is absent in cells at the wound edge but is present outwards, while SA accumulates predominantly at the wound edge and suppresses JA-dependent gene expression in this region. In SA-deficient plants, JA-dependent gene expression expands confluently from the wound edge. These findings reveal a spatial crosstalk between SA and JA that shapes wound responses, extending concepts from pathogen defence to herbivory and mechanical injury.

Our third publication (Robust Quantification of Multiplexed Fluorescent Protein-Based Biosensors in Plant Tissues) identifies a palette of fluorescent proteins that exhibit comparable brightness *in planta*, making them suitable for simultaneous use. It also evaluates different strategies for unmixing of emission-overlapping fluorescent proteins based on linear unmixing and highlights the approach that is the fastest. Thus, it not only allows separation of fluorescent proteins from autofluorescence, originating from chlorophyll or root cell walls, but also facilitates monitoring the dynamics of multiple cellular components, including organelles and proteins, within plant cells.

Chapter 2

Scientific Publications

2.1 Biosensors: A Sneak Peek into Plant Cell's Immunity

Valentina Levak, Tjaša Lukan, Kristina Gruden, Anna Coll

Life, 2021, 11(3):209. DOI: 10.3390/life11030209

This review examines how biosensors can be applied to study plant immunity by monitoring defence signals, such as Ca^{2+} fluxes, ROS, and hormonal signalling pathways, in real time. By enabling dynamic, spatiotemporal observations, these tools shift the focus from static measurements to the timing, intensity, and localization of immune responses, which are often critical for effective defence. Investigating interconnected processes requires the use of multiple biosensors within the same plant, reducing the variability that can arise when comparing different plants. The paper highlights that the simultaneous application of more than one sensor in a single plant has been rarely explored. Additionally, the authors summarize the genetically encoded biosensors that have been implemented in crop species, underscoring the importance of developing sensors directly in target plants rather than relying solely on model systems. Finally, the paper highlights the challenges of applying these tools in plants—such as autofluorescence, low signal-to-noise ratio, and difficulties in quantification—and suggests approaches to overcome them.

The paper was selected as Editor's Choice and was cited in six other papers.

The PhD candidate is the first author of the paper. She contributed to the design of the paper, selected and reviewed the cited literature, was involved in the preparation of the figure and the table, and wrote the first draft.

life

MDPI

Review

Biosensors: A Sneak Peek into Plant Cell's Immunity

Valentina Levak [1,2,*], Tjaša Lukan [1], Kristina Gruden [1] and Anna Coll [1]

[1] National Institute of Biology, Večna pot 111, 1000 Ljubljana, Slovenia;tjasa.lukan@nib.si (T.L.); kristina.gruden@nib.si (K.G.); anna.coll@nib.si (A.C.)
[2] Jožef Stefan International Postgraduate School, Jamova cesta 39, 1000 Ljubljana, Slovenia
* Correspondence: valentina.levak@nib.si

Abstract: Biosensors are indispensable tools to understand a plant's immunity as its spatiotemporal dimension is key in withstanding complex plant immune signaling. The diversity of genetically encoded biosensors in plants is expanding, covering new analytes with ever higher sensitivity and robustness, but their assortment is limited in some respects, such as their use in following biotic stress response, employing more than one biosensor in the same chassis, and their implementation into crops. In this review, we focused on the available biosensors that encompass these aspects. We show that in vivo imaging of calcium and reactive oxygen species is satisfactorily covered with the available genetically encoded biosensors, while on the other hand they are still underrepresented when it comes to imaging of the main three hormonal players in the immune response: salicylic acid, ethylene and jasmonic acid. Following more than one analyte in the same chassis, upon one or more conditions, has so far been possible by using the most advanced genetically encoded biosensors in plants which allow the monitoring of calcium and the two main hormonal pathways involved in plant development, auxin and cytokinin. These kinds of biosensor are also the most evolved in crops. In the last section, we examine the challenges in the use of biosensors and demonstrate some strategies to overcome them.

Keywords: genetically encoded biosensors; live spatiotemporal imaging; crops; plant immune response; multiparameter imaging; biotic stress

check for updates

Citation: Levak, V.; Lukan, T.; Gruden, K.; Coll, A. Biosensors: A Sneak Peek into Plant Cell's Immunity. *Life* **2021**, *11*, 209. https://doi.org/10.3390/life11030209

Academic Editors: Pasquale Stano, Stéphane D. Lemaire and Paul F. South

Received: 27 January 2021
Accepted: 3 March 2021
Published: 7 March 2021

Publisher's Note: MDPI stays neutral with regard to jurisdictional claims in published maps and institutional affiliations.

Copyright: © 2021 by the authors. Licensee MDPI, Basel, Switzerland. This article is an open access article distributed under the terms and conditions of the Creative Commons Attribution (CC BY) license (https://creativecommons.org/licenses/by/4.0/).

1. Biosensors: Exploiting Molecular Hubs to Better Understand the Processes

A biosensor is a sensitive device that detects an analyte or event in a living organism and consequently produces a measurable output [1]. Thus, it consists of two functional parts: detector and reporter [2]. The detector domain must be specific and sensitive to enable detection of the biological concentration of analytes or events. The biosensor as a whole should enable detection with high signal to noise ratio (SNR), high spatiotemporal resolution on the organelle level, enable fast response, and must be functional in different cellular conditions (low pH, different redox states). Besides, it should not interfere with cellular processes and should not be toxic to the cells. Although each of available biosensors has its own limitations and cannot meet all of the abovementioned requirements, they are vital to obtain an insight into cellular events.

According to their mechanism of action, they can be separated into direct and indirect biosensors. Typical direct biosensors report protein activity upon ligand binding. Usually, they consist of two protein domains, one serving as a ligand receptor while the other can sense structural changes upon ligand binding and report it by measurable output. This is the mode of action of one of the first known biosensors named Cameleon, which is still widely used to measure Ca^{2+} concentration (Figure 1). It is translated as a single peptide chain, with two fluorescent proteins on each side, which are either blue and green or cyan and yellow, linked by calmodulin (CaM) and the M13 domain. When the concentration of Ca^{2+} in the cellular compartment increases, Ca^{2+} binds to CaM, which twists around the M13 domain and thereupon the two fluorescent proteins are close enough to enable

Förster resonance energy transfer (FRET) and Ca^{2+} binding can be detected through the change of the fluorescence intensities [3]. Another kind of direct biosensors are degron-based biosensors, which undergo degradation as a result of analyte binding. They exploit the characteristics of the cellular signaling of some plant hormones. In the presence of the hormone in the cell, related transcriptional repressors are degraded and thus the transcription of the hormone-responsive genes is activated. This approach is used, for example, in a plant biosensor for auxin detection, known as DII-VENUS (Figure 1). This is a fusion protein of two domains, of which DII acts as a detector while fast-maturing fluorescent protein VENUS acts as a reporter. The DII domain is a part of the Aux/IAA repressor involved in the binding of auxin and subsequent degradation of the repressor via the ubiquitin/26S proteasome pathway. When auxin concentration in the cell increases, DII-VENUS fusion is degraded and the fluorescence intensity decreases [4]. Direct biosensors can be used for following changes in pH, redox state, ion and metabolite concentrations in the majority of plant cell compartments.

Indirect biosensors are typically transcriptional reporters. Their detector domain is a promoter sequence that contains analyte-responding cis-elements and drives transcription of the reporter gene. The most commonly used reporters are beta-glucuronidase (GUS), fluorescent proteins (FPs) and luciferases. The signal produced by such biosensors is delayed, but amplified in comparison with direct biosensors. In order to gain higher SNR, specificity and sensitivity, native analyte-responsive promoter sequences are usually rebuilt by fusing cis-elements to the minimal Cauliflower mosaic virus (CaMV) 35S promoter sequence [5]. The most known example is the DR5 synthetic promoter, designed on the basis of GH3 gene promoter for auxin detection, which maintains its activity also in reverse orientation (DR5rev, Figure 1) [6]. The latter was improved to version DR5v2 with higher expression and sensitivity and therefore enables detection with better spatial resolution [7].

Recently, another type of indirect biosensor was developed to follow translational regulation of mRNA transcripts in the presence of ethylene. In this biosensor, the detector module is the ethylene-responsive 3′-UTR part of mRNA coding for EBF2, while the coding sequence is translated into reporter protein GFP (Figure 1). The mechanism of this biosensor is based on the action of C-terminal peptide of EIN2, which is cleaved when the concentration of ethylene increases. It can then bind to the 3′-UTR part from EBF2 mRNA fused with the GFP coding sequence, and thus represses its translation. In this way, GFP fluorescence decreases when the concentration of ET is increased [8–10].

During the last ten years, several informative reviews covering the topic of plant biosensors have been published, showing the advances in this technology and its importance for the plant research community. They revise the type of available biosensors and the recent results obtained [1], the use of biosensors to monitor plant hormones [11–13], the principles of most widely used biosensors in plants [14] and quantitative measurements with biosensors [15]. Some reviews are focused on biosensors of a single analyte such as abscisic acid (ABA) [16], auxin [17], Ca^{2+} [18], ethylene (ET) [10], gibberellins (GA) [19] and reactive oxygen species (ROS) [20]. The span of the developed biosensors goes hand in hand with advances of methodology, which exploits various principles and physical properties of the fluorescent proteins and other reporter proteins. The spectrum of advanced fluorescence imaging methods available nowadays for the use in plants is reviewed in Komis et al. [21]. The Fluorescent Biosensor Database [22] merges fluorescent genetically encoded biosensors regardless of the chassis and welcomes new updates by the community.

Variability of the biosensors available nowadays is broad. However, their use in plants is still limited to certain aspects. The majority of studies focus on the use of biosensors in roots to follow development in the model plant *Arabidopsis thaliana*. Consequently, the vast majority of biosensors were designed in this regard, providing even more than one sensor for a single analyte involved in a plant's growth and development, each of them exploiting another cellular event. On the other hand, the span of available biosensors for immune response is narrow. While Ca^{2+} and ROS, involved in the first stages of signal transmission in general, are satisfactorily covered, the main hormones of immune response,

salicylic acid (SA), jasmonic acid (JA) and ET, lack specific, sensitive and thus reliable biosensors to choose between. Leading research in plant development is also seen from the reports on following more than one analyte simultaneously and the transmission of the biosensors from model organisms to crops. Here, we report these findings. Finally, we also discuss difficulties associated with the application of the biosensors in plants with the aim of supporting the advancement of immune response biosensors and their application to crops.

2. Genetically Encoded Biosensors for Following Plant Immune Response

Plants respond to biotic stress by reprogramming a complex signaling network that results in gene activity and metabolic changes. Translation of pathogen recognition into effective defense response strongly depends on the action of several plant hormones and other signaling molecules [23–25]. Early signaling events include changes of intracellular Ca^{2+} levels and a rapid increase of reactive oxygen species. Among plant hormones, SA, JA and ET have been identified as main players [24,26]. In addition, recent evidence shows that the effects of these three hormonal signaling pathways are balanced by ABA, GA, auxins, cytokinins and brassinosteroids (reviewed by Verma et al. [27]), thus adding another layer of regulation. Therefore, these are the best candidate analytes to follow general immune response (Figure 1).

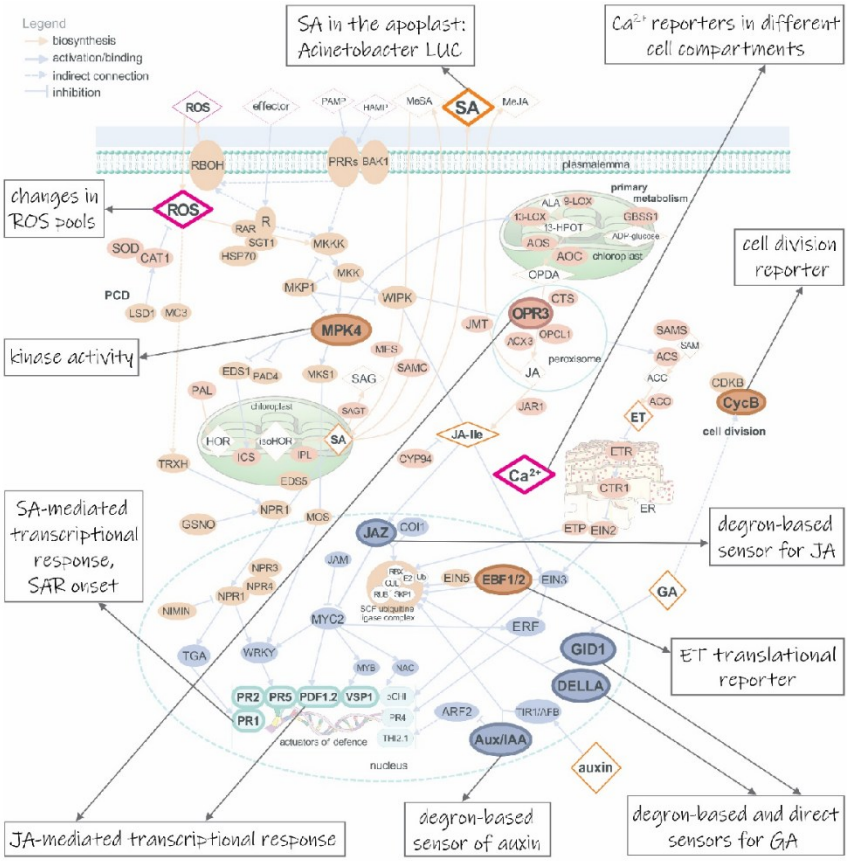


Figure 1. Diversity of available biosensors for following immune response in plants. During the first stage of the immune

response, Ca^{2+} influx in the cytosol can be monitored with diverse reporter proteins. They can be Förster resonance energy transfer (FRET) based, employing two FPs linked by calmodulin-sensing domain, e.g. Cameleons [3], or colourful GECOs (genetically encoded Ca^{2+} indicators for optical imaging) [28], employing one, circularly permutated fluorescent protein. Prominent sensors of reactive oxygen species (ROS) are redox-sensitive GFPs in fusion with oxidant receptor peroxidase-1 (roGFP2-Orp1) [29] and glutaredoxin 1 (Grx1-roGFP2) [30], H_2O_2 and glutathione sensors, respectively, that were used to distinguish the patterns of these two molecular species in the cytosol, chloroplast and mitochondria upon illumination [31]. The main three hormones of immune response, salicylic acid (SA), jasmonic acid (JA) and ethylene (ET), can be followed with a direct degron-based sensor Jas9-VENUS in case of JA or with indirect transcriptional reporters based on defense genes' promoters, such as pathogen-responsive PR1, PR2 and PR5 for SA- and plant defensin 1.2 (PDF1.2) and vegetative storage protein (VSP) for JA-involving response. They can be additionally followed by transcriptional reporters that exploit promoters of genes involved in hormone biosynthesis, e.g. the promoter of 12-oxo-phytodienoic acid reductase 3 (OPR3) gene, a constituent of JA biosynthesis. However, these transcriptional reporters can only complement other biosensors as they are not sufficiently specific. SA in the apoplast can be followed through *Acinetobacter* sp. ADPWH_*lux* luciferase (LUC) activity [32]. ET presence can be followed with translational reporter, joining 3'-UTR mRNA of EBF2, repressor of ET-responsive genes, and coding sequence of FP [8,9]. Other hormones, such as auxin and gibberellins (GA), can also be followed with degron-based sensors, employing DII domain of Aux/IAA repressor (in case of auxin [4]) and DELLA repressor (in case of GA [33]). Auxin can also be monitored through more of its actions, not just directly with DII-FP, but also indirectly with transcriptional reporters of auxin-responsive genes. These can employ synthetic (DR5 [6]) promoter as a detector. On the other hand, GA can be followed with FRET-based direct biosensor exploiting interaction between GID1 and DELLA repressor [34]. Interplay of immune response and plant's growth and development can be followed with biosensors of cell division, employing cyclins, e.g. CycB [35]. AtMPK4 and some other kinases' activity can be detected with kinase localization reporters, employing a domain for kinase docking and a phosphorylation site. When phosphorylated, fluorescent reporter is exported from the nucleus [36]. Signaling proteins are presented as orange, enzymes as brown-red and transcription factors as grey ovals, respectively; metabolites are presented as rhombs and genes as squircles. Full and dotted arrows represent direct and indirect connection; orange and grey arrows represent biosynthetic pathways and binding; point and block arrows represent activation and inhibition, respectively. ARF2, auxin response factor 2; Aux/IAA, a member from the protein family of auxin-sensitive transcriptional repressors; CDPK, cyclin dependent phosphokinase; DELLA, a member of the protein family of GA-sensitive transcriptional repressors; GID1, gibberellin insensitive dwarf 1; JAZ, jasmonate ZIM-domain; MPK4, mitogen-activated protein kinase 4; PR1, 2 and 5, pathogenesis-related protein 1, 2 and 5, respectively. Figure was adapted on the basis of Figure 1c from Lukan et al. [37] with author's permission.

Ca^{2+} is the most versatile messenger regulating a wide range of responses, including biotic stress. After pathogen recognition, one of the earliest signaling events is the Ca^{2+} influx into the plant cell cytosol. Ca^{2+} signatures are also induced in the nucleus, mitochondria or chloroplasts and there is a complex interplay between Ca^{2+} and other messengers and their signaling pathways [38]. Moreover, it has been shown that Ca^{2+}-mediated signaling is also involved in negative regulation of plant immunity [39]. Thus, there are still many questions that should be addressed. Ca^{2+} sensors are to date the most advanced among all biosensors. They have progressed from bioluminescent aequorin, which is natively anchoring calcium [40], to a wide range of designed fluorescent reporters employing calcium-binding domain CaM, e.g. FRET-based Cameleons (Figure 1) [3,41], single fluorophore GCaMPs (composed of circularly permutated enhanced GFP, CaM and M13 peptide) [42] and GECOs (genetically encoded Ca^{2+} indicators for optical imaging) [28] (Figure 1), and even GFP-aequorin, exploiting bioluminescence resonance energy transfer (BRET) [43]. Ca^{2+} response is fast and thus demands constitutively and strongly expressed direct biosensors, enabling subcellular [28], tissue and whole-plant imaging of calcium release reaching very high temporal resolution measured in seconds [44].

Despite the new insights that have been brought into the role of redox mechanisms in plant defence response, one of the major challenges still is to understand the spatial and temporal redox processes occurring during the defence response and to associate the transcriptional activity with the complex dynamics of these signaling molecules [45,46]. Several related biosensors have been successfully used in plants (reviewed in Choi et al. [47]) to help unravel the spatiotemporal redox signaling occurring during plant defense response.

As an example, roGFPs are mutated GFP molecules sensitive to redox levels in the cell [48], which were later fused to signal sequences to allow targeting to different subcellular organelles, such as mitochondria [49] and chloroplasts [50]. Fusion partners known to be targets of redox transitions by glutathione (Figure 1) [30] or H_2O_2 (Figure 1) [29] were also designed and recently used for time-resolved measurements of both molecular species in the cytosol, chloroplasts and mitochondria [31]. This allowed for better understanding of the role of the mitochondria in sensing and signaling the cellular redox challenge in response to abiotic stress [51], deciphering the role of redox state in intercellular transport [50] or exploring the central role of glutathione in mediating redox signaling [52]. Another genetically encoded redox sensor used in plants is HyPer, based on circularly permutated YFP coupled with the H_2O_2-sensitive domain of OxyR, a transcription factor found in *Escherichia coli* [53]. A newly developed biosensor in plants, CROST (change in redox state of thioredoxin) employs a FRET-pair linked with redox-sensitive domain CP12 from *A. thaliana*, known to be reduced in vivo by thioredoxin [54]. Still, available H_2O_2 and redox sensors are frequently limited by extreme pH and redox conditions which must be considered when choosing the appropriate sensor for certain cellular compartments: apoplast, vacuole, endoplasmic reticulum, chloroplast, and mitochondria [20].

Recent advances in the development of plant biosensors (see review Novák et al. [11]) have helped to better understand dynamics of plant signaling, in particular in developmental processes [55]. Some of these can also be applied to monitor the immune response as some parts of the signaling network modules overlap. The most successful biosensors for hormones are transcriptional reporters, based on hormone-responsive promoter motifs fused to a reporter element. The first generation used the synthetic promoter fused to GUS, but, more recently, FPs have shown to be more versatile and have become the reporter of choice [56].

Transcriptional reporters have worked well not just in case of the abovementioned DR5 for auxin, but also in the case of the cytokinin Two Component System (TCS) [57] that was developed and used to uncover the roles of cytokinin signaling in *A. thaliana* root regeneration. It is named after the two-component phosphorelay cascade, the basis of the cytokinin signaling. The final target of the phosphorylation-triggered activation are transcription factors named B-type response regulators which activate the expression of cytokinin responsive genes. Their DNA binding sites are highly conserved and are thus exploited by TCS biosensors, joining six direct repeats to a minimal CaMV 35S promoter. The synthetic sensor TCS and its improved variants TCSnew (TCSn) [58] and TCS version 2 (TCSv2) [59] have been widely used in the model plant *A. thaliana*. Recently, a new synthetic transcriptional reporter for ABA was designed as six repeats of ABA-responsive elements (ABRE) from RD29A or ABI1 promoters fused to a minimal promoter, driving expression of either GUS or GFP targeted to endoplasmic reticulum. It was shown that both transcriptional reporters respond to osmotic stress [60].

Entanglement of the signaling pathways of the main three immune response hormones, SA, JA and ET, challenges the search for their specific transcriptional reporters. Promoters of pathogenesis-related proteins (PRs) are usually employed as transcriptional markers for SA signaling (Figure 1), while promoters of genes involved in JA biosynthesis (e.g. 12-oxo-phytodienoic acid reductase 3, OPR3), regulators of transcription (jasmonate-ZIM-domain 10, JAZ10) or target genes, e.g. plant defensin 1.2 (PDF1.2) and vegetative storage protein (VSP), are analyzed in connection with JA signaling (Figure 1). However, these promoters exhibit significant crosstalk between SA, JA and ET signaling pathways and are thus treated as defense-responsive genes. To our knowledge, specific genetically encoded promoter-based biosensors for SA and JA have not yet been developed in plants. ET transcriptional reporters are based on a synthetic promoter composed of five repeats of the Ethylene insensitive 3 (EIN3) binding site attached to the minimal CaMV 35S promoter [61]. So far, this has been used in combination with either luciferase or GUS due to its low strength [10]. Lately, some new promoters responding to ABA, auxin, cytokinin, SA and JA were identified in *A. thaliana* as promising candidates for transcriptional reporters [62].

Available direct biosensors that track plant hormone concentrations are based on either FRET or degrons. Recently, a major advance in high-resolution quantification of spatiotemporal GA distribution was achieved with the development of a sensor directly measuring GA. This exploits the interaction of GA receptor gibberellin insensitive dwarf 1 (GID1) with members of the DELLA family. Rizza et al. developed and implemented this FRET-based sensor (Gibberellin Perception Sensor 1, GPS1, Figure 1) in *A. thaliana* [34]. In fact, the first FRET-biosensors were developed for ABA measurement and were published in parallel by two different research groups: ABA concentration and uptake sensor (ABACUS) [63], and ABAleons [64].

Using a degron design, Larrieu et al. developed a biosensor for JA perception (Jas9-VENUS, Figure 1) and demonstrated its value for quantitative and dynamic analysis of JA response in *A. thaliana* roots [65]. The Jas9-VENUS biosensor uses the Jas motif of Jasmonate-ZIM-Domain (JAZ) proteins that are targeted to degradation via the ubiquitin/26S proteasome pathway in the presence of the bioactive form of JA. Another degron-based biosensor designed to monitor GA is the GFP-tagged DELLA protein repressor of GA1-3 (GFP-RGA, Figure 1) that was used in the model plant *A. thaliana* and revealed asymmetric distribution of GA and GA signaling during root gravitropic growth [33]. StrigoQuant is also a degron-based but luminescent reporter which includes two luciferases, firefly and Renilla luciferase (FLUC and RLUC, respectively) that are expressed under the same promoter. Co-translationally, fusion of FLUC and RLUC is cleaved by 2A self-cleaving peptide which links both reporters: one is degraded upon presence of strigolactons, the other is used for normalization of expression [66].

Both direct and indirect biosensors are now frequently designed along with their non-responsive counterparts, which were constructed in the same way but are not responsive to the analyte. Thus, they show the background signal from the biosensor itself, and can be used directly for normalization when fused to another reporter protein. Some examples are nlsGPS1 and nlsGPS1-NR (gibberellin) [67], Jas9-VENUS and mJas9-VENUS [65], DII and mDII (e.g. R2D2: DII-3xVENUS and mDII-ntdTomato) [7], TCS and TCSm [57].

Other useful biosensors of immune response are those following the activity of mitogen-activated protein kinases (MAPKs) through the use of docking domain and phosphorylation site (FRET biosensors and KTRs, kinase translocation reporters, in which a reporter changes its intracellular localization when phosphorylated), namely *A. thaliana*'s MPK3, MPK4, MPK6, which take part in response to flg22, chitin and NaCl (Figure 1) [36,68]. The SnRK2 (sucrose nonfermenting-1-related kinase 2) activity sensor (SNACS) is another kinase activity FRET biosensor for ABA-responsive SnRK2 protein kinases involved in stomata closure, stably transformed in *A. thaliana* and its mutants [69].

To follow the outcome of defence and growth antagonism in the whole plant, it is possible to engage cell division reporters based on cyclins, for example, CYCB1;1, B-type cyclin that is present only in late G2 phase and early M phase of the cell cycle: AtpCYCB1;1::CYCB1;1-tYFPnls (Figure 1), also available in fusion with GUS [35], or CYCD6;1, driving S-phase of DNA replication: CYCD6;1::GFP [70]. Recently, a three-component biosensor was designed to follow the whole cell cycle in *A. thaliana* [71]. It contains a multigene cassette expressing fusions of CDT1a-eCFP, HTR13-mCherry and N-CYCB1;1-YFP, each under the control of the native promoter of the first fusion partner. CDT1a is involved in initiation of DNA replication and is expressed during the S and G2 phases, HTR13 is histone H3.1 protein and is expressed during the M and G1 phases, while N-CYCB1;1 is expressed during the late G2 and prophase and metaphase of mitosis [71]. Some possible solutions have not yet been applied to plants. Recently, another promising type of biosensor was established in the animalia kingdom, FlipGFP, for following protease activity. This is based on tripartite GFP, which fluoresces only when reconstituted with two missing beta-strands. These become available after the cleavage of their fusion by a specific protease [72].

3. Getting a Broader View and Deeper Understanding: More Than One Biosensor in the Same Chassis

In the field, plants are rarely exposed to a single stress. They often interact with different organisms, either simultaneously or sequentially, and can be affected by several abiotic stresses such as drought, heat or salinity. The effects of these adverse conditions in plant growth and yield can be devastating and are becoming more problematic with the advent of climate change. Understanding the response of plants to environmental conditions and how the different signaling pathways interact is crucial to guarantee efficient crop protection strategies. Several studies have reported that the involvement of different signaling pathways in response to multiple stresses and three-way interactions cannot be inferred from the response to a single stress [73,74]. Therefore, it is of high importance to gain better insights into the plant response to multiple stresses and the use of combined biosensors could be a promising tool to greatly advance this field.

Employing more than one biosensor simultaneously can provide information for more than one analyte or for the same analyte in more than one cell compartment. Although it demands additional efforts in cloning, transforming, imaging and analysis, examples have recently shown the value of this approach. Waadt et al. [75] investigated the interdependence of calcium and ABA signaling in *A. thaliana* roots. The authors performed multiparameter imaging of both analytes combining the red-emitting single-FP genetically encoded Ca^{2+} indicators for optical imaging (R-GECO1) [76] and the FRET-based ABA reporter ABAleon2.1 emitting in cyan/yellow [64]. Taking advantage of the high sensitivity of GECOs, a dual sensor for monitoring Ca^{2+} signal dynamics in the cytoplasm and the nuclear compartments was developed by assembling the nuclear-R-GECO1 (NR-GECO1) and the cytoplasmic green GECO1 (CG-GECO1) in a single construct [28]. The dual GECO sensor was shown to be a useful tool to monitor Ca^{2+} signal response to biotic and abiotic stress of *Medicago truncatula* and *A. thaliana* roots [28]. Another example of dual sensors is the use of transgenic *A. thaliana* plants simultaneously expressing DR5::3xVENUS-N7 [77] and TCS::GFP [57] reporters to study the spatial patterns of auxin and cytokinins, respectively [78].

The analysis of several analytes simultaneously requires the generation of transgenic plants that express several genetically encoded sensors by co-transformations with single transcriptional units or transformation with a multigene cassette following the assembly of single sensors. The generation of transgenic plants is time-consuming and the insertion of multiple transgenes into the *A. thaliana* genome could result in epigenetic silencing effects [79]. In contrast, it has been shown that the inducible co-expression of two interacting proteins, each tagged with FP, in a single multigene expression cassette reduces variability in expression of the proteins in a single cell, avoids mosaicism and can increase FRET [80]. By expressing two biosensors from one single mRNA Waadt et al. introduced the concept of dual-reporting transcriptionally linked genetically encoded fluorescent indicators (2-in-1-GEFIs). The two fluorescent proteins are separated by 2A self-cleaving peptide. This sensor was used for the multiparametric analysis of ABA, Ca^{2+}, protons, chloride, the glutathione redox potential, and H_2O_2 in *A. thaliana* roots [81].

Many of these approaches are not specific to fluorescent proteins, but can be also applied to the constructs with luciferases. Recent research provided new luciferases that emit light of different wavelengths and can thus be used simultaneously (similar to FPs), or even in fusion with FPs in BRET experiments [82]. Apart from StrigoQuant [66], a pair of FLUC and RLUC was used as a sensor for miRNA silencing, where FLUC transcript was miRNA's target while RLUC was used for normalization [83]. More recent luciferases that complement each other with respect to emission wavelength are the red firefly luciferase (redLUC) and Gaussia Dura luciferase (gLUC) that have already been used in a similar manner to StrigoQuant [84]. NanoLUC is smaller than other luciferases, does not use ATP and allows higher temporal resolution [85]. Light produced from another luciferase, GeNL, performs high transmittance through plant tissue when used with appropriate substrate [86].

In order to follow various molecules and more aspects of a response in a spatiotemporal manner, different approaches can be used simultaneously. We can exploit the options of non-genetically encoded biosensors such as nanosensors which are applied onto the surface, such as carbon nanotubes that change their fluorescence when exposed to higher H_2O_2 concentrations [87]. It has also been shown in *A. thaliana*, wheat and maize that plants can be fumigated with permeable fluorescent probes that irreversibly react with ROS [88]. Microbial biosensors, such as *Acinetobacter* sp. ADPWH_*lux*, can use SA as a sole carbon source and can therefore be exploited for SA detection (Figure 1) [32]. Such an approach is especially useful to gain appropriate time resolution when we want to avoid laborious and time-consuming stable transformation or when stably and constitutively expressed reporters cannot be obtained.

Single or multiple sensors can be used in parallel with reporter microorganisms that allow monitoring of the spatiotemporal response over the plant in relation to the signal from the genetically encoded sensor. Among these we can find GFP-coding viral genome or GFP-tagged infectious viral particles such as plum pox virus [89], potato virus X [90], cowpea mosaic virus [91] or potato virus Y [92]. Several FP-tagged parasitic and (endo)symbiotic bacteria have also been developed, while GUS reporter must be used cautiously because some microorganisms show strong GUS or GUS-like background activity [93,94]. However, the use of lacZ-labelled *Rhizobium leguminosarum* to study infection and nodule development in legumes [95] and the efficiency of luminescent *Ralstonia solanacearum* reporter [96] as a tool to assist potato breeding programs have been recently published. In the case of bacteria, an improved variant of self-assembling split super-folder green fluorescent protein system was optimized to investigate the spatiotemporal dynamics of effectors delivered by the bacterial type III secretion system into the plant cells [97]. Moreover, some FP-tagged fungi are also available, such as *Magnaporthe oryzae* [98,99], *Fusarium graminearum* [100] and *Fusarium solani* [101]. The availability of reporter-incorporated microorganisms is useful for studying biofilm formation, to follow plant-host interaction and, in case of fungi, it enables imaging of hyphae formation, from its passage through the apoplast to its entry into plant cells. Combined with multiple genetically encoded sensors, this approach would allow us to follow the plant response at the site of the interaction with spatiotemporal resolution.

4. Responses of the Cultivated: Biosensors in Crops

While *A. thaliana* serves as the playground where functionality of biosensors developed for animalia kingdom are usually first used, crops seem left behind, as only the most used examples reach them after a delay. The reason for this frequently lies in unsuccessful attempts to produce functionally stable transformants. Stable transformations of some plant species are demanding due to the larger genome and higher ploidy, higher content of repetitive regions and topologically associated domains (TADs), local intra-chromosomal contacts that are species-specific [102]. Added to the challenge of transforming crops is the fact that most can be unresponsive to tissue culture protocols and they have longer growing seasons. Some crops lack (fertile) seed production which also makes it harder to produce crossed lines that contain two or more stacked transgenes. Consequently, the analyses of responses of crops to various stimuli mostly depend on transcriptomics studies while the confirmation of results using biosensors is limited to the transient transformation of *Nicotiana* spp. or *A. thaliana* protoplasts, which can provide much faster but less accurate results. However, this restricts the span of the observable genes to those that have orthologues in further-related species while those with different functions often fail to be more closely observed in their native species.

Despite the limitations, there are some crops available with biosensory properties (Table 1). Ideally, the use of stable transformants is the most desirable approach but it is time consuming and frequently unsuccessful. In some species, mainly in the family of the legumes (but also many other species, e.g. barley [103]), *Agrobacterium rhizogenes*-mediated transformation of roots provides an alternative approach [104]. These can suffice for following various aspects of root development, interaction with microbiota and nodulation.

Table 1. Examples of genetically encoded biosensors applied to crops. Comments are added to those biosensors that were used in multiparameter imaging.

Analyte	Biosensor	Crop	Transformation	Comments	Reference
Ca^{2+}	NES-YC3.6	*Lotus japonicus*	stable		[105]
	NLS-YC3.6	*L. japonicus*	stable		[105]
	NRCG-GECO1	*Medicago truncatula*	roots - transient	dual sensor localized in nucleus and cytoplasm	[28]
	NupYC2.1	*M. truncatula*	roots - transient		[106]
	aequorin	potato	stable		[107]
	aequorin	tomato	stable		[108]
	YC3.6	tomato	stable		[109]
ROS	roGFP1	tomato	stable		[110]
ROS: GSH	chl-roGFP2	potato	stable		[111]
ROS: H_2O_2	HyPer	*M. truncatula*	roots - transient		[112]
auxin	DII-VENUS	*Brachypodium distachyon*	stable		[113]
	DR5::nlsGFP	*Hieracium piloselloides*	stable		[114]
	DR5::GFP-NLS	*L. japonicus*	roots - transient		[115]
	DR5::GUS	*L. japonicus*	roots - transient	inoculated with DsRed-tagged rhizobium	[116]
	DR5::mCherry-NLS	*L. japonicus*	roots - transient	co-expressed with TCSn::YFP-NLS	[35]
	DR5::tYFPnls	*L. japonicus*	roots - transient		[35]
	R2D2	*L. japonicus*	roots - transient	co-expression of DII-tYFPnls and mDII-NLS-DsRed	[35]
	DII-VENUS-NLS	maize	stable		[117]
	DR5rev::mRFPer	maize	stable		[118]
	DR5::GUS	*M. truncatula*	stable		[119]
	DR5::VENUS-N7	*M. truncatula*	stable		[120]
	DR5rev::GFP	*M. truncatula*	stable		[119]
	DR5::GUS	poplar	stable		[121]
	DR5rev::3XVENUS-N7	potato	stable		[122]
	DR5rev::3xVENUS-N7	rice	stable		[123]
	DII-VENUS	rice	stable		[123]
	DR5::GUS	*Senecio vulgaris*	stable		[124]
	DR5::GFP-NLS	soybean	roots - transient	co-expressed with TCSn::tdTomato-NLS	[125]
	DR5::tdTomato	soybean	roots - transient	co-expressed with sUbi::GFP	[126]
	DR5::GUS	tomato	stable		[127]
	DR5rev::3xVENUS-N7	tomato	stable		[128]
	DR5rev::mRFPer	tomato	stable		[129]
cytokinin	TCSn::VENUS-H2B	barley	roots - transient		[130]
	TCSn::YFP-NLS	*L. japonicus*	roots -transient	co-expressed with DR5::mCherry-NLS	[35]
	TCSn::YFP-NLS	*L. japonicus*	stable	inoculated with DsRed-tagged rhizobium	[131]
	TCSn::GUS	rice	stable		[132]
	TCSn::tdTomato-NLS	soybean	roots - transient	co-expressed with DR5::GFP-NLS	[125]
	TCSv2::3xVENUS	tomato	stable		[133]
	TCSv2::GUS	tomato	stable		[133]
cell division	CycB1;1::GUS	potato	stable		[122]

NES- and NLS-YC3.6, yellow cameleon 3.6 with nuclear export and nuclear localization signal, respectively; NRCG-GECO1, nucleus-red, cytosol-green GECO1; NupYC2.1, nucleoplasmin-tagged yellow cameleon 2.1; tYFPnls, triple repeat YFP with nuclear localization signal; R2D2, biosensor composed of DII-3xVENUS (fusion of DII and triple repeat VENUS yellow fluorescent protein) and mDII-ntdTomato (fusion of mDII and nuclear tandem dimer Tomato red fluorescent protein); mRFPer, monomeric RFP targeted to endoplasmic reticulum; N7 and H2B, nuclear localization signals, derived from ankyrin-like protein and histone H2B.

Usually, the sensors that have been applied to crops are the widely used transcriptional reporters for cytokinin or auxin responses consisting of a synthetic promoter and a reporter. In contrast, from the wide range of remaining available sensors, to our knowledge, only the ones that enable monitoring Ca^{2+}, ROS and cell division have been applied to a reduced number of plant species other than *A. thaliana* (Table 1).

Interestingly, multiparameter imaging has already been used in roots of legumes to follow relations between auxin and cytokinin signaling during root growth and nodulation. Fisher et al. assembled a multigene cassette carrying the GFP under the control of synthetic promoter DR5 and the tandem-dimer Tomato (tdTomato) under the control of the TCSn promoter, which enabled them to determine auxin and cytokinin response and their ratios in root and nodule tissues of soybean [125]. Similarly, Nadzieja et al. monitored auxin and cytokinin response of *Lotus japonica* roots, transformed with DR5::mCherry-NLS and TCSn::YFP-NLS sensors, expressed from the same multigene cassette [35]. To detect the spatial correlation between inoculation with symbiotic bacteria *Mesorhizobium loti* and cytokinin or auxin response, DsRed-marked bacteria were applied to roots of *L. japonicus* expressing either TCSn::YFP-NLS [131] or DR5::GUS [116] biosensor, respectively. DR5::tdTomato biosensor was co-expressed in soybean with GFP under constitutive promoter super ubiquitin (sUbi::GFP). Spatial overlap of the signals from FPs enabled discrimination between the red signal from the sensor and bright red autofluorescence [126] (Table 1).

5. Challenges of Plant Biosensors' Development and Use

There are many successful reported uses of biosensors, though their development can be challenging and obtained results are not always straightforward to interpret. While the vast majority of biosensor detection has been performed in plant roots, protoplasts and transiently transformed tobacco pavement cells, imaging of photosynthetic tissue is far less commonly reported. It is often limited to whole plant imaging which does not allow high spatial resolution, while leaf tissue close-ups with subcellular resolution are rare. Besides some general instrumentation constraints, for instance focus drift and unstable laser power in the first couple of hours, uneven illumination and time-consuming high-quality image acquisition [134], imaging of FPs in plants is affected by fluorescent compounds found in cuticle, cell walls, plastids and vacuoles, such as lignin, chlorophyll and other pigments, etc. [135]. These components generate high background and cause low SNR in detection of fluorescent reporters. Apart from that, they can mislead our interpretation of subcellular organization and structures. For example, during their imaging of GFP-tagged plasmodesmata, Liu et al. reported strong reflection from the cell wall, which could be mistakenly interpreted as plasmodesmata structure in both of the neighboring cells [136]. They were able to avoid misinterpretation due to gene gun transformation with lower density of transformed cells compared to agrobacteria-mediated transformation. As microscopy is very time consuming it is in some cases not the method of choice, especially in the first phases of biosensor development, such as optimization of promoter sequences. Microplate reader fluorimetry/luminometry enables fast screening of many biological replicates simultaneously and detection of crucial time points for further more detailed observation [137,138], but lacks spatial resolution.

To follow a plant's dynamic response through space and time with high resolution, the problem of SNR should be addressed. Partly, we can achieve optimal SNR with proper image acquisition and processing, and also region of interest (ROI) selection [134,139], but this is not always sufficient. There are different strategies to overcome the problem of low SNR at the level of biosensor construction. One option aims to overpower autofluorescence with high expression of fluorescent proteins. This is commonly achieved with the help of minimal CaMV 35S promoter. For transcriptional reporters the promoter can be coupled with CaMV 35S enhancer region and two or more repeats of inducible parts of a certain promoter, e.g. PR2 (from parsley) or AtCMPG1 [140,141]. Higher expression can also be achieved with the use of proper combinations of 5′-UTR and 3′-UTR enhancer regions [142], compatible with the plant of choice [143] as it is done for protein production in planta. When a transcriptional reporter is under the control of a weak promoter, an additional transcriptional regulator between the two can amplify its activity [144]. However, this effort is frequently opposed by silencing [137].

The proper choice of localization can also heighten SNR. The signal in plant cytoplasm is weak, variable among cells, hard to quantify and more prone to silencing. On the other hand, localization in other compartments can also have some constraints. Reporter protein localized in vacuole and apoplast should be pH stable, a condition refusing many widely used fluorescent proteins [145]. For this reason, red variants of redox sensors roGFP and HyPer were designed, namely Grx1-roCherry [146] and HyPerRed [147], respectively. Additionally, HyPer and HyPerRed have their redox-non-sensitive and pH-sensitive counterparts and can be used in parallel as a control of pH effect on measurements [147]. However, we have not found any report on their use in plants so far. Nucleus and mitochondrial localizations also have drawbacks. For example, small fluorescent proteins can exhibit leaking when tagged with either nuclear localization signal (NLS) or nuclear exportation signal (NES), while the mutants expressing fluorescent biosensors in the mitochondrial matrix were shown to grow more slowly than others [29].

Higher analyte specificity is also helpful when dealing with low SNR. This can be reached with a chimeric effector/detector module [148]. This often comes with lower constant of dissociation for the chosen analyte and can therefore interfere with the analyte's availability for endogenous targets, which was the case in ABA sensors (reviewed in Isoda et al. [13]). Potential slow release of the analyte from the binding pocket of direct biosensors must also be considered to avoid misinterpretations of temporal dimension of the analyte availability in vivo [67].

Lower SNR in transformants after agrobacteria-mediated transient transformations can be caused by the expression of reporter proteins in agrobacteria, which can be overcome by the promoter exchange [149] or the insertion of an intron [150], the last resulting in higher expression in plant cells through intron-mediated enhancement [151].

Another common problem affecting the use of biosensors is their capacity for analyte quantification. Cell responses are not binary, but rather pattern- and concentration-dependent, so the need for biosensors enabling dynamic quantitative imaging arises, especially when high spatiotemporal resolution and quantitative data are needed for systems biology approaches [152]. Aequorin is a perfect example of absolute intensiometric biosensor for Ca^{2+} imaging as it enables measurement of absolute in vivo concentration [153]. Non-FRET ratiometric biosensors use a duet of reporter proteins, one as a reporter of analyte and another as a reporter of expression in a certain cell or tissue. The second can be expressed separately as a normalization transcriptional unit under constitutive promoter. Expression under strong viral constitutive promoter CaMV 35S can experience silencing or patterns in dividing cells [7] and is therefore often exchanged with plant constitutive promoters, such as rice actin and maize ubiquitin promoters. Still, variable expression in different species forces the exploration of novel options [154,155]. On the other hand, it is possible to opt for separation of two or more reporters at the protein stage. One possibility is co-translational separation by a self-cleaving peptide [84,156]. However, after the cleavage, the peptide is not excised but remains attached to the C-terminus of the upstream protein sequence which can affect its folding or function. This can be overcome by attachment of a peptide linker, which is a target of endogenous peptidases [157,158], or mini-intein with N-terminal autocleavage ability [159]. Synchronized expression of two proteins can also be obtained by using a polyprotein vector system that is based on a pair of self-excising mini-inteins, called dual-intein domain, which allow the release of both proteins (shown for tripartite sfGFP) [160]. In contrast, the use of internal ribosomal entry site (IRES) was not successful and is not recommended, as the level of IRES-driven translation can vary among cells [160].

To alleviate the problems associated with fluorescence imaging in plants, one can also use luciferases as the reporter domain in biosensor. One of the drawbacks of luciferases is the need for external application of the substrate which might not readily penetrate into plant tissue. To overcome this issue, autoluminescent *N. benthamiana* plants were engineered by the insertion of a fungal bioluminescence gene cluster (all with CaMV 35S promoter) [161]. Thus, the transgenic plants do not need any external substrate addition,

as they produce fungal luciferin from caffeic acid. Treatment with methyl jasmonate, ethylene and wounding caused higher luminescence within seconds [161,162]. However, the use of the plant's metabolite impacts the final luminescence produced according to availability. For example, older leaves showed lower luminescence [161,162]. A similar approach, avoiding exogenous substrate application, was explored in the reporter RUBY which produces red betalain pigment. The three enzymes that cooperate in its biosynthetic pathway from tyrosine were expressed under the control of various promoters in *A. thaliana* and were co-translationally separated due to the addition of 2A self-cleaving peptide [163].

6. Concluding Remarks

Biosensors have become indispensable tools to gain new insights in molecular biology with high spatiotemporal resolution. When being transferred to plants, especially crops, the community experiences challenges. However, overcoming these challenges is more and more supported by new achievements in synthetic biology, imaging and plant transformation fields, and can lead to new discoveries. Biosensors have so far been used individually, tracking only one analyte per experiment, with rare exceptions. We believe that the field of biosensors is now ready for multiparameter imaging. Therefore, this approach should now be used to obtain (quantitative) data with high spatiotemporal resolution that offer high-quality input for mathematical modeling of the dynamic network of plant responses to environment. Biosensors are promising tools to uncover the mysteries of a plant's orchestrated signaling network that leads to discrimination between specific immune responses.

Author Contributions: All authors together conceptualized and wrote the manuscript. K.G. and A.C. acquired funding. All authors have read and agreed to the published version of the manuscript.

Funding: This research was funded by the Slovenian Research Agency (research core funding No. P4-0165, projects J4-1777, J1-2467 and 1000-20-0105) and by the European Union's Horizon 2020 research and innovation programme under grant agreement No. 862858.

Institutional Review Board Statement: Not applicable.

Informed Consent Statement: Not applicable.

Data Availability Statement: Not applicable.

Acknowledgments: We wish to apologize to those colleagues whose work could not be cited due to space limitations.

Conflicts of Interest: The authors declare no conflict of interest. The funders had no role in the design of the study; in the collection, analyses, or interpretation of data; in the writing of the manuscript, or in the decision to publish the results.

References

1. Walia, A.; Waadt, R.; Jones, A.M. Genetically encoded biosensors in plants: Pathways to discovery. *Annu. Rev. Plant Biol.* **2018**, *69*, 497–524. [CrossRef]
2. Sadanandom, A.; Napier, R.M. Biosensors in plants. *Curr. Opin. Plant Biol.* **2010**, *13*, 736–743. [CrossRef]
3. Miyawaki, A.; Llopis, J.; Heim, R.; McCaffery, J.M.; Adams, J.A.; Ikura, M.; Tsien, R.Y.; Michael McCaffery, J.; Adams, J.A.; Ikura, M.; et al. Fluorescent indicators for Ca^{2+} based on green fluorescent proteins and calmodulin. *Nature* **1997**, *388*, 882–887. [CrossRef]
4. Brunoud, G.; Wells, D.M.; Oliva, M.; Larrieu, A.; Mirabet, V.; Burrow, A.H.; Beeckman, T.; Kepinski, S.; Traas, J.; Bennett, M.J.; et al. A novel sensor to map auxin response and distribution at high spatio-temporal resolution. *Nature* **2012**, *482*, 103–106. [CrossRef]
5. Ali, S.; Kim, W.C. A Fruitful Decade Using Synthetic Promoters in the Improvement of Transgenic Plants. *Front. Plant Sci.* **2019**, *10*, 1433. [CrossRef] [PubMed]
6. Ulmasov, T.; Murfett, J.; Hagen, G.; Guilfoyle, T.J. Aux/IAA proteins repress expression of reporter genes containing natural and highly active synthetic auxin response elements. *Plant Cell* **1997**, *9*, 1963–1971. [CrossRef]
7. Liao, C.Y.; Smet, W.; Brunoud, G.; Yoshida, S.; Vernoux, T.; Weijers, D. Reporters for sensitive and quantitative measurement of auxin response. *Nat. Methods* **2015**, *12*, 207–210. [CrossRef]
8. Li, W.; Ma, M.; Feng, Y.; Li, H.; Wang, Y.; Ma, Y.; Li, M.; An, F.; Guo, H. EIN2-directed translational regulation of ethylene signaling in Arabidopsis. *Cell* **2015**, *163*, 670–683. [CrossRef]

9. Merchante, C.; Brumos, J.; Yun, J.; Hu, Q.; Spencer, K.R.; Enríquez, P.; Binder, B.M.; Heber, S.; Stepanova, A.N.; Alonso, J.M. Gene-specific translation regulation mediated by the hormone-signaling molecule EIN2. *Cell* **2015**, *163*, 684–697. [CrossRef] [PubMed]
10. Fernandez-Moreno, J.P.; Stepanova, A.N. Monitoring ethylene in plants: Genetically encoded reporters and biosensors. *Small Methods* **2020**, *4*, 1900260. [CrossRef]
11. Novák, O.; Napier, R.; Ljung, K. Zooming in on plant hormone analysis: Tissue- and cell-specific approaches. *Annu. Rev. Plant Biol.* **2017**, *68*, 323–348. [CrossRef] [PubMed]
12. Waadt, R. Phytohormone signaling mechanisms and genetic methods for their modulation and detection. *Curr. Opin. Plant Biol.* **2020**, *57*, 31–40. [CrossRef] [PubMed]
13. Isoda, R.; Yoshinari, A.; Ishikawa, Y.; Sadoine, M.; Simon, R.; Frommer, W.B.; Nakamura, M. Sensors for the quantification, localization and analysis of the dynamics of plant hormones. *Plant J.* **2020**. [CrossRef]
14. Martin-Arevalillo, R.; Vernoux, T. Shining light on plant hormones with genetically encoded biosensors. *Biol. Chem.* **2019**, *400*, 477–486. [CrossRef]
15. Okumoto, S.; Jones, A.; Frommer, W.B. Quantitative imaging with fluorescent biosensors. *Annu. Rev. Plant Biol.* **2012**, *63*, 663–706. [CrossRef]
16. Jones, A.M. A new look at stress: Abscisic acid patterns and dynamics at high-resolution. *New Phytol.* **2016**, *210*, 38–44. [CrossRef] [PubMed]
17. Pařízková, B.; Pernisová, M.; Novák, O. What has been seen cannot be unseen—Detecting auxin in vivo. *Int. J. Mol. Sci.* **2017**, *18*, 2736. [CrossRef] [PubMed]
18. Costa, A.; Navazio, L.; Szabo, I. The contribution of organelles to plant intracellular calcium signalling. *J. Exp. Bot.* **2018**, *69*, 4175–4193. [CrossRef] [PubMed]
19. Rizza, A.; Jones, A.M. The makings of a gradient: Spatiotemporal distribution of gibberellins in plant development. *Curr. Opin. Plant Biol.* **2019**, *47*, 9–15. [CrossRef] [PubMed]
20. Ortega-Villasante, C.; Burén, S.; Barón-Sola, Á.; Martínez, F.; Hernández, L.E. In vivo ROS and redox potential fluorescent detection in plants: Present approaches and future perspectives. *Methods* **2016**, *109*, 92–104. [CrossRef] [PubMed]
21. Komis, G.; Novák, D.; Ovečka, M.; Šamajová, O.; Šamaj, J. Advances in imaging plant cell dynamics. *Plant Physiol.* **2018**, *176*, 80–93. [CrossRef]
22. Greenwald, E.; Zhang, J. Fluorescent Biosensor Database. Available online: https://biosensordb.ucsd.edu/index.php (accessed on 20 November 2020).
23. Pieterse, C.M.J.; Leon-Reyes, A.; Van Der Ent, S.; Van Wees, S.C.M. Networking by small-molecule hormones in plant immunity. *Nat. Chem. Biol.* **2009**, *5*, 308–316. [CrossRef]
24. Pieterse, C.M.J.; Van der Does, D.; Zamioudis, C.; Leon-Reyes, A.; Van Wees, S.C.M. Hormonal modulation of plant immunity. *Annu. Rev. Cell Dev. Biol.* **2012**, *28*, 489–521. [CrossRef]
25. Mandadi, K.K.; Scholthof, K.-B.G. Plant immune responses against viruses: How does a virus cause disease? *Plant Cell* **2013**, *25*, 1489–1505. [CrossRef]
26. Bari, R.; Jones, J.D.G. Role of plant hormones in plant defence responses. *Plant Mol. Biol.* **2009**, *69*, 473–488. [CrossRef]
27. Verma, V.; Ravindran, P.; Kumar, P.P. Plant hormone-mediated regulation of stress responses. *BMC Plant Biol.* **2016**, *16*, 86. [CrossRef]
28. Kelner, A.; Leitão, N.; Chabaud, M.; Charpentier, M.; de Carvalho-Niebel, F. Dual Color Sensors for Simultaneous Analysis of Calcium Signal Dynamics in the Nuclear and Cytoplasmic Compartments of Plant Cells. *Front. Plant Sci.* **2018**, *9*, 245. [CrossRef] [PubMed]
29. Nietzel, T.; Elsässer, M.; Ruberti, C.; Steinbeck, J.; Ugalde, J.M.; Fuchs, P.; Wagner, S.; Ostermann, L.; Moseler, A.; Lemke, P.; et al. The fluorescent protein sensor roGFP2-Orp1 monitors in vivo H2O2 and thiol redox integration and elucidates intracellular H2O2 dynamics during elicitor-induced oxidative burst in Arabidopsis. *New Phytol.* **2019**, *221*, 1649–1664. [CrossRef] [PubMed]
30. Aller, I.; Rouhier, N.; Meyer, A.J. Development of roGFP2-derived redox probes for measurement of the glutathione redox potential in the cytosol of severely glutathione-deficient rml1 seedlings. *Front. Plant Sci.* **2013**, *4*, 506. [CrossRef] [PubMed]
31. Ugalde, J.M.; Fuchs, P.; Nietzel, T.; Cutolo, E.A.; Homagk, M.; Vothknecht, U.C.; Holuigue, L.; Schwarzländer, M.; Müller-Schüssele, S.J.; Meyer, A.J. Chloroplast-derived photo-oxidative stress causes changes in H2O2 and GSH in other subcellular compartments. *Plant Physiol.* **2021**, kiaa095. [CrossRef]
32. Huang, W.E.; Huang, L.; Preston, G.M.; Naylor, M.; Carr, J.P.; Li, Y.; Singer, A.C.; Whiteley, A.S.; Wang, H. Quantitative in situ assay of salicylic acid in tobacco leaves using a genetically modified biosensor strain of Acinetobacter sp. ADP1. *Plant J.* **2006**, *46*, 1073–1083. [CrossRef] [PubMed]
33. Löfke, C.; Zwiewka, M.; Heilmann, I.; Van Montagu, M.C.E.; Teichmann, T.; Friml, J. Asymmetric gibberellin signaling regulates vacuolar trafficking of PIN auxin transporters during root gravitropism. *Proc. Natl. Acad. Sci. USA* **2013**, *110*, 3627–3632. [CrossRef] [PubMed]
34. Rizza, A.; Walia, A.; Lanquar, V.; Frommer, W.B.; Jones, A.M. In vivo gibberellin gradients visualized in rapidly elongating tissues. *Nat. Plants* **2017**, *3*, 803–813. [CrossRef] [PubMed]
35. Nadzieja, M.; Stougaard, J.; Reid, D. A toolkit for high resolution imaging of cell division and phytohormone signaling in legume roots and root nodules. *Front. Plant Sci.* **2019**, *10*, 1000. [CrossRef]

36. Seitz, K.; Krysan, P.J. Expanding the toolkit of fluorescent biosensors for studying mitogen activated protein kinases in plants. *Int. J. Mol. Sci.* **2020**, *21*, 5350. [CrossRef]
37. Lukan, T.; Pompe-Novak, M.; Baebler, Š.; Tušek-Žnidarič, M.; Kladnik, A.; Križnik, M.; Blejec, A.; Zagorščak, M.; Stare, K.; Dušak, B.; et al. Precision transcriptomics of viral foci reveals the spatial regulation of immune-signaling genes and identifies RBOHD as an important player in the incompatible interaction between potato virus Y and potato. *Plant J.* **2020**, *104*, 645–661. [CrossRef]
38. Yuan, P.; Jauregui, E.; Du, L.; Tanaka, K.; Poovaiah, B.W. Calcium signatures and signaling events orchestrate plant–microbe interactions. *Curr. Opin. Plant Biol.* **2017**, *38*, 173–183. [CrossRef] [PubMed]
39. Seybold, H.; Trempel, F.; Ranf, S.; Scheel, D.; Romeis, T.; Lee, J. Ca^{2+} signalling in plant immune response: From pattern recognition receptors to Ca^{2+} decoding mechanisms. *New Phytol.* **2014**, *204*, 782–790. [CrossRef]
40. Knight, M.R.; Campbell, A.K.; Smith, S.M.; Trewavas, A.J. Transgenic plant aequorin reports the effects of touch and cold-shock and elicitors on cytoplasmic calcium. *Nature* **1991**, *352*, 524–526. [CrossRef] [PubMed]
41. Allen, G.J.; Kwak, J.M.; Chu, S.P.; Llopis, J.; Tsien, R.Y.; Harper, J.F.; Schroeder, J.I. Cameleon calcium indicator reports cytoplasmic calcium dynamics in Arabidopsis guard cells. *Plant J.* **1999**, *19*, 735–747. [CrossRef]
42. Nakai, J.; Ohkura, M.; Imoto, K. A high signal-to-noise Ca^{2+} probe composed of a single green fluorescent protein. *Nat. Biotechnol.* **2001**, *19*, 137–141. [CrossRef] [PubMed]
43. Xiong, T.C.; Ronzier, E.; Sanchez, F.; Corratgé-Faillie, C.; Mazars, C.; Thibaud, J.B. Imaging long distance propagating calcium signals in intact plant leaves with the BRET-based GFP-aequorin reporter. *Front. Plant Sci.* **2014**, *5*, 43. [CrossRef]
44. Toyota, M.; Spencer, D.; Sawai-Toyota, S.; Jiaqi, W.; Zhang, T.; Koo, A.J.; Howe, G.A.; Gilroy, S. Glutamate triggers long-distance, calcium-based plant defense signaling. *Science* **2018**, *361*, 1112–1115. [CrossRef] [PubMed]
45. Herrera-Vásquez, A.; Salinas, P.; Holuigue, L. Salicylic acid and reactive oxygen species interplay in the transcriptional control of defense genes expression. *Front. Plant Sci.* **2015**, *6*, 171. [CrossRef] [PubMed]
46. Wrzaczek, M.; Brosché, M.; Kangasjärvi, J. ROS signaling loops—Production, perception, regulation. *Curr. Opin. Plant Biol.* **2013**, *16*, 575–582. [CrossRef]
47. Choi, W.G.; Swanson, S.J.; Gilroy, S. High-resolution imaging of Ca^{2+}, redox status, ROS and pH using GFP biosensors. *Plant J.* **2012**, *70*, 118–128. [CrossRef]
48. Hanson, G.T.; Aggeler, R.; Oglesbee, D.; Cannon, M.; Capaldi, R.A.; Tsien, R.Y.; Remington, S.J. Investigating mitochondrial redox potential with redox-sensitive green fluorescent protein indicators. *J. Biol. Chem.* **2004**, *279*, 13044–13053. [CrossRef]
49. Jiang, K.; Schwarzer, C.; Lally, E.; Zhang, S.; Ruzin, S.; Machen, T.; Remington, S.J.; Feldman, L. Expression and characterization of a redox-sensing green fluorescent protein (reduction-oxidation-sensitive green fluorescent protein) in Arabidopsis. *Plant Physiol.* **2006**, *141*, 397–403. [CrossRef]
50. Stonebloom, S.; Brunkard, J.O.; Cheung, A.C.; Jiang, K.; Feldman, L.; Zambryski, P. Redox states of plastids and mitochondria differentially regulate intercellular transport via plasmodesmata. *Plant Physiol.* **2012**, *158*, 190–199. [CrossRef]
51. Schwarzländer, M.; Fricker, M.D.; Sweetlove, L.J. Monitoring the in vivo redox state of plant mitochondria: Effect of respiratory inhibitors, abiotic stress and assessment of recovery from oxidative challenge. *Biochim. Biophys. Acta Bioenerg.* **2009**, *1787*, 468–475. [CrossRef] [PubMed]
52. Meyer, A.J.; Brach, T.; Marty, L.; Kreye, S.; Rouhier, N.; Jacquot, J.P.; Hell, R. Redox-sensitive GFP in Arabidopsis thaliana is a quantitative biosensor for the redox potential of the cellular glutathione redox buffer. *Plant J.* **2007**, *52*, 973–986. [CrossRef]
53. Hernández-Barrera, A.; Quinto, C.; Johnson, E.A.; Wu, H.M.; Cheung, A.Y.; Cárdenas, L. Using hyper as a molecular probe to visualize hydrogen peroxide in living plant cells: A method with virtually unlimited potential in plant biology. *Methods Enzymol.* **2013**, *527*, 275–290. [CrossRef] [PubMed]
54. Sugiura, K.; Yokochi, Y.; Fu, N.; Fukaya, Y.; Yoshida, K.; Mihara, S.; Hisabori, T. The thioredoxin (Trx) redox state sensor protein can visualize Trx activities in the light/dark response in chloroplasts. *J. Biol. Chem.* **2019**, *294*, 12091–12098. [CrossRef]
55. Uslu, V.V.; Grossmann, G. The biosensor toolbox for plant developmental biology. *Curr. Opin. Plant Biol.* **2016**, *29*, 138–147. [CrossRef]
56. Mylle, E.; Codreanu, M.C.; Boruc, J.; Russinova, E. Emission spectra profiling of fluorescent proteins in living plant cells. *Plant Methods* **2013**, *9*, 10. [CrossRef] [PubMed]
57. Muller, B.; Sheen, J. Cytokinin and auxin interaction in root stem-cell specification during early embryogenesis. *Nature* **2008**, *453*, 1094–1097. [CrossRef]
58. Zurcher, E.; Tavor-Deslex, D.; Lituiev, D.; Enkerli, K.; Tarr, P.T.; Muller, B. A robust and sensitive synthetic sensor to monitor the transcriptional output of the cytokinin signaling network in planta. *Plant Physiol.* **2013**, *161*, 1066–1075. [CrossRef] [PubMed]
59. Steiner, E.; Livne, S.; Kobinson-Katz, T.; Tal, L.; Pri-tal, O.; Mosquna, A.; Tarkowská, D.; Muller, B.; Tarkowski, P.; Weiss, D. The putative O-linked N-acetylglucosamine transferase SPINDLY inhibits class I TCP proteolysis to promote sensitivity to cytokinin 1. *Plant Physiol.* **2016**, *171*, 1485–1494. [CrossRef] [PubMed]
60. Wu, R.; Duan, L.; Pruneda-Paz, J.L.; Oh, D.H.; Pound, M.; Kay, S.; Dinneny, J.R. The 6xABRE synthetic promoter enables the spatiotemporal analysis of ABA-mediated transcriptional regulation. *Plant Physiol.* **2018**, *177*, 1650–1665. [CrossRef]
61. Stepanova, A.N.; Yun, J.; Likhacheva, A.V.; Alonso, J.M. Multilevel interactions between ethylene and auxin in Arabidopsis roots. *Plant Cell* **2007**, *19*, 2169–2185. [CrossRef]
62. Lehmann, S.; Dominguez-Ferreras, A.; Huang, W.J.; Denby, K.; Ntoukakis, V.; Schäfer, P. Novel markers for high-throughput protoplast-based analyses of phytohormone signaling. *PLoS ONE* **2020**, *15*, e0234154. [CrossRef]

63. Jones, A.M.; Danielson, J.Å.H.; Manojkumar, S.N.; Lanquar, V.; Grossmann, G.; Frommer, W.B. Abscisic acid dynamics in roots detected with genetically encoded FRET sensors. *Elife* **2014**, e01741. [CrossRef]
64. Waadt, R.; Hitomi, K.; Nishimura, N.; Hitomi, C.; Adams, S.R.; Getzoff, E.D.; Schroeder, J.I. FRET-based reporters for the direct visualization of abscisic acid concentration changes and distribution in Arabidopsis. *Elife* **2014**, e01739. [CrossRef]
65. Larrieu, A.; Champion, A.; Legrand, J.; Lavenus, J.; Mast, D.; Brunoud, G.; Oh, J.; Guyomarc'h, S.; Pizot, M.; Farmer, E.E.; et al. A fluorescent hormone biosensor reveals the dynamics of jasmonate signalling in plants. *Nat. Commun.* **2015**, *6*, 6043. [CrossRef] [PubMed]
66. Samodelov, S.L.; Beyer, H.M.; Guo, X.; Augustin, M.; Jia, K.P.; Baz, L.; Ebenhöh, O.; Beyer, P.; Weber, W.; Al-Babili, S.; et al. StrigoQuant: A genetically encoded biosensor for quantifying strigolactone activity and specificity. *Sci. Adv.* **2016**, *2*, e1601266. [CrossRef] [PubMed]
67. Rizza, A.; Walia, A.; Tang, B.; Jones, A.M. Visualizing cellular gibberellin levels using the nlsGPS1 Förster resonance energy transfer (FRET) biosensor. *J. Vis. Exp.* **2019**, e58739. [CrossRef]
68. Zaman, N.; Seitz, K.; Kabir, M.; George-Schreder, L.S.; Shepstone, I.; Liu, Y.; Zhang, S.; Krysan, P.J. A Förster resonance energy transfer sensor for live-cell imaging of mitogen-activated protein kinase activity in Arabidopsis. *Plant J.* **2019**, *97*, 970–983. [CrossRef]
69. Zhang, L.; Takahashi, Y.; Hsu, P.K.; Kollist, H.; Merilo, E.; Krysan, P.J.; Schroeder, J.I. FRET kinase sensor development reveals SnRK2/OST1 activation by ABA but not by MeJA and high CO2 during stomatal closure. *Elife* **2020**, *9*, e56351. [CrossRef] [PubMed]
70. Sozzani, R.; Cui, H.; Moreno-Risueno, M.A.; Busch, W.; Van Norman, J.M.; Vernoux, T.; Brady, S.M.; Dewitte, W.; Murray, J.A.H.; Benfey, P.N. Spatiotemporal regulation of cell-cycle genes by SHORTROOT links patterning and growth. *Nature* **2010**, *466*, 128–132. [CrossRef]
71. Desvoyes, B.; Arana-Echarri, A.; Barea, M.D.; Gutierrez, C. A comprehensive fluorescent sensor for spatiotemporal cell cycle analysis in Arabidopsis. *Nat. Plants* **2020**, *6*, 1330–1334. [CrossRef]
72. Zhang, Q.; Schepis, A.; Huang, H.; Yang, J.; Ma, W.; Torra, J.; Zhang, S.Q.; Yang, L.; Wu, H.; Nonell, S.; et al. Designing a green fluorogenic protease reporter by flipping a beta strand of GFP for imaging apoptosis in animals. *J. Am. Chem. Soc.* **2019**, *141*, 4526–4530. [CrossRef]
73. Gruden, K.; Lidoy, J.; Petek, M.; Podpečan, V.; Flors, V.; Papadopoulou, K.K.; Pappas, M.L.; Martinez-Medina, A.; Bejarano, E.; Biere, A.; et al. Ménage à trois: Unraveling the mechanisms regulating plant–microbe–arthropod interactions. *Trends Plant Sci.* **2020**, *25*, 1215–1226. [CrossRef]
74. Devireddy, A.R.; Zandalinas, S.I.; Fichman, Y.; Mittler, R. Integration of reactive oxygen species and hormone signaling during abiotic stress. *Plant J.* **2020**. [CrossRef]
75. Waadt, R.; Krebs, M.; Kudla, J.; Schumacher, K. Multiparameter imaging of calcium and abscisic acid and high-resolution quantitative calcium measurements using R-GECO1-mTurquoise in Arabidopsis. *New Phytol.* **2017**, *216*, 303–320. [CrossRef] [PubMed]
76. Zhao, Y.; Araki, S.; Wu, J.; Tramoto, T.; Chang, Y.-F.; Nakano, M.; Abderfattah, A.; Fujiwara, M.; Ishihara, T.; Nagai, T.; et al. An expanded palette of genetically encoded Ca^{2+} indicators. *Science* **2011**, *557*, 1888–1891. [CrossRef]
77. Nakamura, A.; Higuchi, K.; Goda, H.; Fujiwara, M.T.; Sawa, S.; Koshiba, T.; Shimada, Y.; Yoshida, S. Brassinolide induces IAA5, IAA19, and DR5, a synthetic auxin response element in Arabidopsis, implying a cross talk point of brassinosteroid and auxin signaling. *Plant Physiol.* **2003**, *133*, 1843–1853. [CrossRef]
78. Zhu, M.; Chen, W.; Mirabet, V.; Hong, L.; Bovio, S.; Strauss, S.; Schwarz, E.M.; Tsugawa, S.; Wang, Z.; Smith, R.S.; et al. Robust organ size requires robust timing of initiation orchestrated by focused auxin and cytokinin signalling. *Nat. Plants* **2020**, *6*, 686–698. [CrossRef] [PubMed]
79. Behera, S.; Wang, N.; Zhang, C.; Schmitz-Thom, I.; Strohkamp, S.; Schültke, S.; Hashimoto, K.; Xiong, L.; Kudla, J. Analyses of Ca^{2+} dynamics using a ubiquitin-10 promoter-driven Yellow Cameleon 3.6 indicator reveal reliable transgene expression and differences in cytoplasmic Ca^{2+} responses in Arabidopsis and rice (Oryza sativa) roots. *New Phytol.* **2015**, *206*, 751–760. [CrossRef] [PubMed]
80. Denay, G.; Schultz, P.; Hänsch, S.; Weidtkamp-Peters, S.; Simon, R. Over the rainbow: A practical guide for fluorescent protein selection in plant FRET experiments. *Plant Direct* **2019**, *3*, e00189. [CrossRef]
81. Waadt, R.; Köster, P.; Andrés, Z.; Waadt, C.; Bradamante, G.; Lampou, K.; Kudla, J.; Schumacher, K. Dual-reporting transcriptionally linked genetically encoded fluorescent indicators resolve the spatiotemporal coordination of cytosolic abscisic acid and second messenger dynamics in Arabidopsis. *Plant Cell* **2020**, *32*, 2582–2601. [CrossRef]
82. Xu, X.; Soutto, M.; Xie, Q.; Servick, S.; Subramanian, C.; Von Arnim, A.G.; Johnson, C.H. Imaging protein interactions with bioluminescence resonance energy transfer (BRET) in plant and mammalian cells and tissues. *Proc. Natl. Acad. Sci. USA* **2007**, *104*, 10264–10269. [CrossRef]
83. Moyle, R.L.; Carvalhais, L.C.; Pretorius, L.-S.; Nowak, E.; Subramaniam, G.; Dalton-Morgan, J.; Schenk, P.M. An optimized transient dual luciferase assay for quantifying microRNA directed repression of targeted sequences. *Front. Plant Sci.* **2017**, *8*, 1631. [CrossRef]
84. Khosla, A.; Rodriguez-Furlan, C.; Kapoor, S.; Van Norman, J.M.; Nelson, D.C. A series of dual-reporter vectors for ratiometric analysis of protein abundance in plants. *Plant Direct* **2020**, *4*, e00231. [CrossRef]

85. Urquiza-García, U.; Millar, A.J. Expanding the bioluminescent reporter toolkit for plant science with NanoLUC. *Plant Methods* **2019**, *15*, 68. [CrossRef]
86. Furuhata, Y.; Sakai, A.; Murakami, T.; Nagasaki, A.; Kato, Y. Bioluminescent imaging of Arabidopsis thaliana using an enhanced Nano-lantern luminescence reporter system. *PLoS ONE* **2020**, *15*, e0227477. [CrossRef] [PubMed]
87. Lew, T.T.S.; Koman, V.B.; Silmore, K.S.; Seo, J.S.; Gordiichuk, P.; Kwak, S.Y.; Park, M.; Ang, M.C.Y.; Khong, D.T.; Lee, M.A.; et al. Real-time detection of wound-induced H_2O_2 signalling waves in plants with optical nanosensors. *Nat. Plants* **2020**, *6*, 404–415. [CrossRef] [PubMed]
88. Fichman, Y.; Miller, G.; Mittler, R. Whole-plant live imaging of reactive oxygen species. *Mol. Plant* **2019**, *12*, 1203–1210. [CrossRef]
89. Pasin, F.; Kulasekaran, S.; Natale, P.; Simón-Mateo, C.; García, J.A. Rapid fluorescent reporter quantification by leaf disc analysis and its application in plant-virus studies. *Plant Methods* **2014**, *10*, 22. [CrossRef] [PubMed]
90. Oparka, K.J.; Roberts, A.G.; Cruz, S.S.; Boevink, P.; Prior, D.A.M.; Smallcombe, A.; Oparka, K.J.; Roberts, A.G.; Cruz, S.S.; Boevink, P.; et al. Using GFP to study virus invasion and spread in plant tissues. *Nature* **1997**, *388*, 401–402. [CrossRef]
91. Verver, J.; Wellink, J.; Van Lent, J.; Gopinath, K.; Van Kammen, A. Studies on the movement of cowpea mosaic virus using the jellyfish green fluorescent protein. *Virology* **1998**, *242*, 22–27. [CrossRef]
92. Rupar, M.; Faurez, F.; Tribodet, M.; Gutiérrez-Aguirre, I.; Delaunay, A.; Glais, L.; Kriznik, M.; Dobnik, D.; Gruden, K.; Jacquot, E.; et al. Fluorescently tagged Potato Virus Y: A versatile tool for functional analysis of plant-virus interactions. *Mol. Plant Microbe Interact.* **2015**, *28*, 739–750. [CrossRef]
93. Egener, T.; Hurek, T.; Reinhold-Hurek, B. Use of green fluorescent protein to detect expression of nif genes of Azoarcus sp. BH72, a grass-associated diazotroph, on rice roots. *Mol. Plant Microbe Interact.* **1998**, *11*, 71–75. [CrossRef]
94. Jefferson, R.A.; Kavanagh, T.A.; Bevan, M.W. GUS fusions: Beta-glucuronidase as a sensitive and versatile gene fusion marker in higher plants. *EMBO J.* **1987**, *6*, 3901–3907. [CrossRef] [PubMed]
95. McAdam, E.L.; Reid, J.B.; Foo, E. Gibberellins promote nodule organogenesis but inhibit the infection stages of nodulation. *J. Exp. Bot.* **2018**, *69*, 2117–2130. [CrossRef]
96. Cruz, A.P.Z.; Ferreira, V.; Pianzzola, M.J.; Siri, M.I.; Coll, N.S.; Valls, M. A novel, sensitive method to evaluate potato germplasm for bacterial wilt resistance using a luminescent Ralstonia solanacearum reporter strain. *Mol. Plant Microbe Interact.* **2014**, *27*, 277–285. [CrossRef] [PubMed]
97. Park, E.; Lee, H.Y.; Woo, J.; Choi, D.; Dinesh-Kumar, S.P. Spatiotemporal monitoring of Pseudomonas syringae effectors via type III secretion using split fluorescent protein fragments. *Plant Cell* **2017**, *29*, 1571–1584. [CrossRef]
98. Campos-Soriano, L.; San Segundo, B. Assessment of blast disease resistance in transgenic PRms rice using a GFP-expressing Magnaporthe oryzae strain. *Plant Pathol.* **2009**, *58*, 677–689. [CrossRef]
99. Jones, K.; Kim, D.W.; Park, J.S.; Khang, C.H. Live-cell fluorescence imaging to investigate the dynamics of plant cell death during infection by the rice blast fungus Magnaporthe oryzae. *BMC Plant Biol.* **2016**, *16*, 69. [CrossRef]
100. Qiu, H.; Zhao, X.; Fang, W.; Wu, H.; Abubakar, Y.S.; Lu, G.; Wang, Z.; Zheng, W. Spatiotemporal nature of Fusarium graminearum-wheat coleoptile interactions. *Phytopathol. Res.* **2019**, *1*, 26. [CrossRef]
101. Skiada, V.; Faccio, A.; Kavroulakis, N.; Genre, A.; Bonfante, P.; Papadopoulou, K.K. Colonization of legumes by an endophytic Fusarium solani strain FsK reveals common features to symbionts or pathogens. *Fungal Genet. Biol.* **2019**, *127*, 60–74. [CrossRef]
102. Dong, P.; Tu, X.; Chu, P.Y.; Lü, P.; Zhu, N.; Grierson, D.; Du, B.; Li, P.; Zhong, S. 3D Chromatin Architecture of Large Plant Genomes Determined by Local A/B Compartments. *Mol. Plant* **2017**, *10*, 1497–1509. [CrossRef] [PubMed]
103. Imani, J.; Li, L.; Schäfer, P.; Kogel, K.-H. STARTS—A stable root transformation system for rapid functional analyses of proteins of the monocot model plant barley. *Plant J.* **2011**, *67*, 726–735. [CrossRef]
104. Chabaud, M.; Boisson-Dernier, A.; Zhang, J.; Taylor, C.G.; Yu, O.; Barker, D.G. Agrobacterium rhizogenes-mediated root transformation. In *Medicago Truncatula Handbook*; Mathesius, U., Journet, E.P., Sumner, L.W., Eds.; Noble Research Institute: Ardmore, OK, USA, 2006; ISBN 0-9754303-1-9.
105. Krebs, M.; Held, K.; Binder, A.; Hashimoto, K.; Den Herder, G.; Parniske, M.; Kudla, J.; Schumacher, K. FRET-based genetically encoded sensors allow high-resolution live cell imaging of Ca^{2+} dynamics. *Plant J.* **2012**, *69*, 181–192. [CrossRef] [PubMed]
106. Sieberer, B.J.; Chabaud, M.; Timmers, A.C.; Monin, A.; Fournier, J.; Barker, D.G. A nuclear-targeted cameleon demonstrates intranuclear Ca^{2+} spiking in Medicago truncatula root hairs in response to rhizobial nodulation factors. *Plant Physiol.* **2009**, *151*, 1197–1206. [CrossRef]
107. Moroz, N.; Tanaka, K. FlgII-28 is a major flagellin-derived defense elicitor in potato. *Mol. Plant Microbe Interact.* **2020**, *33*, 247–255. [CrossRef] [PubMed]
108. Zhang, X.-R.; Xu, Y.-P.; Cai, X.-Z. SlCNGC1 and SlCNGC14 suppress Xanthomonas oryzae pv. oryzicola-induced hypersensitive response and non-host resistance in tomato. *Front. Plant Sci.* **2018**, *9*, 285. [CrossRef]
109. Wang, R.; Li, R.; Xu, T.; Li, T. Optimization of the pollen-tube pathway method of plant transformation using the Yellow Cameleon 3.6 calcium sensor in Solanum lycopersicum. *Biologia* **2017**, *72*, 1147–1155. [CrossRef]
110. Huang, W.J.; Liu, H.K.; McCormick, S.; Tang, W.H. Tomato pistil factor STIG1 promotes in vivo pollen tube growth by binding to phosphatidylinositol 3-phosphate and the extracellular domain of the pollen receptor kinase LePRK2. *Plant Cell* **2014**, *26*, 2505–2523. [CrossRef]
111. Hipsch, M.; Lampl, N.; Zelinger, E.; Barda, O.; Rosenwasser, S. Sensing stress responses in potato with whole-plant redox imaging. *bioRxiv* **2020**. [CrossRef]

112. Andrio, E.; Marino, D.; Marmeys, A.; de Segonzac, M.D.; Damiani, I.; Genre, A.; Huguet, S.; Frendo, P.; Puppo, A.; Pauly, N. Hydrogen peroxide-regulated genes in the Medicago truncatula—Sinorhizobium meliloti symbiosis. *New Phytol.* **2013**, *198*, 179–189. [CrossRef]
113. O'Connor, D.L.; Elton, S.; Ticchiarelli, F.; Hsia, M.M.; Vogel, J.P.; Leyser, T. Cross-species functional diversity within the PIN auxin efflux protein family. *Elife* **2017**, *6*, e31804. [CrossRef]
114. Tucker, M.R.; Okada, T.; Johnson, S.D.; Takaiwa, F.; Koltunow, A.M.G. Sporophytic ovule tissues modulate the initiation and progression of apomixis in Hieracium. *J. Exp. Bot.* **2012**, *63*, 3229–3241. [CrossRef]
115. Suzaki, T.; Yano, K.; Ito, M.; Umehara, Y.; Suganuma, N.; Kawaguchi, M. Positive and negative regulation of cortical cell division during root nodule development in Lotus japonicus is accompanied by auxin response. *Development* **2012**, *139*, 3997–4006. [CrossRef]
116. Nadzieja, M.; Kelly, S.; Stougaard, J.; Reid, D. Epidermal auxin biosynthesis facilitates rhizobial infection in Lotus japonicus. *Plant J.* **2018**, *95*, 101–111. [CrossRef]
117. Mir, R.; Aranda, L.Z.; Biaocchi, T.; Luo, A.; Sylvester, A.W.; Rasmussen, C.G. A DII domain-based auxin reporter uncovers low auxin signaling during telophase and early G1. *Plant Physiol.* **2017**, *173*, 863–871. [CrossRef] [PubMed]
118. Gallavotti, A.; Yang, Y.; Schmidt, R.J.; Jackson, D. The relationship between auxin transport and maize branching. *Plant Physiol.* **2008**, *147*, 1913–1923. [CrossRef] [PubMed]
119. Zhou, C.; Han, L.; Hou, C.; Metelli, A.; Qi, L.; Tadege, M.; Mysore, K.S.; Wang, Z.Y. Developmental analysis of a Medicago truncatula smooth leaf margin1 mutant reveals context-dependent effects on compound leaf development. *Plant Cell* **2011**, *23*, 2106–2124. [CrossRef] [PubMed]
120. Herrbach, V.; Remblière, C.; Gough, C.; Bensmihen, S. Lateral root formation and patterning in Medicago truncatula. *J. Plant Physiol.* **2014**, *171*, 301–310. [CrossRef]
121. Chen, Y.; Yordanov, Y.S.; Ma, C.; Strauss, S.; Busov, V.B. DR5 as a reporter system to study auxin response in Populus. *Plant Cell Rep.* **2013**, *32*, 453–463. [CrossRef] [PubMed]
122. Joshi, M.; Fogelman, E.; Belausov, E.; Ginzberg, I. Potato root system development and factors that determine its architecture. *J. Plant Physiol.* **2016**, *205*, 113–123. [CrossRef] [PubMed]
123. Yang, J.; Yuan, Z.; Meng, Q.; Huang, G.; Périn, C.; Bureau, C.; Meunier, A.-C.; Ingouff, M.; Bennett, M.J.; Liang, W.; et al. Dynamic Regulation of Auxin Response during Rice Development Revealed by Newly Established Hormone Biosensor Markers. *Front. Plant Sci.* **2017**, *8*, 256. [CrossRef] [PubMed]
124. Zoulias, N.; Duttke, S.H.C.; Garcês, H.; Spencer, V.; Kim, M. The role of auxin in the pattern formation of the Asteraceae flower head (Capitulum). *Plant Physiol.* **2019**, *179*, 391–401. [CrossRef] [PubMed]
125. Fisher, J.; Gaillard, P.; Fellbaum, C.R.; Subramanian, S.; Smith, S. Quantitative 3D imaging of cell level auxin and cytokinin response ratios in soybean roots and nodules. *Plant Cell Environ.* **2018**, *41*, 2080–2092. [CrossRef]
126. Turner, M.; Nizampatnam, N.R.; Baron, M.; Coppin, S.; Damodaran, S.; Adhikari, S.; Arunachalam, S.P.; Yu, O.; Subramanian, S. Ectopic expression of miR160 results in auxin hypersensitivity, cytokinin hyposensitivity, and inhibition of symbiotic nodule development in soybean. *Plant Physiol.* **2013**, *162*, 2042–2055. [CrossRef] [PubMed]
127. Dubrovsky, J.G.; Sauer, M.; Napsucialy-Mendivil, S.; Ivanchenko, M.G.; Friml, J.; Shishkova, S.; Celenza, J.; Benková, E. Auxin acts as a local morphogenetic trigger to specify lateral root founder cells. *Proc. Natl. Acad. Sci. USA* **2008**, *105*, 8790–8794. [CrossRef] [PubMed]
128. Ben-Gera, H.; Shwartz, I.; Shao, M.-R.R.; Shani, E.; Estelle, M.; Ori, N. ENTIRE and GOBLET promote leaflet development in tomato by modulating auxin response. *Plant J.* **2012**, *70*, 903–915. [CrossRef] [PubMed]
129. Pattison, R.J.; Catalá, C. Evaluating auxin distribution in tomato (Solanum lycopersicum) through an analysis of the PIN and AUX/LAX gene families. *Plant J.* **2012**, *70*, 585–598. [CrossRef]
130. Kirschner, G.K.; Stahl, Y.; Imani, J.; von Korff, M.; Simon, R. Fluorescent reporter lines for auxin and cytokinin signalling in barley (Hordeum vulgare). *PLoS ONE* **2018**, *13*, e0196086. [CrossRef]
131. Reid, D.; Nadzieja, M.; Novák, O.; Heckmann, A.B.; Sandal, N.; Stougaard, J. Cytokinin biosynthesis promotes cortical cell responses during nodule development. *Plant Physiol.* **2017**, *175*, 361–375. [CrossRef] [PubMed]
132. Tao, J.; Sun, H.; Gu, P.; Liang, Z.; Chen, X.; Lou, J.; Xu, G.; Zhang, Y. A sensitive synthetic reporter for visualizing cytokinin signaling output in rice. *Plant Methods* **2017**, *13*, 89. [CrossRef] [PubMed]
133. Farber, M.; Attia, Z.; Weiss, D. Cytokinin activity increases stomatal density and transpiration rate in tomato. *J. Exp. Bot.* **2016**, *67*, 6351–6362. [CrossRef] [PubMed]
134. Jonkman, J.; Brown, C.M.; Wright, G.D.; Anderson, K.I.; North, A.J. Tutorial: Guidance for quantitative confocal microscopy. *Nat. Protoc.* **2020**, *15*, 1585–1611. [CrossRef]
135. Donaldson, L. Autofluorescence in plants. *Molecules* **2020**, *25*, 2393. [CrossRef]
136. Liu, D.Y.T.; Kuhlmey, B.T.; Smith, P.M.C.; Day, D.A.; Faulkner, C.R.; Overall, R.L. Reflection across plant cell boundaries in confocal laser scanning microscopy. *J. Microsc.* **2008**, *231*, 349–357. [CrossRef]
137. De Col, V.; Fuchs, P.; Nietzel, T.; Elsässer, M.; Voon, C.P.; Candeo, A.; Seeliger, I.; Fricker, M.D.; Grefen, C.; Møller, I.M.; et al. ATP sensing in living plant cells reveals tissue gradients and stress dynamics of energy physiology. *Elife* **2017**, *6*, e26770. [CrossRef] [PubMed]

138. Kato, H.; Onai, K.; Abe, A.; Shimizu, M.; Takagi, H.; Tateda, C.; Utsushi, H.; Singkarabanit-Ogawa, S.; Kitakura, S.; Ono, E.; et al. Lumi-Map, a real-time luciferase bioluminescence screen of mutants combined with MutMap, reveals Arabidopsis genes involved in PAMP-triggered immunity. *Mol. Plant Microbe Interact.* **2020**, *33*, 1366–1380. [CrossRef]
139. Vaz Martins, T.; Livina, V.N. What drives symbiotic calcium signalling in legumes? Insights and challenges of imaging. *Int. J. Mol. Sci.* **2019**, *20*, 2245. [CrossRef] [PubMed]
140. Liu, W.; Mazarei, M.; Rudis, M.R.; Fethe, M.H.; Stewart, C.N. Rapid in vivo analysis of synthetic promoters for plant pathogen phytosensing. *BMC Biotechnol.* **2011**, *11*, 108. [CrossRef]
141. Shokouhifar, F.; Bahrabadi, M.; Bagheri, A.; Mamarabadi, M. Transient expression analysis of synthetic promoters containing F and D cis-acting elements in response to Ascochyta rabiei and two plant defense hormones. *AMB Express* **2019**, *9*, 195. [CrossRef] [PubMed]
142. Peyret, H.; Brown, J.K.M.; Lomonossoff, G.P. Improving plant transient expression through the rational design of synthetic 5′ and 3′ untranslated regions. *Plant Methods* **2019**, *15*, 108. [CrossRef]
143. Matsui, T.; Sawada, K.; Takita, E.; Kato, K. Compatibility of translational enhancers with various plant species. *Plant Biotechnol.* **2015**, *32*, 309–316. [CrossRef]
144. Persad, R.; Reuter, D.N.; Dice, L.T.; Nguyen, M.A.; Rigoulot, S.B.; Layton, J.S.; Schmid, M.J.; Poindexter, M.R.; Occhialini, A.; Stewart, C.N.; et al. The Q-System as a synthetic transcriptional regulator in plants. *Front. Plant Sci.* **2020**, *11*, 245. [CrossRef] [PubMed]
145. Stoddard, A.; Rolland, V. I see the light! Fluorescent proteins suitable for cell wall/apoplast targeting in Nicotiana benthamiana leaves. *Plant Direct* **2019**, *3*, e00112. [CrossRef] [PubMed]
146. Shokhina, A.G.; Kostyuk, A.I.; Ermakova, Y.G.; Panova, A.S.; Staroverov, D.B.; Egorov, E.S.; Baranov, M.S.; van Belle, G.J.; Katschinski, D.M.; Belousov, V.V.; et al. Red fluorescent redox-sensitive biosensor Grx1-roCherry. *Redox Biol.* **2019**, *21*, 101071. [CrossRef]
147. Ermakova, Y.G.; Bilan, D.S.; Matlashov, M.E.; Mishina, N.M.; Markvicheva, K.N.; Subach, O.M.; Subach, F.V.; Bogeski, I.; Hoth, M.; Enikolopov, G.; et al. Red fluorescent genetically encoded indicator for intracellular hydrogen peroxide. *Nat. Commun.* **2014**, *5*, 5222. [CrossRef] [PubMed]
148. De Paepe, B.; Maertens, J.; Vanholme, B.; De Mey, M. Chimeric LysR-type transcriptional biosensors for customizing ligand specificity profiles toward flavonoids. *ACS Synth. Biol.* **2019**, *8*, 318–331. [CrossRef]
149. Raman, V.K.; Aggarwal, D.; Rao, R.S.; Sreevathsa, R.; Singh, A.; Abdin, M.; Mohapatra, T.; Pattanayak, D. Rapid and efficient Agrobacterium mediated transformation of early scutellum derived calli of indica rice. *Indian J. Exp. Biol.* **2018**, *56*, 20–28.
150. Mankin, S.L.; Allen, G.C.; Thompson, W.F. Introduction of a plant intron into the luciferase gene of Photinus pyralis. *Plant Mol. Biol. Rep.* **1997**, *15*, 186–196. [CrossRef]
151. Laxa, M. Intron-mediated enhancement: A tool for heterologous gene expression in plants? *Front. Plant Sci.* **2017**, *7*, 1977. [CrossRef] [PubMed]
152. Machado, D.; Costa, R.S.; Rocha, M.; Ferreira, E.C.; Tidor, B.; Rocha, I. Modeling formalisms in systems biology. *AMB Express* **2011**, *1*, 1–14. [CrossRef]
153. Mithöfer, A.; Mazars, C. Aequorin-based measurements of intracellular Ca^{2+}-signatures in plant cells. *Biol. Proc. Online* **2002**, *4*, 105–118. [CrossRef] [PubMed]
154. Jiang, P.; Zhang, K.; Ding, Z.; He, Q.; Li, W.; Zhu, S.; Cheng, W.; Zhang, K.; Li, K. Characterization of a strong and constitutive promoter from the Arabidopsis serine carboxypeptidase-like gene AtSCPL30 as a potential tool for crop transgenic breeding. *BMC Biotechnol.* **2018**, *18*, 59. [CrossRef] [PubMed]
155. Cai, Y.-M.; Kallam, K.; Tidd, H.; Gendarini, G.; Salzman, A.; Patron, N.J. Rational design of minimal synthetic promoters for plants. *Nucleic Acids Res.* **2020**, *48*, 11845–11856. [CrossRef]
156. Liu, Z.; Chen, O.; Wall, J.B.J.; Zheng, M.; Zhou, Y.; Wang, L.; Ruth Vaseghi, H.; Qian, L.; Liu, J. Systematic comparison of 2A peptides for cloning multi-genes in a polycistronic vector. *Sci. Rep.* **2017**, *7*, 2193. [CrossRef] [PubMed]
157. François, I.E.J.A.; Van Hemelrijck, W.; Aerts, A.M.; Wouters, P.F.J.; Proost, P.; Broekaert, W.F.; Cammue, B.P.A. Processing in Arabidopsis thaliana of a heterologous polyprotein resulting in differential targeting of the individual plant defensins. *Plant Sci.* **2004**, *166*, 113–121. [CrossRef]
158. Sun, H.; Zhou, N.; Wang, H.; Huang, D.; Lang, Z. Processing and targeting of proteins derived from polyprotein with 2A and LP4/2A as peptide linkers in a maize expression system. *PLoS ONE* **2017**, *12*, e0174804. [CrossRef]
159. Zhang, B.; Rapolu, M.; Kumar, S.; Gupta, M.; Liang, Z.; Han, Z.; Williams, P.; Su, W.W. Coordinated protein co-expression in plants by harnessing the synergy between an intein and a viral 2A peptide. *Plant Biotechnol. J.* **2017**, *15*, 718–728. [CrossRef]
160. Liu, T.-Y.; Chou, W.-C.; Chen, W.-Y.; Chu, C.-Y.; Dai, C.-Y.; Wu, P.-Y. Detection of membrane protein-protein interaction in planta based on dual-intein-coupled tripartite split-GFP association. *Plant J.* **2018**, *94*, 426–438. [CrossRef] [PubMed]
161. Mitiouchkina, T.; Mishin, A.S.; Somermeyer, L.G.; Markina, N.M.; Chepurnyh, T.V.; Guglya, E.B.; Karataeva, T.A.; Palkina, K.A.; Shakhova, E.S.; Fakhranurova, L.I.; et al. Plants with genetically encoded autoluminescence. *Nat. Biotechnol.* **2020**, *38*, 944–946. [CrossRef]
162. Khakhar, A.; Starker, C.G.; Chamness, J.C.; Lee, N.; Stokke, S.; Wang, C.; Swanson, R.; Rizvi, F.; Imaizumi, T.; Voytas, D.F. Building customizable auto-luminescent luciferase-based reporters in plants. *Elife* **2020**, *9*, e52786. [CrossRef]
163. He, Y.; Zhang, T.; Sun, H.; Zhan, H.; Zhao, Y. A reporter for noninvasively monitoring gene expression and plant transformation. *Hortic. Res.* **2020**, *7*, 152. [CrossRef] [PubMed]

2.2 Jasmonic Acid and Salicylic Acid Interact to Determine Spatial Regulation of Gene Expression Responses in Potato Leaf to Herbivory by Colorado Potato Beetle and Mechanical Wounding

Valentina Levak, Tjaša Mahkovec Povalej, Karmen Pogačar, Katja Stare, Maja Zagorščak, Tim Hawkins, Joanne Robson, David Dobnik, Tjaša Lukan, Kristina Gruden

Plant and Cell Physiology, 2025, 66, 1878–1890. DOI: 10.1093/pcp/pcaf120

The study examines the spatial dynamics of JA and SA signalling in potato (*S. tuberosum* L.) leaves in response to herbivory by the CPB and to mechanical wounding. Using genetically encoded biosensors, the authors found that JA-dependent gene expression was absent in cells immediately adjacent to the wound, while JA signalling spread outward from the wound site. In contrast, SA accumulated near the wound, and in SA-depleted plants, JA signalling spread uniformly, indicating that SA locally suppresses JA responses. These results reveal a distinct spatiotemporal crosstalk between SA and JA that shapes wound responses in potato, extending concepts previously established in pathogen-plant interactions to herbivory and mechanical damage. By illustrating how these hormones interact to regulate gene expression in a spatially precise manner, the study provides new insights into the local regulation of plant immune responses and advances our understanding of the complex mechanisms underlying plant defence.

The paper was selected as Editor's Choice.

The PhD candidate is the first author of the paper. She contributed to experimental design, execution of most experiments, reviewed the relevant literature, prepared all figures and wrote the first draft.

PCP
PLANT & CELL PHYSIOLOGY

Jasmonic acid and salicylic acid interact to determine spatial regulation of gene expression responses in potato leaf to herbivory by Colorado potato beetle and mechanical wounding

Valentina Levak[1,2,*], Tjaša Mahkovec Povalej[1], Karmen Pogačar[1,2], Katja Stare[1], Maja Zagorščak[1], Tim Hawkins[3], Joanne Robson[3], David Dobnik[1], Tjaša Lukan[1,†] and Kristina Gruden[1,†,*]

[1]Department of Biotechnology and Systems Biology, National Institute of Slovenia, Večna pot 121, 1000 Ljubljana, Slovenia, [2]Jožef Stefan International Postgraduate School, Jamova 39, 1000 Ljubljana, Slovenia, [3]Department of Biosciences, Durham University, South Rd, Durham DH1 3LE, UK

*Corresponding authors: Valentina Levak, E-mail, valentina.levak@nib.si; Kristina Gruden, E-mail, kristina.gruden@nib.si
†Shared last authorship.

Received 19 June 2025; Accepted 22 September 2025

Regular Paper

Downloaded from https://academic.oup.com/pcp/advance-article/doi/10.1093/pcp/pcaf120/8262811 by National and University Library Ljubljana user on 11 December 2025

Abstract

We investigated the spatial dynamics of potato (*Solanum tuberosum*) responses to herbivory and mechanical wounding. We first followed the spatiotemporal response of jasmonic acid (JA) signaling, known to be involved in the response. We generated two potato sensor lines: a JAZ degradation sensor and a downstream multicystatin (MC) transcriptional reporter. Both sensors revealed concentric, locally restricted responses on wounded leaves. Notably, JA-dependent gene expression was absent in cells immediately adjacent to the wound, whereas JAZ degradation spread continuously outward from the wound site. This pattern occurred after both herbivore attack and mechanical injury by the needle. To probe the mechanism, a salicylic acid (SA) reporter showed SA accumulation near the wound. Introducing the MC reporter into SA-depleted *NahG* plants produced a uniform spread of MC expression, confirming that SA attenuates the JA response in proximal cells. Together, these results show that a locally distinct, spatiotemporal SA–JA crosstalk shapes wound responses in potato, extending principles known from pathogen–plant interactions to herbivory and mechanical damage.

Keywords: Colorado potato beetle • herbivore • hormonal crosstalk • jasmonic acid • potato • salicylic acid • wounding

Introduction

Plants rely on two interconnected arms of innate immunity to perceive and respond to pathogen attack (Jones et al. 2024). Pattern-triggered immunity uses cell-surface pattern-recognition receptors to detect microbe-associated molecular patterns, host-derived damage-associated molecular patterns, and herbivore-associated molecular patterns (Hou et al. 2019). Effector-triggered immunity (ETI) employs disease-resistance (R) proteins to recognize effector molecules delivered by pathogens and herbivores (Nguyen et al. 2021). Invasion by necrotrophic pathogens and herbivore infestation typically causes wounding and initiates cascades of biochemical and cellular signals, including calcium fluxes, phytohormone signaling, and reactive oxygen species production.

Jasmonic acid (JA) is a central phytohormone in wound responses. Its biosynthesis begins within minutes via 13-lipoxygenase (13-LOX)-mediated oxidation of plastid fatty acids and does not require *de novo* transcription or translation (Chung et al. 2008, Glauser et al. 2008, Chauvin et al. 2013, Kimberlin et al. 2022). Subsequent steps yield 12-oxo-phytodienoic acid, which is transported to peroxisomes and converted to JA. JA then enters the cytosol, where JAR1 conjugates it to isoleucine (JA–Ile), the most bioactive JA derivative. JA–Ile promotes assembly of the SCF^{COI1} complex with JAZ transcriptional repressors, triggering proteasomal degradation of JAZ within minutes and releasing transcriptional activators such as MYC2/3/4 (Chini et al. 2007, Fernández-Calvo et al. 2011, Larrieu et al. 2015). These can then drive JA-dependent gene expression. JA-dependent transcription is temporally tuned. In *Arabidopsis*, transcripts encoding JA biosynthesis regulators (e.g. MYC2, ORA47, MYB75, JAZs) rise about 15 min after JA treatment, followed by downregulation of primary metabolism and salicylic acid (SA)-pathway regulators (e.g. WRKY transcription factors) about 30 min after, and upregulation of JA biosynthetic genes and defense proteins (e.g. LOX, AOC, AOS, JAR1, VSP1/2) by 1 h after JA treatment (Koo et al. 2009, Hickman et al. 2017).

Plant defense—including responses to wounding—is coordinated not only by JA but also by other signaling pathways that can be activated independently and intersect at distinct

© The Author(s) 2025. Published by Oxford University Press on behalf of the Japanese Society of Plant Physiologists.
This is an Open Access article distributed under the terms of the Creative Commons Attribution-NonCommercial License (https://creativecommons.org/licenses/by-nc/4.0/), which permits non-commercial re-use, distribution, and reproduction in any medium, provided the original work is properly cited. For commercial re-use, please contact reprints@oup.com for reprints and translation rights for reprints. All other permissions can be obtained through our RightsLink service via the Permissions link on the article page on our site—for further information please contact journals.permissions@oup.com.

stages (Ramšak et al. 2018, Vega-Muñoz et al. 2020, Xu et al. 2024). Such orchestration constrains runaway responses that could cause extensive tissue damage, including systemic cell death or hypersensitivity to wounding (Cui et al. 2013, 2019, Zhang et al. 2019). Although defense is often framed as SA-dependent against biotrophs versus JA-dependent against necrotrophs and herbivores, accumulating evidence shows that processes once considered pathway-specific frequently require integrated hormonal networks. For example, JA can drive induced resistance to bacterial infection—previously viewed as primarily SA dependent (Gaikwad et al. 2023). The exact mechanisms of how the defense signaling network functions are, however, currently not well understood. Crosstalk can manifest in spatial separation of processes, as seen during ETI in *Arabidopsis* infected with *Pseudomonas syringae* DC3000 (AvrRpt2) (Betsuyaku et al. 2018). By contrast, the contribution of SA to wound responses is still unclear, aside from a single report noting a transient SA increase after wounding (Ogawa et al. 2010).

Cultivated potato (*Solanum tuberosum* L.) is the world's most important dicot crop, with annual production of about 370 million tons (FAO statistical database, fao.org/faostat/en/). The Colorado potato beetle (CPB), *Leptinotarsa decemlineata*, is a major global pest of potato, driving substantial economic losses; without effective protection, yield losses to CPB and other insect pests can reach up to 70% (Oerke 2006). As a chewing herbivore, CPB causes intense defoliation, eliciting defenses that overlap with mechanically induced responses largely mediated by JA, though responses to herbivory and mechanical wounding are not identical (Walling 2000). In solanaceous plants, canonical markers of wounding and JA signaling include proteinase inhibitors (Graham et al. 1986, Farmer and Ryan 1990, Farmer et al. 1992), which can reduce foliar nutritional value for herbivores (Martinez et al. 2016, Divekar et al. 2022). CPB, however, has evolved countermeasures, such as expressing proteolytic or inhibitor-insensitive digestive proteinases (Bouchard et al. 2003, Gruden et al. 2003, 2004) and deploying oral secretions containing SA-inducible microbiota that modulate host signaling (Chung et al. 2013, 2017). CPB can also suppress the emission of defense-inducible volatiles (Abdala-Roberts et al. 2022), a hallmark of herbivory responses in other plant–pest systems (Grandi et al. 2024).

Understanding the mechanisms that confer crop resistance to biotic and abiotic stress is essential for sustainable, environmentally friendly protection. Although *Arabidopsis* provides powerful mechanistic insight, its genes or their functions do not always translate directly to potato or other crops. For example, *Arabidopsis* JA-response markers *AtVSP2* and *AtPDF1.2* show different expression profiles or do not have an ortholog in potato, respectively (Wiesel et al. 2015).

Here, we use genetically encoded sensors of the JA pathway in potato to resolve the spatiotemporal dynamics of responses to herbivory and wounding. JA–Ile accumulation was monitored with the Jas9 degradation sensor (Larrieu et al. 2015), and JA-dependent gene expression was tracked using a newly engineered reporter in which the potato multicystatin (*MC*) promoter drives a fluorescent protein expression. Both sensors revealed a locally confined wound response; however, their activities diverged in cells closest to the wound. Specifically, JA-dependent gene expression was suppressed in these proximal cells despite detectable JA–Ile. This pattern was not dependent on insect saliva, as it also occurred after needle wounding. We next pursued the underlying mechanisms of the detected phenomena and showed that it is SA-dependent. Together, these findings indicate that spatially patterned SA–JA crosstalk, previously characterized during bacterial and fungal infections (Betsuyaku et al. 2018, Ghareeb et al. 2020, Liu et al. 2023, Calabria et al. 2025), also governs the spatial dynamics of plant responses to herbivory and mechanical injury.

Results

Promoter of potato MC is a reliable transcriptional reporter of JA-signaling in potato leaves

To build a JA-responsive transcriptional reporter in potato, we selected the *MC* gene (Sotub06g027390/PGSC0003DMG400005950/Soltu.DM.06G028940), previously shown to be induced by CPB feeding and methyl jasmonate (MeJA) (Petek et al. 2014, Wiesel et al. 2015). Canonical JA regulation was validated using *coi1* mutants, in which *MC* was not induced upon CPB larvae feeding (Petek et al. 2014). *MC* encodes a cysteine proteinase inhibitor with multiple cystatin domains; its orthologues are present in other solanaceous species but absent from *Arabidopsis* (PLAZA database, bioinformatics.psb.ugent.be/plaza; Green et al. 2014). Within the 1-kb *MC* promoter, we identified multiple JA-associated cis-elements, including MYC-recognition sites, as well as motifs linked to SA (e.g. TGA1A and WRKY binding sites), Ca^{2+}, and ethylene signaling (Supplementary Data S1; Supplementary Fig. S1; Supplementary Table S1). We generated two independent *pMC::EYFP* transgenic lines in potato cv. Désirée (lines 14 and 18) that displayed normal growth and robust MeJA inducibility by qPCR and confocal microscopy (Fig. 1a; Supplementary Fig. S2a; 10.5281/zenodo.16875336), and used these lines for subsequent experiments.

pMC::EYFP reporter reveals unexpected spatiotemporal gene expression response after herbivore feeding

After confirming MeJA inducibility, we exposed *pMC::EYFP* reporter lines to herbivore, CPB larvae. We observed that larvae exhibited two distinguishable behaviors on leaves (Ruan et al. 2020): the first we termed probing, characterized by light wounding with lateral mouthparts (maxillary palps and mandibles) while moving across the surface, and the second we termed biting, larva being located and biting the leaf with medial mouthparts (labrum) (Fig. 1b; 10.5281/zenodo.16875336). In both cases, *pMC::EYFP* signal formed a locally confined, concentric zone around wounds. Notably, *MC* expression was not continuous from the wound edge outward; instead, cells immediately adjacent to the wound showed a

Downloaded from https://academic.oup.com/pcp/advance-article/doi/10.1093/pcp/pcaf120/8262811 by National and University Library Ljubljana user on 11 December 2025

Downloaded from https://academic.oup.com/pcp/advance-article/doi/10.1093/pcp/pcaf120/8262811 by National and University Library Ljubljana user on 11 December 2025

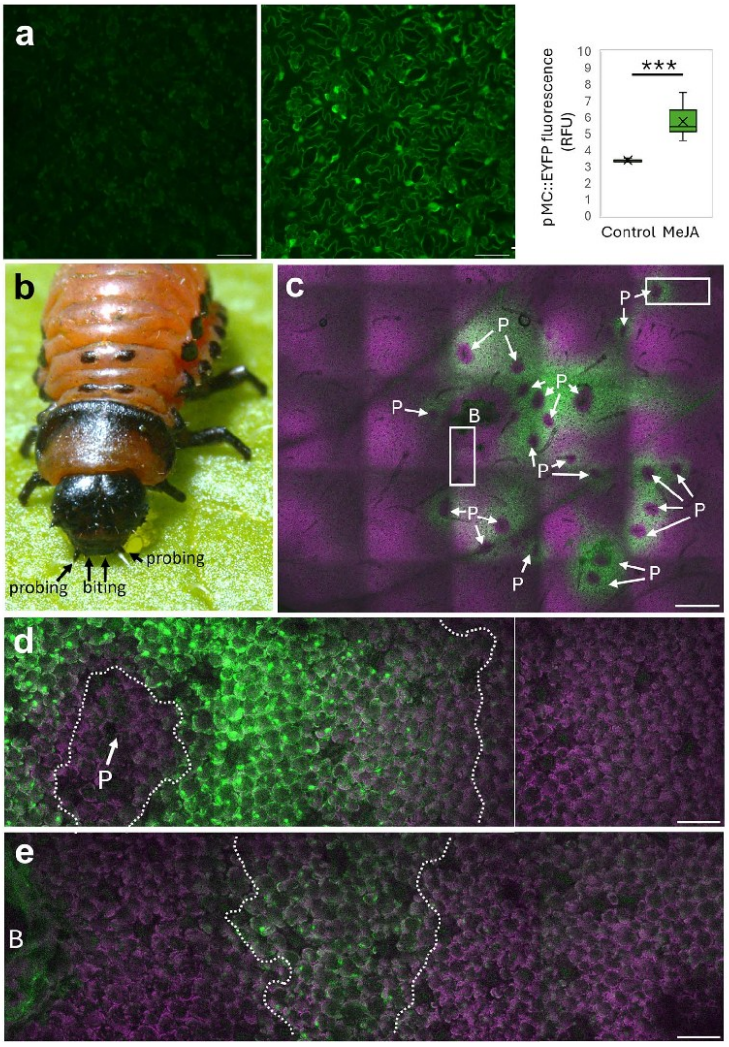


Figure 1. Transcriptional response of *MC* gene, downstream target of JA-signaling to larval feeding, is attenuated in the cells close to the wound. (a) *pMC::EYFP* biosensor fluorescence in leaves of stable transformants of potato cv. Désirée (line 14) after 24 h mock (left) or MeJA treatment (middle). *pMC::EYFP* fluorescence was measured in a Z-stack spanning the epidermis and mesophyll. Right: mean fluorescence intensity was quantified in images of samples from 2–3 leaves of 3 plants per group. Student's *t*-test was used to assess the significant difference between mock and MeJA-treated plants ($P < .001$). JA-dependent induction of *MC* gene expression was also shown by using *coi1*-deficient plants (Petek et al. 2014). Scale bar, 50 µm. (b) CPB larva feeding on a potato leaf. The arrows indicate larva's mouthparts used in distinct feeding behaviors, probing (maxillary palpi and mandibles) and biting (labrum). (c) CPB-fed region on the leaf of *pMC::EYFP* potato sensor plant 20 h after feeding. Green: EYFP fluorescence, purple: chlorophyll fluorescence. B: bite wound, P: wounds made during probing. Scale bar, 1 mm. Close-ups of response to one of each wound are enlarged in (d) after probing, P, and (e) near the bite wound, B. The border of the observable response is shown with dotted lines. Scale bar, 100 µm. Raw images for all experiments are available at Zenodo: https://doi.org/10.5281/zenodo.16875336.

no-MC-response zone lacking *pMC::EYFP* signal. Probing and biting elicited distinct patterns: the no-MC-response zone was broader and more variable in width after biting than after probing (Fig. 1c–e; Supplementary Fig. S2b and c; 10.5281/zenodo.16875336). The same response was observed in an independent transgenic line (Supplementary Fig. S2b and c; 10.5281/zenodo.16875336).

Mechanical wounding elicits similar spatiotemporal response as herbivore feeding

To track *in vivo* dynamics, we imaged nondetached leaves on soil-grown plants for 24 h after CPB feeding and quantified *pMC::EYFP* activity (Fig. 2a; Supplementary Movies S1 and S2; 10.5281/zenodo.16875336). This analysis resolved three wound-proximal regions of interest—ROI A, B, and C—contrasted with a distal control (ROI Ctr) (Fig. 2b). ROIs were defined at the first appearance of *pMC::EYFP* signal. ROI A—a band immediately surrounding the wound—lacked a detectable reporter signal. The width of ROI A was greater after biting (0.3–0.8 mm) than after probing (0.15–0.5 mm). ROI B (0.2–1.3 mm wide), encircling ROI A, showed the highest induction. In ROI C, *pMC::EYFP* signal increased with a slight delay compared to ROI B and plateaued before ROI B, indicating that the response is locally confined once established (Fig. 2b–d; 10.5281/zenodo.16875336). ROI Ctr displayed only background reporter activity over time. These features were reproducible across experimental repeats.

Because herbivore oral secretions can repress JA-dependent outputs by inducing SA signaling (e.g. via saliva- or regurgitant-associated microbiota; Weech et al. 2008, Chung et al. 2013), we also tested mechanical wounding performed by needle punctures to exclude saliva effects. Mechanical wounding produced the same *pMC::EYFP* pattern as CPB feeding across all four ROIs (Fig. 2c and d; Supplementary Movie S3; Supplementary Fig. S3; 10.5281/zenodo.16875336). Replicated trials yielded comparable results.

Jas9-Venus-N7 sensor confirms that JA-Ile is produced confluently from the wound edge

Next, we designed experiments to decipher the mechanistic basis for the lack of response in the region immediately adjacent to both herbivore and mechanical wounding. We first tested if spatial response was the same upstream the JA signaling pathway. We introduced the JA–Ile biosensor Jas9-Venus-N7 (Larrieu et al. 2015) into potato plants. This CaMV 35S-driven sensor tracks proteasomal degradation of JAZ repressors of MYC transcription factors that regulate targets such as *MC* (Supplementary Fig. S1; Supplementary Table S1). Jas9-Venus-N7 signal was detectable in mesophyll, epidermis, and stomata. However, the signal was mostly below the limit of detection in the mesophyll and epidermal cells compared to the stomata at low magnification, which was selected for imaging to avoid photodamage. Hence, only stomata nuclei were used for quantitative analysis (Fig. 3a; Supplementary Figs S4–S6; Supplementary Table S2), while the signal in the mesophyll was used to qualitatively validate that spatiotemporal pattern of the JA-Ile abundance is comparable between stomata and mesophyll (see Supplementary Figs S4–S6, also 10.5281/zenodo.16875336: nuclei in palisade tissue with Jas9-Venus-N7 fluorescence are marked with arrows). We imaged at defined times after CPB feeding or single-needle puncture across ROIs matching those used for *pMC::EYFP* (A–C). In both wounding types, Jas9-Venus-N7 was degraded in a continuous front extending outward from the wound, indicating confluent accumulation of JA–Ile (Fig. 3a; Supplementary Figs S4–S6; 10.5281/zenodo.16875336). The radial distance over which JA–Ile increased (sensor's signal decreased) mirrored the *MC*-reporter domain, but—critically—there was no attenuation near the wound (ROI A). Thus, JA–Ile is present in the proximal zone where *MC* transcription is not induced. The *MC* reporter lagged the Jas9-Venus-N7 response by approximately 6 h. An *in silico* JA-pathway model recapitulated a $\geq$2 h delay, arising primarily from fluorescent protein folding/maturation kinetics and translation rates (Fig. 3b and c). Together, these data place the mechanism underlying the proximal no-MC-response downstream of JAZ derepression.

SA accumulation at the wound edge spatially tunes JA-dependent gene expression

Given the known antagonism between JA and SA, we asked whether SA contributes to the proximal suppression of *MC* expression despite the presence of JA–Ile. Using the bacterial SA biosensor *Acinetobacter* sp. ADPWH_*lux* (Huang et al. 2006, Defraia et al. 2008), we quantified SA in nontransgenic leaves microdissected into 0.7-mm (piece A) and 1-mm (pieces B–C and Ctr) sectors corresponding to *pMC::EYFP* ROIs A–C and the distal control (Ctr). Four hours after wounding, SA was highest in piece A at the wound edge and declined with increasing distance (Fig. 3d), consistent with attenuation of JA-dependent transcription in proximal cells.

To test whether SA accumulation causes the proximal no-MC–response zone, we inserted the *pMC::EYFP* reporter into potato plants expressing *NahG*, which disables the accumulation of SA (Halim et al. 2007). Although *NahG* converts SA to catechol and can elevate H_2O_2, prior work showed no shift in chloroplast redox state in *NahG* potato (Lukan et al. 2023), indicating that global homeostasis is not strongly perturbed. We screened transgenic lines for MeJA inducibility (Supplementary Fig. S7; 10.5281/zenodo.16875336) and selected four with normal phenotypes and robust *pMC::EYFP* expression across cell types for spatiotemporal analysis after mechanical wounding.

In *NahG* plants, *pMC::EYFP* was also induced within ROI A, and its onset was comparable in timing to ROI B (Fig. 3e; Supplementary Fig. S8; Supplementary Movies S4 and S5), unlike the nontransgenic background (Supplementary Fig. S9; Supplementary Movie S6; 10.5281/zenodo.16875336). Additionally, to acutely manipulate signaling, we treated leaves with the SA analog INA (2,6-dichloroisonicotinic acid) or JA immediately, 15 min, or 1 h before wounding. INA suppressed *pMC::EYFP* across all ROIs, whereas JA induced and accelerated

Downloaded from https://academic.oup.com/pcp/advance-article/doi/10.1093/pcp/pcaf120/8262811 by National and University Library Ljubljana user on 11 December 2025

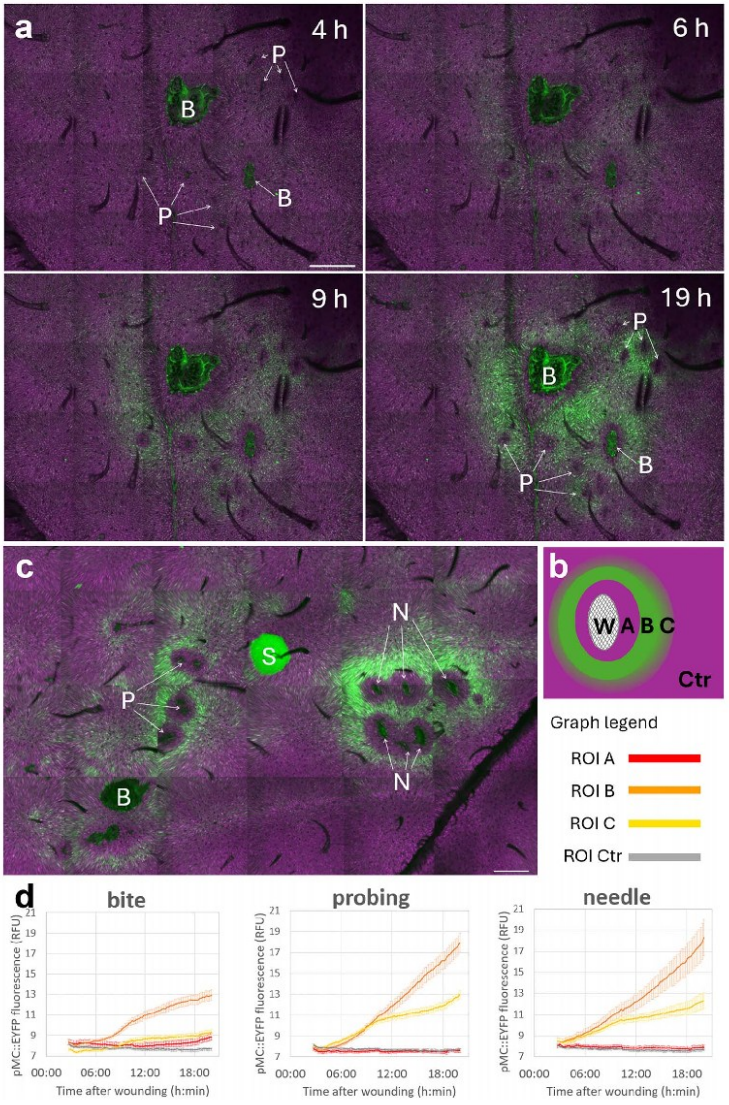


Figure 2. Dynamics of *pMC::EYFP* gene expression after different wounding types is spatially determined. (a) Time series illustrating four representative time points of *pMC::EYFP* induction following CPB feeding. Bite wounds (B) and probing attempts (P) are indicated. Scale bar, 0.5 mm. Transgenic line 18 was used in the experiment. The chlorophyll channel is shown in purple while the EYFP channel is shown in green. (b) Schematic of distinct regions of interest (ROIs) A–C and distal background (Ctr), within which *pMC::EYFP* signal was quantified. (c) *pMC::EYFP* response to needle wound beside CPB woundings 20 h after treatment. Overlay of chlorophyll (purple) and EYFP (green) is shown. Scale bar, 1 mm. (d) Kinetics of *pMC::EYFP* response to bite, probing, and needle wound in different ROIs. ROI A (cells closest to the wound) in red, ROI B (cells with the highest *pMC::EYFP* signal) in orange, ROI C (cells outwards of ROI B) in yellow, ROI Ctr (cells further away without an increase of *pMC::EYFP* signal) in gray. B: bite wound, P: probing wounds, N: needle wounds, S: CPB saliva autofluorescence in EYFP channel. Average response in the distinctive ROIs with SE is shown. All raw images are available at Zenodo: https://doi.org/10.5281/zenodo.16875336.

Downloaded from https://academic.oup.com/pcp/advance-article/doi/10.1093/pcp/pcaf120/8262811 by National and University Library Ljubljana user on 11 December 2025

PCP PLANT & CELL PHYSIOLOGY Levak et al.

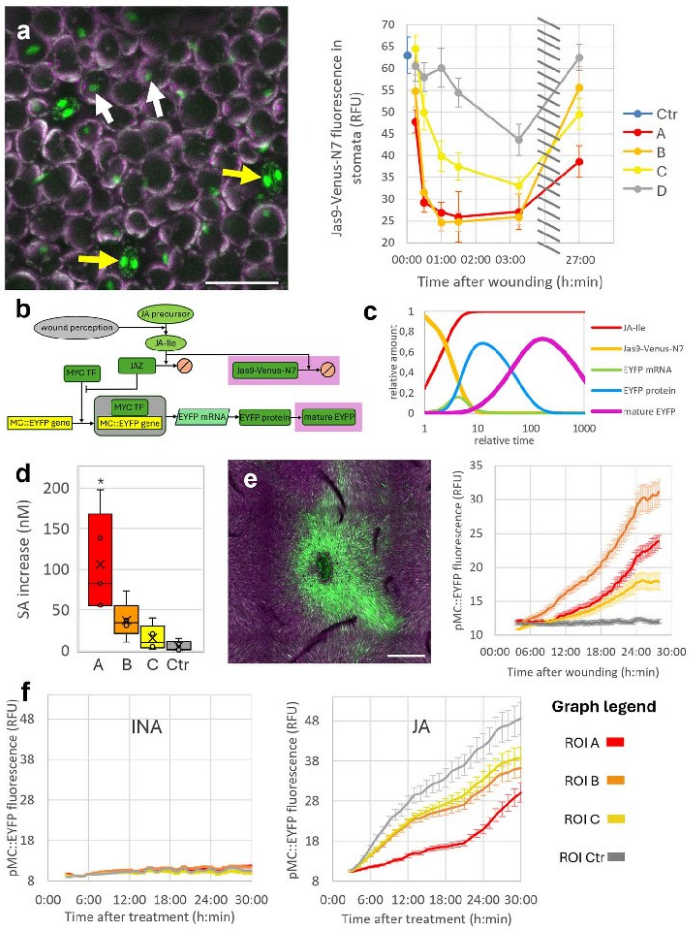


Figure 3. Spatial pattern of *MC*-response is SA-dependent. (a) Response of JA-Ile sensor to CPB wounding. Left: detection of Jas9-Venus-N7 signal before treatment (transgenic line 1). Overlay of Venus signal (green) and chlorophyll autofluorescence (purple). White arrow: Jas9-Venus-N7 sensor's signal in the mesophyll cells, yellow arrows: Jas9-Venus-N7 sensor's signal in the stomata. Scale bar, 100 μm. Results of an experiment performed in an independent transgenic line are shown in Supplementary Fig. S6. Right: Dynamics of JA-Ile sensor response to wounding according to the distance from the wound (ROIs of increasing distance from the wound, A–D). Average response in the ROIs with SE is shown. (B–C) Mechanistic model of JA signaling. (b) Schematic of the model capturing the response of Jas9-Venus-N7 and *pMC::EYFP* sensors in JA signaling cascade. (c) Simulated dynamics showing the expected delay between Jas9-Venus-N7 loss and *pMC::EYFP* accumulation due to fluorescent protein maturation. (d) Measurement of SA accumulation in leaf pieces with increasing distance from the needle wound that corresponds to ROIs A–C of *pMC::EYFP* (A—the closest to the wound, Ctr—distant part of the same leaf). Measurement was performed with Acinetobacter ADPWH_*lux* SA sensor's luminescence on five pooled pieces of the same size, gathered from five plants. Luminescence was analyzed for pairs of ROIs with Student's *t*-test (two-tailed distribution, unequal variance). Only ROI A showed a significant difference from all other ROIs ($P < 0.05$). (e) *pMC::EYFP* response to mechanical wounding in *NahG* plants. Left: *pMC::EYFP* activity 24 h after wounding with a needle (overlay of chlorophyll channel in purple and EYFP channel in green). Scale bar, 1 mm. Right: Dynamics of *pMC::EYFP* sensor response to wounding in *NahG* plants according to the distance from the wound: ROI A (cells closest to the wound) in red, ROI B (next to ROI A) in orange, ROI C (cells outwards of ROI B) in yellow, ROI Ctr (cells further away without increase of *pMC::EYFP* signal) in gray, legend is below the graph. Average response in the distinctive ROIs with SE is shown. (f) In nontransgenic background (without *NahG* transgene), 1 mM INA repressed *pMC::EYFP* induction in all ROIs upon wounding, while 1 mM JA caused the *pMC::EYFP* induction in ROI A. Average response in the distinctive ROIs with SE is shown. Legend of *pMC::EYFP* response in distinct regions is on the right side of the graphs. All raw images are available at Zenodo: https://doi.org/10.5281/zenodo.16875336.

Downloaded from https://academic.oup.com/pcp/advance-article/doi/10.1093/pcp/pcaf120/8262811 by National and University Library Ljubljana user on 11 December 2025

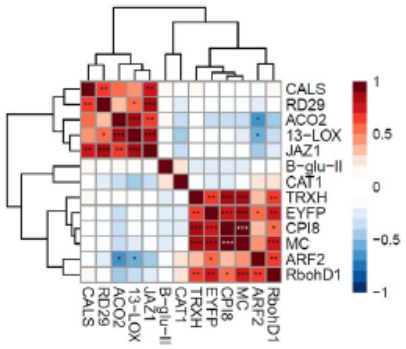


Figure 4. Redox-related genes show a positive correlation with *MC* gene activity. Hierarchical clustering heatmap of Pearson correlation coefficients of marker genes at 1 and 4 h after mechanical (needle) or herbivore bite wounding across different positions (ROIs A-C that correspond to ROIs A–C of *pMC::EYFP* signal). Correlations were adjusted for multiple testing using Benjamini–Hochberg correction and clustered using Euclidean distance. Asterisks denote significance (*$P < 0.05$, **$P < 0.01$, ***$P < 0.001$).

reporter activation in ROI A (Fig. 3f; Supplementary Fig. S10; Supplementary Movies S7–S14; 10.5281/zenodo.16875336). Together, these results demonstrate that local SA signaling—not merely JA availability—governs the proximal attenuation of JA-dependent transcription around wound sites.

ROS-related genes, TRXH and RbohD1, show positive correlation with spatial regulation of MC expression

To probe mechanisms underlying *MC*'s spatiotemporal pattern, we analyzed expression of *MC*, *EYFP*, and immune/signaling genes across regions A–C (matching *pMC::EYFP* ROIs) at 1 h and 4 h after CPB biting or needle wounding. Targets spanned JA signaling (*13-LOX*, *JAZ1*, *CPI8*), ethylene (*ACO2*, *ERF1*, *PTI5*), SA (*PR1b*, *B-glu-2*), auxin (*ARF2*), ABA (*RD29*), and redox pathways (*TRXH*, *CALS*, *RbohD1*, *CAT1*). *ERF1*, *PTI5*, and *PR1b* were largely below quantification limits in these microdissected sections and were excluded from further analysis.

Across remaining genes, *MC* and *EYFP* expression were positively correlated, validating *pMC::EYFP* as a faithful reporter of native *MC* activity. Notably, *TRXH* and *RbohD1* expression correlated with both *EYFP* and *MC* (Fig. 4; Supplementary Table S3), implicating ROS-associated signaling in the proximal wound response. By contrast, SA-marker transcripts showed no significant correlation with *MC* at these time points (Supplementary Table S3).

Discussion

We investigated the spatiotemporal responses of potato to herbivory and mechanical wounding and developed a JA-responsive transcriptional reporter based on the *MC* proteinase inhibitor. In Solanaceae—analogous to *VSP1/2* in Brassicaceae—proteinase inhibitors are canonical markers of JA-dependent gene expression (Ryan 1968, Benedetti et al. 1995, Fujimoto et al. 2011). MC inhibits endogenous papain-like cysteine proteinases (Popovič and Brzin 2007) as well as cysteine proteinases abundant in herbivore guts (Murdock et al. 1987, Orr et al. 1994, Gruden et al. 2003, 2004). We also validated Jas9–Venus–N7 as a sensor of active JA signaling in potato leaves; as in *Arabidopsis*, it is highly sensitive to elevated JA (Larrieu et al. 2015, Förster et al. 2019, Supplementary Figs S4 and S5). The two sensors activated with distinct kinetics: Jas9–Venus–N7 preceded *pMC::EYFP*, which lagged by several hours primarily due to fluorescent protein folding/maturation, as supported by a simple kinetic model (Fig. 3c; Supplementary Data S2). Comparable reporter delays have been observed in *Arabidopsis* time-series imaging, namely *pJAZ10::FP* (Bellandi et al. 2022), *pPR1::FP*, and *VSP1::FP* (Betsuyaku et al. 2018) and *PR1::FP*, *VSP2::FP*, and *pPDF1.2a::FP* (Ghareeb et al. 2020) (where FP stands for fluorescent protein), although this could also depend on other preceding processes.

Both JA-pathway reporters—Jas9–Venus–N7 and *pMC::EYFP*—showed that needle puncture or brief CPB feeding elicits a response confined to a mm-scale zone around the wound, without spreading across the leaf (Supplementary Figs 1 and 2; Supplementary Figs S2 and S3; Supplementary Movies S1–S3). Similar locally restricted, concentric, and confluent signals have been observed in *Arabidopsis* using other genetically encoded sensors, including ROS bursts after mechanical damage (Prasad et al. 2020), Ca^{2+} waves after mechanical or insect wounding (Vincent et al. 2017, Toyota et al. 2018, Bellandi et al. 2022), and Pep1 release (Hander et al. 2019). Consistent with this spatial scale, JA-biosynthetic enzymes and increased oxidized glutathione—both JA-dependent—were enriched within 2.5 mm of distance from a mechanical wound (Gfeller et al. 2011). Notably, Pep1 release was restricted to cells immediately adjacent to the injured cell (Hander et al. 2019). The extent of spread depends on wound intensity: mild wounding produces a strictly local response, as in our assays and the studies above, whereas damage to major veins can trigger systemic signaling (Salvador-Recatalà et al. 2014, Kiep et al. 2015).

We found that wounding alone drives SA accumulation in cells immediately adjacent to the injury (Fig. 3; Supplementary Figs S8 and S9; Supplementary Movies S4 and S5 vs. Supplementary Movie S6). Although spatial antagonism between JA- and SA-dependent transcription has been documented in several biotic interactions (Betsuyaku et al. 2018, Ghareeb et al. 2020, Calabria et al. 2025), it has not, to our knowledge, been shown following wounding *per se*. Our data therefore indicate that ETI is not required to establish spatial JA–SA crosstalk—at least during the first hours after wounding and in potato. Prior non-spatial studies are consistent with this view: *Arabidopsis* exhibits a transient SA increase after toothpick or carborundum wounding (Ogawa et al. 2010, Ang et al. 2024), and *PR1* transcripts accumulate in local and systemic leaves after puncture in wild type but not in *npr1* mutants (Myers et al. 2023).

Downloaded from https://academic.oup.com/pcp/advance-article/doi/10.1093/pcp/pcaf120/8262811 by National and University Library Ljubljana user on 11 December 2025

Herbivores—including CPB—can suppress JA-dependent defenses via saliva or regurgitant that activates SA signaling (McCloud and Baldwin 1997, Weech et al. 2008, Chung et al. 2013, 2017). Because SA antagonizes JA outputs, this shift increases host susceptibility to herbivory (Consales et al. 2012, Wang et al. 2017). SA accumulation may also fortify wound sites against microbial ingress, offering a rationale for the SA-dependent inhibition of *pMC::EYFP* we observed even after sterile needle puncture without larval secretions. Notably, the inhibited zone was broader after larval biting, consistent with the additive effects of saliva-based and plant-based SA. Exogenous JA restored reporter activation in ROI A (Fig. 3f; Supplementary Fig. S10), indicating that output depends on local hormone ratios. Nonetheless, a residual delay in *pMC::EYFP* induction persisted both in *NahG* plants and after JA treatment of nontransgenic leaves, implying that factors beyond SA—while SA is a major contributor—also restrain proximal JA-dependent transcription.

The crosstalk occurred downstream of JA–Ile–mediated JAZ degradation, as the spatial pattern was absent with the Jas9–Venus–N7 sensor. SA-dependent suppression of JA signaling downstream of JA precursors and JA–Ile has likewise been documented in *Arabidopsis* (Leon-Reyes et al. 2010). Given the SA-related cis-regulatory motifs predicted in the *MC* promoter (Supplementary Fig. S1; Supplementary Table S1), the interaction likely occurs at the level of transcriptional regulation. Alternatively, JA–SA crosstalk may arise through protein-level interactions, e.g. NPR1 with MYC2 or EDS1–PAD4 with MYC2 (Cui et al. 2018, Nomoto et al. 2021).

Our gene expression analysis showed that induced proteinase inhibitor genes did not spatially correlate with *13-LOX* or *JAZ1*. Instead, *13-LOX* and *JAZ1* correlated with the ethylene biosynthetic gene *ACO2*, with peak expression in ROI A closest to the wound (Fig. 4; Supplementary Table S3), suggesting these upstream JA/ET nodes are largely insulated from SA–JA antagonism. By contrast, *TRXH* and *RbohD*—key redox regulators—coexpressed with the proteinase inhibitors (Fig. 4; Supplementary Table S3), implicating ROS-linked signaling in shaping the proximal transcriptional landscape. The role of redox signaling in response to wounding was also confirmed on a proteome level and GSH oxidation status, which was JA-dependent, in Arabidopsis leaves (Gfeller et al. 2011). Additionally, in hairy roots of tomato, accumulation of antioxidants, GSH and AsA, and expression of ROS scavenging enzymes were found to be *COI1*-dependent and *si-COI1* mutants showed more oxidative stress (Kadam and Barvkar 2024).

Using genetically encoded, high-resolution reporters, we show that spatial antagonism between JA and SA shapes the response to mechanical wounding—without confounding inputs from pathogens or herbivores. To our knowledge, this proximal SA-mediated attenuation of JA-dependent transcription after wounding has not been reported, helping reconcile prior ambiguities in SA–JA crosstalk. Resolving the dynamics of these interactions is essential for designing durable, sustainable resistance strategies in the field. This and similar studies using genetically encoded sensor plants (Betsuyaku et al. 2018, Ghareeb et al. 2020, Lukan et al. 2020, 2023, Salguero-Linares et al. 2022, Calabria et al. 2025) advance the field of defense signaling in plants by introducing a precise spatiotemporal dimension.

Materials and Methods

Plant material

We used three potato genotypes: cv. Rywal, cv. Désirée, and NahG-Désirée transgenic lines (Baebler et al. 2011). Rywal plantlets were obtained from the Institute of Plant Breeding and Acclimatization–National Research Institute (Młochów, Poland), and Désirée from the Leibniz Institute of Plant Biochemistry (Halle, Germany). Potato plants were grown in stem-node tissue culture as previously described (Baebler et al. 2009). Two weeks after node segmentation, plantlets were transferred to soil and maintained in a growth chamber under previously reported controlled conditions (Baebler et al. 2014). Experiments were performed 3–5 weeks after potting. For soil-grown plants, we carefully avoided mechanical disturbance and any exposure—even via volatiles—to previously treated plants to prevent priming or cross-contamination of biosensor responses.

Insect maintenance

CPB larvae were kindly provided by Primož Žigon (Agricultural Institute of Slovenia). Larvae were maintained in closed glass containers and fed daily exchanged potato leaves. For feeding assays, third–fourth instar larvae were used and starved for 24 h prior to experiments.

Cloning

The *MC* gene (Sotub06g027390/PGSC0003DMG400005950/Soltu.DM.06G028940) sequence was retrieved from the Solanaceae Genomics Resource (http://solanaceae.plantbiology.msu.edu/pgsc_download.shtml) to design PCR primers. Genomic DNA (gDNA) was isolated from potato using the DNeasy Plant Mini Kit (Qiagen) per the manufacturer's instructions. An approximately 1000 bp *MC* promoter fragment was amplified from gDNA by touchdown nested PCR with VELOCITY DNA Polymerase (Bioline) using primer pairs MC_F2.1/MC_R1 and MC_F2.2/MC_R2 (primer sequences and PCR conditions are shown in Supplementary Table S4). Amplicons were gel-purified (Wizard® SV Gel and PCR Clean-Up System, Promega) and cloned into pJET1.2 blunt cloning vector (Thermo Fisher Scientific) according to the manufacturer's protocol. Chemically competent *E. coli* was transformed with the constructs, plasmids were isolated using GenElute™ Plasmid Miniprep Kit (Sigma) and sequenced (GATC Biotech, Supplementary Table S4 Sequencing primers). For reporter construction, the *MC* promoter in pJET and the *EYFP* coding sequence from pH7YWG2 (VIB; Karimi et al. 2005) were each amplified with Phusion® High-Fidelity DNA Polymerase (NEB) using primer sets A/Gr and Gf/D, respectively (Supplementary Table S4), gel-purified as stated above, and fused using the Gibson Assembly® Cloning Kit (Thermo Fisher Scientific). The resulting *pMC::EYFP* cassette was subsequently subcloned into pENTR/D-TOPO (Thermo Fisher Scientific) following the manufacturer's protocol.

Analysis of promoter sequences

The *MC* promoter sequence from potato cv. Désirée was aligned to the reference double-monoploid (DM) genome of *Solanum tuberosum* ssp. *phureja* using AlignX (Lu and Moriyama 2004). Cis-regulatory motifs and transcription factor binding sites were predicted with PlantCARE (Lescot et al. 2002), TRANSFAC (Wingender et al. 1996), and PLACE (Higo et al. 1999).

Stable transformations

Stable transformation of potato cv. Désirée and Désirée–*NahG* with *pMC::EYFP*, and cv. Rywal with Jas9–Venus–N7, was performed via *Agrobacterium tumefaciens* LBA4404 as described in (Lukan et al. 2023). The *pMC::EYFP* cassette was

Downloaded from https://academic.oup.com/pcp/advance-article/doi/10.1093/pcp/pcaf120/8262811 by National and University Library Ljubljana user on 11 December 2025

Downloaded from https://academic.oup.com/pcp/advance-article/doi/10.1093/pcp/pcaf120/8262811 by National and University Library Ljubljana user on 11 December 2025

recombined from pENTR/D-TOPO into the binary destination vector pB7WG (VIB) by LR reaction (Thermo Fisher Scientific). The pH7m34GW plasmid carrying Jas9–Venus–N7 (Larrieu et al. 2015) was kindly provided by Antoine Larrieu (ENS Lyon). gDNA from transgenic lines was isolated from potato plants as described above. Undiluted gDNA from *pMC::EYFP* lines was screened by PCR using primer pair EYFP_C/EYFP_D; Jas9–Venus–N7 insertion was verified with qJas9-VENUS-F/qJas9-VENUS-R (Supplementary Table S4), using the KAPA2G Robust HotStart PCR Kit (Kapa Biosystems) according to the manufacturer's instructions.

Treatments

To validate *pMC::EYFP* reporter function, soil-grown transgenic plants were exposed to methyl jasmonate (MeJA; Sigma) in airtight plexiglass chambers for either 1 h or 24 h. For the 1 h treatment, half of a single leaf per plant was excised 5 h post-exposure for RT–qPCR. For the 24 h treatment, leaves were imaged by confocal microscopy immediately after removal from the chamber. Control plants were sealed in identical empty chambers for the same durations. Jas9–Venus–N7 sensor responsiveness was assessed in tissue-cultured plants following mechanical wounding, and fluorescence was monitored to confirm reporter degradation dynamics. Based on inducibility and signal quality, two independent transgenic lines per sensor were selected for subsequent experiments.

Mechanical wounding was made by piercing the leaf with a sterile needle. Herbivory wounding was performed by the third or fourth instar CPBs' larvae. During experiment, they were put on the leaf and their behavior was observed continuously to distinguish two behaviors: probing—light wounding using lateral mouthparts (maxillary palps and mandibles) while moving across the surface—and biting—once located, larva fed on tissue using medial mouthparts (labrum) (Ruan et al. 2020) (Fig. 1b). The larvae were removed immediately after their first bite. All wound treatments were run in more than three independent experiments.

JA was prepared at 1 mM in water containing 0.1% DMSO. INA (2,6-dichloroisonicotinic acid) was prepared at 1 mM in water with 1% ethanol (Baebler et al. 2011). Solutions were applied with a brush to one half of a leaf (one side from the midrib). To avoid within-plant signaling confounds, mock treatments (0.1% DMSO in water or 1% ethanol in water) were performed on separate plants. Leaves were then mechanically wounded with a sterile needle either immediately, 15 min, or 1 h after treatment.

Confocal microscopy

Spatiotemporal reporter dynamics were imaged on a Leica TCS LSI confocal macroscope (Leica Microsystems, Wetzlar, Germany) with Plan APO 5× and 20× objectives. Nondetached leaves on soil-grown plants were used throughout. For *pMC::EYFP* imaging, leaves were gently secured between two glass slides and imaged for about 24 h after wounding. Time-series tilescans were acquired every 12 min–1 h to minimize photobleaching. For each tilescan, EYFP and chlorophyll signals from epidermis and palisade tissue were recorded sequentially. EYFP: 488 nm excitation; 520–550 nm emission. Chlorophyll: 488 nm excitation; 690–750 nm emission. Z-stacks were collected using Z-galvo (stage movement). For Jas9–Venus–N7 imaging, nondetached leaves were supported with aluminum foil. Z-stacks spanning epidermis and palisade tissue were collected using Z-wide (objective movement). Venus: 488 nm excitation; 515–550 nm emission. The confocal pinhole was set to 6 AU (at 580 nm) in all experiments to increase signal intensity. Within each sensor dataset, images were taken at identical laser power, detector gain, and tissue depth. Because absolute fluorescence varied across experiments and transgenic lines, intensity values should not be compared between separate experiments (see Supplementary Table S5 for full settings). All raw images are deposited at Zenodo (10.5281/zenodo.16875336).

ROIs were defined at the time point when *pMC::EYFP* first became detectable in ROI B. Widths and radial distances were measured at this time point. Observed ranges were: ROI A, 0.15–0.5 mm after probing or needle wounding and 0.3–0.8 mm after biting; ROI B, 0.2–1.3 mm. To enable cross-experiment comparisons, we then standardized ROI dimensions and applied them consistently across assays with other sensors—Jas9–Venus–N7, *Acinetobacter* ADPWH_*lux*, *pMC::EYFP* in the *NahG* background—and for microdissection used in gene-expression analyses. Standardized widths were: ROI A, 0.5–0.7 mm; ROI B, 0.7–1.0 mm; ROI C, 0.7–1.0 mm.

RT-qPCR

We quantified transcripts in *pMC::EYFP* plants for: *MC*, *EYFP*, *13-LOX*, *JAZ1*, *PCPI8*, *ACO2*, *ERF1*, *PTI5*, *PR1b*, *B-glu-2*, *ARF2*, *RD29*, *TRXH*, *CALS*, *RBOHD1*, and *CAT1*. Primers for *MC* and *EYFP* were designed in Primer Express 2 (Applied Biosystems) and synthesized by IDT; all primers/probes are listed in Supplementary Table S4. Samples for RT-qPCR were taken as described in (Lukan et al. 2020). Samples of ROIs A-C (corresponding to distinctive ROIs A–C of *pMC::EYFP* sensor) were processed individually. Total RNA was extracted with Direct-zol RNA Microprep (Zymo Research) per the manufacturer's protocol, treated with DNase I (Qiagen; 0.5 µL per sample), and reverse transcribed using the High-Capacity cDNA Reverse Transcription Kit (Thermo Fisher Scientific). RT–qPCR was run on ViiA 7, QuantStudio™ 7 Flex, and 7900HT Fast systems (Thermo Fisher Scientific) in 384-well plates under universal cycling conditions, 5 µL reaction volume, with technical duplicates. Expression was normalized to *Cox* and *EF1* (Baebler et al. 2011) using quantGenius (http://quantgenius.nib.si, Baebler et al. 2017). Correlation between marker genes was calculated using Pearson correlation coefficient with Benjamini–Hochberg correction and shown as heatmaps with hierarchical clustering on Euclidean distance in R v.4.3.1 (www.R-project.org) using package psych v.2.4.6.

SA measurements

Acinetobacter sp. ADPWH_*lux* (Huang et al. 2005, 2006) was kindly provided by John P. Carr (University of Cambridge). Nontransgenic plants of potato cv. Désirée were used for SA measurements. To assure comparable amount of tissue, sampling was performed with biopunch of 2 mm diameter. Samples were halved to get 0.7 mm wide (one third of each piece encompassed the wound site) or 1 mm wide leaf pieces (for ROIs B and C) that corresponded to the ROIs in confocal microscopy and control piece (Ctr, same leaf, distal piece from the same leaf). Each leaf was pierced by needle three times and samples collected from the same leaf were pooled and snap-frozen in liquid nitrogen. Five plants were processed identically. Samples were homogenized in a TissueLyzer (1 min, 30 Hz). After homogenization, we followed an adapted protocol by (Defraia et al. 2008): 100 µl of buffer (10 mM MES + 10 mM $MgCl_2$ diluted in dH_2O) was added to each homogenate, centrifuged (14 000 rpm, 10 min), and 60 µl of supernatant was transferred to a white 96-well Corning plate. Afterwards, 60 µl of Acinetobacter culture resuspended in the buffer (OD_{600} 0.4) was added. Continuous luminescence measurement was recorded immediately after the plate was filled with Acinetobacter resuspension using Centro XS luminometer (Berthold). The time point of signal quantification was determined according to the time of establishment of linear correlation between $\log_{10}$ of SA concentration of the standard curve and corresponding luminescence (20 min after start of the measurement). The standard curve was generated from homogenized potato cv. Désirée leaves spiked with increasing concentrations of SA (Supplementary Fig. S11).

Modeling sensors response

Temporal response of Jas9-Venus-N7 and *pMC::EYFP* sensors was modeled using CellDesigner (Funahashi et al. 2003, 2008) by reconstructing the JA signaling pathway *in silico* (Data S2). Deterministic simulations used mass-action kinetics (rate = [reactants] × *k*). Relative rate constants (k) were derived from values in BioNumbers (bionumbers.hms.harvard.edu/search.aspx) and FPbase (fpbase.org) and set as follows: binding and transcription = 1; basal degradation = 0.001; JAZ degradation and JAZ–TF binding = 0.5; translation = 0.1; EYFP folding = 0.6; EYFP maturation = 0.033.

Initial concentrations (arbitrary units) were 1 for JA precursor, wound perception, JAR1, JAZ, AtJas9–Venus–N7, MYC2 transcription factor, and the *pMC::EYFP* gene, and 0 for all other species.

Data analyses

For MeJA assays (*pMC::EYFP*), raw EYFP-channel images were exported for whole-field analysis; mean pixel intensity was computed per image. Differences between mock and MeJA treatments were assessed by a two-tailed Student's *t*-test. For wounding assays with *pMC::EYFP* transgenic plants, maximum-intensity projections of merged tilescans were generated for each time point, and 10 regions of interest were selected within each region (ROI A–C and Ctr). Mean EYFP intensity and SE were calculated per region (ROI A–C, Ctr). For wounding assays with Jas9–Venus–N7 transgenic plants, maximum-intensity Z-projections were used to identify paired stomatal nuclei within fields corresponding to *pMC::EYFP* ROIs. Mean Venus intensity and SE were calculated across all nucleus pairs per field; qualitative inspection of micrographs corroborated the quantitative results. All ROI selections and intensity measurements were performed in LAS X (Leica). Exact analysis parameters for each experiment type are listed in Supplementary Table S5. For *Acinetobacter* ADPWH_*lux* measurements, five biological samples (each pooled from three needle wounds) were averaged and SE reported. Pairwise comparisons among regions (ROI A–C and Ctr) used a two-tailed Student's *t*-test.

Acknowledgments

We acknowledge Carissa Robyn Bleker, Nastja Marondini, Rebeka Strah, Ana Žuran, and Alesia Mevlja for their help in the experimental part. We also acknowledge Primož Žigon (Agricultural Institute of Slovenia) for providing third or fourth instar Colorado potato beetles' larvae, Antoine Larrieu (ENS Lyon) for Jas9-Venus-N7 plasmid, and John P. Carr (University of Cambridge) for *Acinetobacter* sp. ADPWH_*lux*. Potato plants were obtained from the Institute of Plant Breeding and Acclimatization—National Research Institute, Młochów, Poland (cv. Rywal) and from the Leibniz Institute of Plant Biochemistry, Halle, Germany (cv. Désirée).

Author Contributions

V.L., T.L., K.G., and D.D. designed the research; V.L., T.L., T.M.P., K.P., K.S., T.H., and J.R. performed the research; V.L., T.L., K.G., K.P., K.S., and M.Z. analyzed the data; V.L., T.L., K.G., K.S., M.Z., T.M.P., K.P., D.D., T.H., and J.R. contributed to the writing or revision of the article.

Supplementary Data

Supplementary data is available at *PCP* online.

Conflict of Interest

None declared.

Funding

This work was supported by the Slovenian Research and Innovation Agency [research core funding No. P4-0165, project J4-1777, and program for young researchers].

Data Availability

The raw data underlying this article are available in Zenodo, at: 10.5281/zenodo.16875336. All materials reported in this paper will be shared by the corresponding authors upon request.

References

Abdala-Roberts, L., Vázquez-González, C., Rasmann, S., Moreira, X. (2022) Test of communication between potato plants in response to herbivory by the Colorado potato beetle. *Agric. For. Entomol.* 24:212–218. https://doi.org/10.1111/AFE.12484

Ang, M.C.Y., Saju, J.M., Porter, T.K., Mohaideen, S., Sarangapani, S., Khong, D.T., et al. (2024) Decoding early stress signaling waves in living plants using nanosensor multiplexing. *Nat. Commun.* 15:1–17. https://doi.org/10.1038/s41467-024-47082-1

Baebler, Š., Krečič-Stres, H., Rotter, A., Kogovšek, P., Cankar, K., Kok, E.J., et al. (2009) PVYNTN elicits a diverse gene expression response in different potato genotypes in the first 12 h after inoculation. *Mol. Plant Pathol.* 10:263–275. https://doi.org/10.1111/j.1364-3703.2008.00530.x

Baebler, Š., Stare, K., Kovač, M., Blejec, A., Prezelj, N., Stare, T., et al. (2011) Dynamics of responses in compatible potato – potato virus Y interaction are modulated by salicylic acid. *PLoS One* 6:e29009. https://doi.org/10.1371/journal.pone.0029009

Baebler, Š., Witek, K., Petek, M., Stare, K., Tušek-Žnidarič, M., Pompe-Novak, M., et al. (2014) Salicylic acid is an indispensable component of the Ny-1 resistance-gene-mediated response against potato virus Y infection in potato. *J. Exp. Bot.* 65:1095–1109. https://doi.org/10.1093/jxb/ert447

Baebler, Š., Svalina, M., Petek, M., Stare, K., Rotter, A., Pompe-Novak, M., et al. (2017) QuantGenius: implementation of a decision support system for qPCR-based gene quantification. *BMC Bioinform.* 18:1–11. https://doi.org/10.1186/S12859-017-1688-7/FIGURES/5

Bellandi, A., Papp, D., Breakspear, A., Joyce, J., Johnston, M.G., de Keijzer, J., et al. (2022) Diffusion and bulk flow of amino acids mediate calcium waves in plants. *Sci. Adv.* 8:eabo6693. https://doi.org/10.1126/sciadv.abo6693

Benedetti, C.E., Xie, D., Turner, J.G. (1995) Coi1-dependent expression of an Arabidopsis vegetative storage protein in flowers and siliques and in response to coronatine or methyl jasmonate. *Plant Physiol.* 109:567–572. https://doi.org/10.1104/PP.109.2.567

Betsuyaku, S., Katou, S., Takebayashi, Y., Sakakibara, H., Nomura, N., Fukuda, H. (2018) Salicylic acid and Jasmonic acid pathways are activated in spatially different domains around the infection site during effector-triggered immunity in *Arabidopsis thaliana*. *Plant Cell Physiol.* 59:8–16. https://doi.org/10.1093/pcp/pcx181

Bouchard, É., Cloutier, C., Michaud, D. (2003) Oryzacystatin I expressed in transgenic potato induces digestive compensation in an insect natural predator via its herbivorous prey feeding on the plant. *Mol. Ecol.* 12:2439–2446. https://doi.org/10.1046/J.1365-294X.2003.01919.X

Calabria, J., Wang, L., Rast-Somssich, M.I., Chen, H.-W., Watt, M., Persson, S., et al. (2025) Resolving spatially distinct phytohormone response zones in Arabidopsis thaliana roots colonized by *Fusarium oxysporum*. *J. Exp. Bot.* 76:2022–2034. https://doi.org/10.1093/JXB/ERAE516

Chauvin, A., Caldelari, D., Wolfender, J., Farmer, E.E. (2013) Four 13-lipoxygenases contribute to rapid jasmonate synthesis in wounded Arabidopsis thaliana leaves: a role for lipoxygenase 6 in responses to long-distance wound signals. *New Phytol.* 197:566–575. https://doi.org/10.1111/nph.12029

Chini, A., Fonseca, S., Fernández, G., Adie, B., Chico, J.M., Lorenzo, O., et al. (2007) The JAZ family of repressors is the missing link in jasmonate signalling. *Nature* 448:666–671. https://doi.org/10.1038/nature06006

Downloaded from https://academic.oup.com/pcp/advance-article/doi/10.1093/pcp/pcaf120/8262811 by National and University Library Ljubljana user on 11 December 2025

Chung, H.S., Koo, A.J.K., Gao, X., Jayanty, S., Thines, B., Jones, A.D., et al. (2008) Regulation and function of Arabidopsis JASMONATE ZIM-domain genes in response to wounding and herbivory. *Plant Physiol.* 146: 952–964. https://doi.org/10.1104/PP.107.115691

Chung, S.H., Rosa, C., Scully, E.D., Peiffer, M., Tooker, J.F., Hoover, K., et al. (2013) Herbivore exploits orally secreted bacteria to suppress plant defenses. *Proc. Natl. Acad. Sci. USA* 110:15728–15733. https://doi.org/10.1073/pnas.1308867110

Chung, S.H., Scully, E.D., Peiffer, M., Geib, S.M., Rosa, C., Hoover, K., et al. (2017) Host plant species determines symbiotic bacterial community mediating suppression of plant defenses. *Sci. Rep.* 7:39690. https://doi.org/10.1038/SREP39690

Consales, F., Schweizer, F., Erb, M., Gouhier-Darimont, C., Bodenhausen, N., Bruessow, F., et al. (2012) Insect oral secretions suppress wound-induced responses in Arabidopsis. *J. Exp. Bot.* 63:727–737. https://doi.org/10.1093/JXB/ERR308

Cui, F., Brosché, M., Sipari, N., Tang, S., Overmyer, K. (2013) Regulation of ABA dependent wound induced spreading cell death by MYB108. *New Phytol.* 200:634–640. https://doi.org/10.1111/NPH.12456

Cui, H., Qiu, J., Zhou, Y., Bhandari, D.D., Zhao, C., Bautor, J., et al. (2018) Antagonism of transcription factor MYC2 by EDS1/PAD4 complexes bolsters salicylic acid defense in Arabidopsis effector-triggered immunity. *Mol. Plant* 11:1053–1066. https://doi.org/10.1016/j.molp.2018.05.007

Cui, F., Wu, W., Wang, K., Zhang, Y., Hu, Z., Brosché, M., et al. (2019) Cell death regulation but not abscisic acid signaling is required for enhanced immunity to Botrytis in Arabidopsis cuticle-permeable mutants. *J. Exp. Bot.* 70:5971–5984. https://doi.org/10.1093/JXB/ERZ345

Defraia, C.T., Schmelz, E.A., Mou, Z. (2008) A rapid biosensor-based method for quantification of free and glucose-conjugated salicylic acid. *Plant Methods* 4:28. https://doi.org/10.1186/1746-4811-4-28

Divekar, P.A., Rani, V., Majumder, S., Karkute, S.G., Molla, K.A., Pandey, K.K., et al. (2022) Protease inhibitors: an induced plant defense mechanism against herbivores. *J. Plant Growth Regul.* 42:6057–6073. https://doi.org/10.1007/S00344-022-10767-2

Farmer, E.E. and Ryan, C.A. (1990) Interplant communication: airborne methyl jasmonate induces synthesis of proteinase inhibitors in plant leaves. *Proc. Natl. Acad. Sci. USA* 87:7713–7716. https://doi.org/10.1073/PNAS.87.19.7713

Farmer, E.E., Johnson, R.R., Ryan, C.A. (1992) Regulation of expression of proteinase inhibitor genes by methyl jasmonate and jasmonic acid. *Plant Physiol.* 98:995–1002. https://doi.org/10.1104/PP.98.3.995

Fernández-Calvo, P., Chini, A., Fernández-Barbero, G., Chico, J.M., Gimenez-Ibanez, S., Geerinck, J., et al. (2011) The Arabidopsis bHLH transcription factors MYC3 and MYC4 are targets of JAZ repressors and act additively with MYC2 in the activation of jasmonate responses. *Plant Cell* 23:701–715. https://doi.org/10.1105/TPC.110.080788

Förster, S., Schmidt, L.K., Kopic, E., Anschütz, O., Huang, S., Schlücking, K., et al. (2019) Wounding-induced stomatal closure requires jasmonate-mediated activation of GORK K + channels by a Ca 2+ sensor-kinase CBL1-CIPK5 complex. *Dev. Cell* 48:87–99.e6. https://doi.org/10.1016/j.devcel.2018.11.014

Fujimoto, T., Tomitaka, Y., Abe, H., Tsuda, S., Futai, K.,Mizukubo, T. (2011). Expression profile of jasmonic acid-induced genes and the induced resistance against the root-knot nematode (Meloidogyne incognita) in tomato plants (Solanum lycopersicum) after foliar treatment with methyl jasmonate. *Journal of Plant Physiology* 168:1084-1097. https://doi.org/10.1016/j.jplph.2010.12.002

Funahashi, A., Morohashi, M., Kitano, H., Tanimura, N. (2003) CellDesigner: a process diagram editor for gene-regulatory and biochemical networks. *BIOSILICO* 1:159–162. https://doi.org/10.1016/S1478-5382(03)02370-9

Funahashi, A., Matsuoka, Y., Jouraku, A., Morohashi, M., Kikuchi, N., Kitano, H. (2008) CellDesigner 3.5: a versatile modeling tool for biochemical networks. *Proc. IEEE* 96:1254–1265. https://doi.org/10.1109/JPROC.2008.925458

Gaikwad, T., Breen, S., Breeze, E., Hussain, R.M.F., Kulasekaran, S., de Torres-Zabala, M., et al. (2023) Rapid local and systemic jasmonate signalling drives initiation and establishment of plant systemic immunity. *BioRxiv* 2023:22.541689. https://doi.org/10.1101/2023.05.22.541689

Gfeller, A., Baerenfaller, K., Loscos, J., Chételat, A., Baginsky, S., Farmer, E.E. (2011) Jasmonate controls polypeptide patterning in undamaged tissue in wounded Arabidopsis leaves. *Plant Physiol.* 156:1797–1807. https://doi.org/10.1104/PP.111.181008

Ghareeb, H., El-Sayed, M., Pound, M., Tetyuk, O., Hanika, K., Herrfurth, C., et al. (2020) Quantitative hormone signaling output analyses of *Arabidopsis thaliana* interactions with virulent and avirulent *Hyaloperonospora* arabidopsidis isolates at single-cell resolution. *Front. Plant Sci.* 11:603693. https://doi.org/10.3389/FPLS.2020.603693/BIBTEX

Glauser, G., Grata, E., Dubugnon, L., Rudaz, S., Farmer, E.E., Wolfender, J.-L. (2008) Spatial and temporal dynamics of jasmonate synthesis and accumulation in Arabidopsis in response to wounding. *J. Biol. Chem.* 283: 16400–16407. https://doi.org/10.1074/jbc.M801760200

Graham, J.S., Hall, G., Pearce, G., Ryan, C.A. (1986) Regulation of synthesis of proteinase inhibitors I and II mRNAs in leaves of wounded tomato plants. *Planta* 169:399–405. https://doi.org/10.1007/BF00392137

Grandi, L., Ye, W., Clancy, M.V., Vallat, A., Glauser, G., Abdala-Roberts, L., et al. (2024) Plant-to-plant defence induction in cotton is mediated by delayed release of volatiles upon herbivory. *New Phytol.* 244:2505–2517. https://doi.org/10.1111/NPH.20202

Green, A.R., Nissen, M.S., Mohan Kumar, G.N., Knowles, N.R., Kang, C.H. (2014) Characterization of *Solanum tuberosum* multicystatin and the significance of core domains. *Plant Cell* 25:5043–5052. https://doi.org/10.1105/TPC.113.121004

Gruden, K., Popovič, T., Cimerman, N., Križaj, I., Štrukelj, B. (2003) Diverse enzymatic specificities of digestive proteases, 'intestains', enable Colorado potato beetle larvae to counteract the potato defence mechanism. *Biol. Chem.* 384:305–310. https://doi.org/10.1515/BC.2003.034/MACHINEREADABLECITATION/RIS

Gruden, K., Kuipers, A.G.J., Gunčar, G., Slapar, N., Štrukelj, B., Jongsma, M.A. (2004) Molecular basis of Colorado potato beetle adaptation to potato plant defence at the level of digestive cysteine proteinases. *Insect Biochem. Mol. Biol.* 34:365–375. https://doi.org/10.1016/J.IBMB.2004.01.003

Halim, V.A., Eschen-Lippold, L., Altmann, S., Birschwilks, M., Scheel, D., Rosahl, S. (2007) Salicylic acid is important for basal defense of *Solanum tuberosum* against *Phytophthora infestans*. *Mol. Plant-Microbe Interact.* 20: 1346–1352. https://doi.org/10.1094/MPMI-20-11-1346

Hander, T., Fernández-Fernández, Á.D., Kumpf, R.P., Willems, P., Schatowitz, H., Rombaut, D., et al. (2019) Damage on plants activates Ca2+ −dependent metacaspases for release of immunomodulatory peptides. *Science* 363:eaar7486. https://doi.org/10.1126/SCIENCE.AAR7486/SUPPL_FILE/AAR7486S7.MOV

Hickman, R., Van Verk, M.C., Van Dijken, A.J.H., Mendes, M.P., Vroegop-Vos, I.A., Caarls, L., et al. (2017) Architecture and dynamics of the jasmonic acid gene regulatory network. *Plant Cell* 29:2086–2105. https://doi.org/10.1105/TPC.16.00958

Higo, K., Ugawa, Y., Iwamoto, M., Korenaga, T. (1999) Plant cis-acting regulatory DNA elements (PLACE) database: 1999. *Nucleic Acids Res.* 27: 297–300. https://doi.org/10.1093/nar/27.1.297

Hou, S., Liu, Z., Shen, H., Wu, D. (2019) Damage-associated molecular pattern-triggered immunity in plants. *Front. Plant Sci.* 10:646. https://doi.org/10.3389/FPLS.2019.00646

Huang, W.E., Wang, H., Zheng, H., Huang, L., Singer, A.C., Thompson, I., et al. (2005) Chromosomally located gene fusions constructed in Acinetobacter sp. ADP1 for the detection of salicylate. *Environ. Microbiol.* 7:1339–1348. https://doi.org/10.1111/J.1462-5822.2005.00821.X

Huang, W.E., Huang, L., Preston, G.M., Naylor, M., Carr, J.P., Li, Y., et al. (2006) Quantitative in situ assay of salicylic acid in tobacco leaves using a

Downloaded from https://academic.oup.com/pcp/advance-article/doi/10.1093/pcp/pcaf120/8262811 by National and University Library Ljubljana user on 11 December 2025

genetically modified biosensor strain of Acinetobacter sp. ADP1. *Plant J.* 46:1073–1083. https://doi.org/10.1111/J.1365-313X.2006.02758.X

Jones, J.D.G., Staskawicz, B.J., Dangl, J.L. (2024) The plant immune system: from discovery to deployment. *Cell* 187:2095–2116. https://doi.org/10.1016/J.CELL.2024.03.045

Kadam, S.B. and Barvkar, V.T. (2024) COI1 dependent jasmonic acid signalling positively modulates ROS scavenging system in transgenic hairy root culture of tomato. *Plant Physiol. Biochem.* 206:108229. https://doi.org/10.1016/J.PLAPHY.2023.108229

Karimi, M., De Meyer, B., Hilson, P. (2005) Modular cloning in plant cells. *Trends Plant Sci.* 10:103–105. https://doi.org/10.1016/J.TPLANTS.2005.01.008

Kiep, V., Vadassery, J., Lattke, J., Maaß, J.P., Boland, W., Peiter, E., et al. (2015) Systemic cytosolic Ca2+ elevation is activated upon wounding and herbivory in Arabidopsis. *New Phytol.* 207:996–1004. https://doi.org/10.1111/NPH.13493

Kimberlin, A.N., Holtsclaw, R.E., Zhang, T., Mulaudzi, T., Koo, A.J. (2022) On the initiation of jasmonate biosynthesis in wounded leaves. *Plant Physiol.* 189:1925–1942. https://doi.org/10.1093/plphys/kiac163

Koo, A.J.K., Gao, X., Daniel Jones, A., Howe, G.A. (2009) A rapid wound signal activates the systemic synthesis of bioactive jasmonates in Arabidopsis. *Plant J.* 59:974–986. https://doi.org/10.1111/J.1365-313X.2009.03924.X

Larrieu, A., Champion, A., Legrand, J., Lavenus, J., Mast, D., Brunoud, G., et al. (2015) A fluorescent hormone biosensor reveals the dynamics of jasmonate signalling in plants. *Nat. Commun.* 6:6043–6049. https://doi.org/10.1038/ncomms7043

Leon-Reyes, A., Van der Does, D., De Lange, E.S., Delker, C., Wasternack, C., Van Wees, S.C.M., et al. (2010) Salicylate-mediated suppression of jasmonate-responsive gene expression in arabidopsis is targeted downstream of the jasmonate biosynthesis pathway. *Planta* 232:1423–1432. https://doi.org/10.1007/S00425-010-1265-Z/FIGURES/4

Lescot, M., Déhais, P., Thijs, G., Marchal, K., Moreau, Y., Van De Peer, Y., et al. (2002) PlantCARE, a database of plant cis-acting regulatory elements and a portal to tools for in silico analysis of promoter sequences. *Nucleic Acids Res.* 30:325–327. https://doi.org/10.1093/nar/30.1.325

Liu, X., Igarashi, D., Hillmer, R.A., Stoddard, T., Lu, Y., Tsuda, K., et al. (2023) Dynamic decomposition of transcriptome responses during plant effector-triggered immunity revealed conserved responses in two distinct cell populations. *BioRxiv* 2022:30.522333. https://doi.org/10.1101/2022.12.30.522333

Lu, G. and Moriyama, E.N. (2004) Vector NTI, a balanced all-in-one sequence analysis suite. *Brief. Bioinform.* 5:378–388. https://doi.org/10.1093/bib/5.4.378

Lukan, T., Pompe-Novak, M., Baebler, Š., Tušek-Žnidarič, M., Kladnik, A., Križnik, M., et al. (2020) Precision transcriptomics of viral foci reveals the spatial regulation of immune-signaling genes and identifies RBOHD as an important player in the incompatible interaction between potato virus Y and potato. *Plant J.* 104:645–661. https://doi.org/10.1111/tpj.14953

Lukan, T., Županič, A., Mahkovec Povalej, T., Brunkard, J.O., Kmetič, M., Juteršek, M., et al. (2023) Chloroplast redox state changes mark cell-to-cell signaling in the hypersensitive response. *New Phytol.* 237:548–562. https://doi.org/10.1111/nph.18425

Martinez, M., Santamaria, M.E., Diaz-Mendoza, M., Arnaiz, A., Carrillo, L., Ortego, F., et al. (2016) Phytocystatins: defense proteins against phytophagous insects and Acari. *Int. J. Mol. Sci.* 17:1747. https://doi.org/10.3390/IJMS17101747

McCloud, E.S. and Baldwin, I.T. (1997) Herbivory and caterpillar regurgitants amplify the wound-induced increases in jasmonic acid but not nicotine in *Nicotiana sylvestris*. *Planta* 203:430–435.

Murdock, L.L., Brookhart, G., Dunn, P.E., Foard, D.E., Kelley, S., Kitch, L., et al. (1987) Cysteine digestive proteinases in Coleoptera. *Comp. Biochem. Physiol. Part B: Comp. Biochem.* 87:783–787. https://doi.org/10.1016/0305-0491(87)90388-9

Myers, R.J., Fichman, Y., Zandalinas, S.I., Mittler, R. (2023) Jasmonic acid and salicylic acid modulate systemic reactive oxygen species signaling during stress responses. *Plant Physiol.* 191:862–873. https://doi.org/10.1093/PLPHYS/KIAC449

Nguyen, Q.M., Iswanto, A.B.B., Son, G.H., Kim, S.H. (2021) Recent advances in effector-triggered immunity in plants: new pieces in the puzzle create a different paradigm. *Int. J. Mol. Sci.* 22:4709. https://doi.org/10.3390/IJMS22094709

Nomoto, M., Skelly, M.J., Itaya, T., Mori, T., Suzuki, T., Matsushita, T., et al. (2021) Suppression of MYC transcription activators by the immune cofactor NPR1 fine-tunes plant immune responses. *Cell Rep.* 37:110125. https://doi.org/10.1016/J.CELREP.2021.110125

Oerke, E.C. (2006) Crop losses to pests. *J. Agric. Sci.* 144:31–43. https://doi.org/10.1017/S0021859605005708

Ogawa, T., Ara, T., Aoki, K., Suzuki, H., Shibata, D. (2010) Transient increase in salicylic acid and its glucose conjugates after wounding in Arabidopsis leaves. *Plant Biotechnol.* 27:205–209.

Orr, G.L., Strickland, J.A., Walsh, T.A. (1994) Inhibition of Diabrotica larval growth by a multicystatin from potato tubers. *J. Insect Physiol.* 40:893–900. https://doi.org/10.1016/0022-1910(94)90023-X

Petek, M., Rotter, A., Kogovšek, P., Baebler, Š., Mithöfer, A., Gruden, K. (2014) Potato virus Y infection hinders potato defence response and renders plants more vulnerable to Colorado potato beetle attack. *Mol. Ecol.* 23:5378–5391. https://doi.org/10.1111/mec.12932

Popovič, T. and Brzin, J. (2007) Purification and characterization of two cysteine proteinases from potato leaves and the mode of their inhibition with endogenous inhibitors. *Croat. Chem. Acta* 80:45–52.

Prasad, A., Sedlářová, M., Balukova, A., Rác, M., Pospíšil, P. (2020) Reactive oxygen species as a response to wounding: in vivo imaging in *Arabidopsis thaliana*. *Front. Plant Sci.* 10:1660. https://doi.org/10.3389/fpls.2019.01660

Ramšak, Ž., Coll, A., Stare, T., Tzfadia, O., Baebler, Š., Van de Peer, Y., et al. (2018) Network Modeling unravels mechanisms of crosstalk between ethylene and salicylate signaling in potato. *Plant Physiol.* 178:488–499. https://doi.org/10.1104/PP.18.00450

Ruan, Y., Konstantinov, A.S., Damaška, A.F. (2020) The biology and immature stages of the moss-eating flea beetle *Cangshanaltica fuanensis* sp. nov. (Coleoptera, Chrysomelidae, Galerucinae, Alticini), with description of a fan-driven high-power Berlese funnel. *Insects* 11:571. https://doi.org/10.3390/insects11090571

Ryan, C.A. (1968) An inducible protein in potato and tomato leaflets. *Plant Physiol.* 43:1880–1881. https://doi.org/10.1104/PP.43.11.1880

Salguero-Linares, J., Serrano, I., Ruiz-Solani, N., Salas-Gómez, M., Phukan, U.J., González, V.M., et al. (2022) Robust transcriptional indicators of immune cell death revealed by spatiotemporal transcriptome analyses. *Mol. Plant* 15:1059–1075. https://doi.org/10.1016/j.molp.2022.04.010

Salvador-Recatalà, V., Tjallingii, W.F., Farmer, E.E. (2014) Real-time, in vivo intracellular recordings of caterpillar-induced depolarization waves in sieve elements using aphid electrodes. *New Phytol.* 203:674–684. https://doi.org/10.1111/nph.12807

Toyota, M., Spencer, D., Sawai-Toyota, S., Jiaqi, W., Zhang, T., Koo, A.J., et al. (2018) Glutamate triggers long-distance, calcium-based plant defense signaling. *Science* 361:1112–1115. https://doi.org/10.1126/SCIENCE.AAT7744/SUPPL_FILE/AAT7744S9.MP4

Vega-Muñoz, I., Duran-Flores, D., Fernández-Fernández, Á.D., Heyman, J., Ritter, A., Stael, S. (2020) Breaking bad news: dynamic molecular mechanisms of wound response in plants. *Front. Plant Sci.* 11:610445. https://doi.org/10.3389/FPLS.2020.610445/BIBTEX

Vincent, T.R., Canham, J., Toyota, M., Avramova, M., Mugford, S.T., Gilroy, S., et al. (2017) Real-timei vivo recording of Arabidopsis calcium signals during insect feeding using a fluorescent biosensor. *J. Vis. Exp.* 126:56142. https://doi.org/10.3791/56142

Downloaded from https://academic.oup.com/pcp/advance-article/doi/10.1093/pcp/pcaf120/8262811 by National and University Library Ljubljana user on 11 December 2025

Walling, L.L. (2000) The myriad plant responses to herbivores. *J. Plant Growth Regul.* 19:195–216. https://doi.org/10.1007/S003440000026/METRICS

Wang, J., Peiffer, M., Hoover, K., Rosa, C., Zeng, R., Felton, G.W. (2017) *Helicoverpa zea* gut-associated bacteria indirectly induce defenses in tomato by triggering a salivary elicitor(s). *New Phytol.* 214:1294–1306. https://doi.org/10.1111/NPH.14429

Weech, M.H., Chapleau, M., Pan, L., Ide, C., Bede, J.C. (2008) Caterpillar saliva interferes with induced *Arabidopsis thaliana* defence responses via the systemic acquired resistance pathway. *J. Exp. Bot.* 59:2437–2448. https://doi.org/10.1093/JXB/ERN108

Wiesel, L., Davis, J.L., Milne, L., Redondo Fernandez, V., Herold, M.B., Middlefell Williams, J., et al. (2015) A transcriptional reference map of defence hormone responses in potato. *Sci. Rep.* 5:1–12. https://doi.org/10.1038/srep15229.

Wingender, E., Dietze, P., Karas, H., Knüppel, R. (1996) TRANSFAC: a database on transcription factors and their DNA binding sites. *Nucleic Acids Res.* 24:238–241. https://doi.org/10.1093/nar/24.1.238

Xu, H., Dong, C., Wu, Y., Fu, S., Tauqeer, A., Gu, X., et al. (2024) The JA-to-ABA signaling relay promotes lignin deposition for wound healing in Arabidopsis. *Mol. Plant* 17:1594–1605. https://doi.org/10.1016/j.molp.2024.09.003

Zhang, G., Zhao, F., Chen, L., Pan, Y., Sun, L., Bao, N., et al. (2019) Jasmonate-mediated wound signalling promotes plant regeneration. *Nature Plants* 5:491–497. https://doi.org/10.1038/s41477-019-0408-x

Downloaded from https://academic.oup.com/pcp/advance-article/doi/10.1093/pcp/pcaf120/8262811 by National and University Library Ljubljana user on 11 December 2025

© The Author(s) 2025. Published by Oxford University Press on behalf of the Japanese Society of Plant Physiologists. This is an Open Access article distributed under the terms of the Creative Commons Attribution-NonCommercial License (https://creativecommons.org/licenses/by-nc/4.0/), which permits non-commercial re-use, distribution, and reproduction in any medium, provided the original work is properly cited. For commercial re-use, please contact reprints@oup.com for reprints and translation rights for reprints. All other permissions can be obtained through our RightsLink service via the Permissions link on the article page on our site—for further information please contact journals.permissions@oup.com.
Plant and Cell Physiology, 2025, 00(00), 1–13. https://doi.org/10.1093/pcp/pcaf120
Regular Paper

2.3 Robust Quantification of Multiplexed Fluorescent Protein-Based Biosensors in Plant Tissues

Valentina Levak, Anže Županič, Karmen Pogačar, Nastja Marondini, Katja Stare, Tina Arnšek, Katja Fink, Kristina Gruden, Tjaša Lukan

bioRxiv, 2026, 711581. DOI: 10.64898/2026.03.13.711581. Accepted for publication in The Plant Journal, 19 June 2026.

This study tackles the challenges of multiplexing genetically encoded fluorescent biosensors in living plant samples, with an emphasis on separating and quantifying overlapping fluorophores. Eight fluorescent proteins were characterized in *Nicotiana benthamiana* for emission spectra, fluorescence lifetimes, and brightness. Three fluorescent proteins were stably expressed in *S. tuberosum* to compare signal intensity with transient expression in *N. benthamiana*. Using Leica's LAS X Dye Separation module, the authors assessed Spectral Unmixing and Channel Dye Separation tools, highlighting their strengths, limitations, and ability to reduce autofluorescence and mitigate effects of specimen movement. The paper also provides a MATLAB script for the objective segmentation of cellular compartments, such as nuclei and chloroplasts.

The PhD candidate is the first author of the paper. She contributed to the experimental design, execution of most experiments, reviewed the relevant literature, prepared all figures and tables and wrote the first draft.

bioRxiv preprint doi: https://doi.org/10.64898/2026.03.13.711581; this version posted June 18, 2026. The copyright holder for this preprint (which was not certified by peer review) is the author/funder, who has granted bioRxiv a license to display the preprint in perpetuity. It is made available under a CC-BY-NC 4.0 International license.

Robust quantification of multiplexed fluorescent protein-based biosensors in plant tissues

Valentina Levak[1, 2,*], Anže Županič[1], Karmen Pogačar[1, 2], Nastja Marondini[1], Katja Stare[1], Tina Arnšek[1], Katja Fink[1], Kristina Gruden[1], Tjaša Lukan[1,*]

1 Department of Biotechnology and Systems Biology, National Institute of Biology, Ljubljana, Slovenia

2 Jožef Stefan International Postgraduate School, Ljubljana, Slovenia

* corresponding authors

valentina.levak@nib.si (ORCID: 0000-0001-5975-4032), anze.zupanic@nib.si (ORCID: 0000-0003-3303-9086), karmen.pogacar@nib.si (ORCID: 0000-0001-5190-7217), nastja.marondini@nib.si, katja.stare@nib.si (ORCID: 0000-0002-3999-9400), tina.arnsek@nib.si, katja.fink@nib.si (ORCID: 0000-0002-3663-7543), kristina.gruden@nib.si (ORCID: 0000-0001-5906-8569), tjasa.lukan@nib.si (ORCID: 0000-0002-6235-2816)

DATA AVAILABILITY

Raw image data supported with metadata were deposited to Zenodo: 10.5281/zenodo.19691651and can be opened with LAS X available at https://www.leica-microsystems.com/products/microscope-software/p/leica-las-x-ls/downloads/. MATLAB script was deposited to GitHub: https://github.com/NIB-SI/Nuclei-segmentation.

FUNDING

This research was funded by the Slovenian Research and Innovation Agency (research core funding No. P4-0165, P4-0463, projects J4-1777, J4-60073, J4-70169 and ARIS program for young researchers).

CONFLICT OF INTEREST

The authors declare no conflicts of interest. This article does not contain any studies with human or animal participants.

bioRxiv preprint doi: https://doi.org/10.64898/2026.03.13.711581; this version posted June 18, 2026. The copyright holder for this preprint (which was not certified by peer review) is the author/funder, who has granted bioRxiv a license to display the preprint in perpetuity. It is made available under a CC-BY-NC 4.0 International license.

Robust quantification of multiplexed fluorescent protein-based biosensors in plant tissues

Valentina Levak[1, 2,*], Anže Županič[1], Karmen Pogačar[1, 2], Nastja Marondini[1], Katja Stare[1], Tina Arnšek[1], Katja Fink[1], Kristina Gruden[1], Tjaša Lukan[1,*]

1 Department of Biotechnology and Systems Biology, National Institute of Biology, Ljubljana, Slovenia

2 Jožef Stefan International Postgraduate School, Ljubljana, Slovenia

* corresponding authors

Summary

Genetically encoded biosensors are one of the essential tools in biological research. They enable visualization of molecules of interest from the subcellular level to entire organism level *in vivo* and can be used to monitor presence of small molecules, gene expression, protein activity, and protein degradation. However, multiplexing fluorescent biosensors in plants is notoriously difficult due to signal bleed-through and strong autofluorescence from chlorophyll. In this study, we investigated the potential of multiplexing biosensors based on the selection of reporter fluorescent proteins. We characterized the emission spectra, fluorescence lifetimes, and relative brightness of diverse fluorescent proteins in plant leaves. We show that selected proteins exhibit comparable brightness, supporting their use in co-expression experiments and reliable quantification of individual signals. To separate three overlapping signals, we applied two different linear unmixing approaches and compared them to results obtained without unmixing. We identified channel separation unmixing approach as the most suitable for biosensors. Additionally, we show how unmixing with the selected approach can be applied to separate autofluorescence and five fluorescent proteins. We further validated this approach in virus-infected cells by following organelle dynamics *in vivo*. Finally, we demonstrate the feasibility of high-throughput segmentation and quantification with a custom MATLAB workflow for nuclei, chloroplasts, and cytoplasm signal analysis. Overall, our work demonstrates that biosensors can be multiplexed, even when their emission spectra overlap.

Significance statement

Multiplexing genetically encoded biosensors in plants has been limited by overlapping fluorescent signals and strong autofluorescence. This study presents an optimized framework for linear unmixing and provides a MATLAB-based organelle segmentation tool,

bioRxiv preprint doi: https://doi.org/10.64898/2026.03.13.711581; this version posted June 18, 2026. The copyright holder for this preprint (which was not certified by peer review) is the author/funder, who has granted bioRxiv a license to display the preprint in perpetuity. It is made available under a CC-BY-NC 4.0 International license.

allowing precise quantification of multiple fluorescent reporters *in vivo* and advancing real-time visualization of complex cellular processes in plants.

Keywords

Genetically encoded biosensors, fluorescent proteins, linear unmixing, fluorescent protein multiplexing, autofluorescence, organelle segmentation, potato transgenics, *Solanum tuberosum*

Introduction

Since its discovery in 1961, green fluorescent protein (GFP) and its homologs from other organisms have become indispensable tools in biological research (Shimomura, 2005). Over the years, the fluorescent protein palette has expanded to include variants spanning from UV-excitable to IR-emitting (Day & Davidson, 2009; Matlashov et al., 2020; Shu et al., 2009). These proteins are widely employed in the development of genetically encoded biosensors, enabling studies with high temporal (millisecond) and spatial resolution across scales—from subcellular to organism level. Despite the availability of a broad range of biosensors, their multiplexed use remains relatively uncommon, particularly in plant research. One of the main challenges arises from the broader excitation and emission spectra of fluorescent proteins compared to spectra of chemical dyes, which complicates simultaneous detection due to spectral overlap. Simultaneous detection of multiple fluorescent proteins in plant tissues—without spectral overlap between the fluorescent proteins or with autofluorescence—is typically limited to two or three fluorescent proteins, each excited by a different laser. However, multiplexing of existing spectrally overlapping biosensors would give an insight into precise spatiotemporal coordination of multiple interacting proteins or processes. Moreover, this approach is particularly advantageous in experimental settings that necessitate the simultaneous use of a large number of fluorescent proteins, for which a sufficient set of variants with non-overlapping spectral properties is not available.

Plant responses to environmental conditions, pathogens, and pests involve a wide range of molecular players, including Ca^{2+}, reactive oxygen species (ROS), hormones, and protein kinases (Zhang et al., 2020, 2021). These signalling components interact through sequential cascades and complex crosstalk to regulate and balance diverse physiological processes (Lukan & Coll, 2022). To truly understand plant immune response, we need a way to simultaneously visualize several molecular responses in the same cells at the same time. Multiplexing of genetically encoded biosensors within the same organism and the evaluation of their spatial and temporal interdependence is crucial for understanding how plants integrate multiple signalling pathways (Xiao et al., 2025). The outcome of plant responses to

bioRxiv preprint doi: https://doi.org/10.64898/2026.03.13.711581; this version posted June 18, 2026. The copyright holder for this preprint (which was not certified by peer review) is the author/funder, who has granted bioRxiv a license to display the preprint in perpetuity. It is made available under a CC-BY-NC 4.0 International license.

environmental stressors depends not only on the qualitative presence of specific molecules but also on their abundance (Delplace et al., 2020; Jones et al., 2024), making accurate quantification of these biomolecules using genetically encoded biosensors essential. In our observation, the relative brightness of fluorescent proteins strongly influences the successful multiplexing, as sensors with markedly different brightness exhibit unequal sensitivity range of quantification under the same imaging conditions. Moreover, imaging in plant tissues presents additional difficulties due to strong autofluorescence, primarily from chlorophyll and secondary metabolites (Donaldson, 2020).

In this study, we address the challenges of multiplexing genetically encoded biosensors based on fluorescent proteins in plants and suggest optimal protocol for imaging considering the error associated with it. We characterized eight fluorescent proteins—mTagBFP2, mTurquoise2, Venus, mKO2, mCherry, mKate2, mCardinal, and miRFP713—in *Nicotiana benthamiana* leaves, evaluating their emission spectra, fluorescence lifetimes, and brightness. From this set, Venus, mKO2, and mKate2 were also assessed in *Solanum tuberosum* in addition to *N. benthamiana*. To separate overlapping signals, we successfully applied two different linear unmixing approaches. Our protocols could separate overlapping fluorescent protein signals as well as fluorescent protein signal and autofluorescence. Finally, we demonstrate the feasibility of high-throughput segmentation and quantification with a MATLAB workflow for nuclei, chloroplasts, and cytoplasm signal analysis.

Results and Discussion

The emission spectra of fluorescent proteins depend more on the imaging system than on the plant matrix

Efficient separation of fluorescent proteins depends on differences in their excitation and emission spectra or fluorescence lifetimes (Tau, τ), as well as comparable brightness to ensure accurate spectral unmixing. Therefore, we first checked if the published emission spectra are comparable to the ones acquired with different confocal systems and in different plant matrices. Additionally, we assayed the fluorescent proteins and autofluorescence of chlorophyll for their fluorescence lifetimes to provide experimental evidence that they can be separated based on their lifetimes *in planta*.

We selected a palette of reported highly bright proteins (mTagBFP2, mTurquoise2, Venus, mKO2, mCherry, mKate2, mCardinal, and miRFP713) and measured their emission spectra and fluorescence lifetimes in plant leaves to detect any potential matrix dependent effects. To enable quantitative imaging, each protein was localized in *N. benthamiana* nuclei using N7 nuclear localization signal and expressed under strong constitutive CaMV 35S promoter in a transient setup. Imaging was performed using Leica's TCS LSI, Stellaris 5, and Stellaris 8

bioRxiv preprint doi: https://doi.org/10.64898/2026.03.13.711581; this version posted June 18, 2026. The copyright holder for this preprint (which was not certified by peer review) is the author/funder, who has granted bioRxiv a license to display the preprint in perpetuity. It is made available under a CC-BY-NC 4.0 International license.

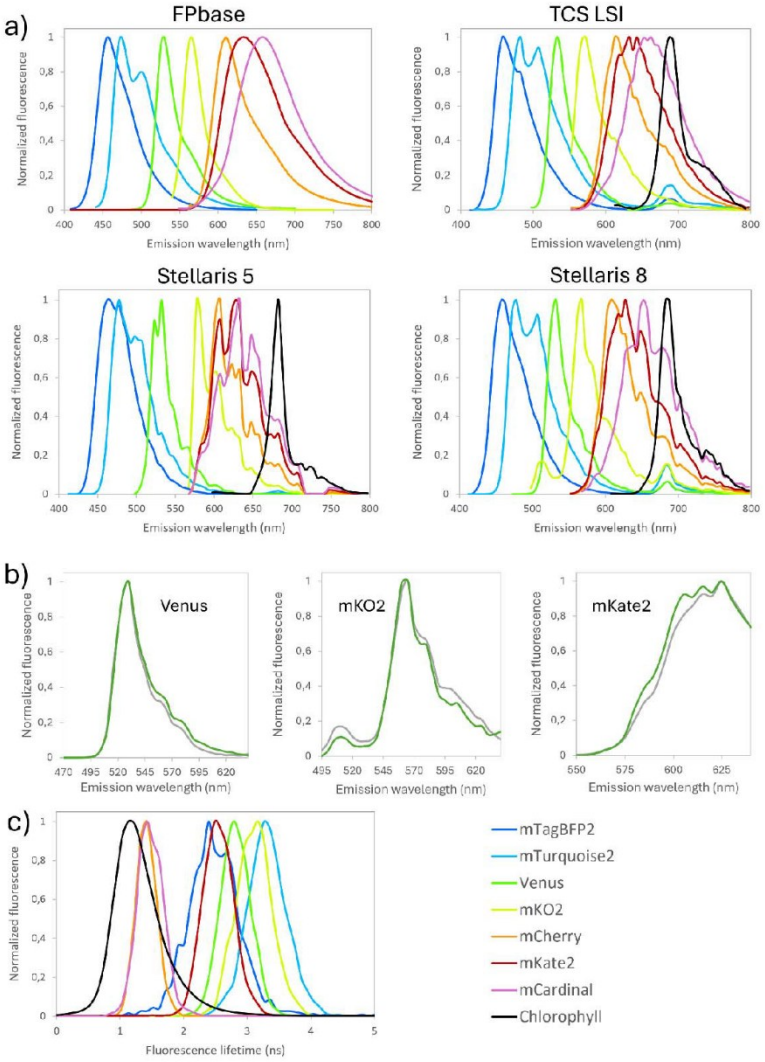
129 systems. All proteins except miRFP713 were detectable by all three imaging systems under
130 these conditions; the lack of miRFP713 signal likely reflects insufficient cytoplasmic and
131 nuclear biliverdin, its required cofactor (Matlashov et al., 2020). Notably, we successfully
132 detected mCardinal in plant leaves for the first time, while mKO2 and mTagBFP2 detection
133 had been previously reported *in planta* (Rigoulot et al., 2021). The use of other fluorescent
134 proteins is well-documented in plants (Brunoud et al., 2012; Ghareeb et al., 2016; Mylle et
135 al., 2013).

136 We first compared the emission spectra of the selected fluorescent proteins obtained by
137 different confocal systems. Consistent with previous observations (Mylle et al., 2013), we
138 noted discrepancies relative to the spectra reported in FPbase (Lambert, 2019), particularly
139 in the red range when using HyD S detectors (Figure 1a, Stellaris 5 and Stellaris 8).

140 To evaluate the influence of the plant matrix, we compared the emission spectra of Venus,
141 mKO2, and mKate2 in stable potato transformants, which closely matched those obtained in
142 transient *N. benthamiana* expression (Figure 1b). These results suggest that while the
143 recorded emission spectra highly depend on the used confocal system, they can be used
144 interchangeably across different plant matrices.

145 In addition to spectral properties, fluorescence lifetime offers an alternative means of
146 separation. Chlorophyll autofluorescence generally exhibits shorter lifetimes than fluorescent
147 proteins, enabling separation via Tau gating. Our measurements showed that all proteins
148 except mCardinal and mCherry could be fully separated from chlorophyll autofluorescence
149 using Tau gating, even in cases of overlapping emission spectra, such as with mKate2
150 (Figure 1c). Tau gating imaging can thus aid separation when these proteins are used as
151 reporters.

bioRxiv preprint doi: https://doi.org/10.64898/2026.03.13.711581; this version posted June 18, 2026. The copyright holder for this preprint (which was not certified by peer review) is the author/funder, who has granted bioRxiv a license to display the preprint in perpetuity. It is made available under a CC-BY-NC 4.0 International license.



152

153 **Figure 1: Emission and fluorescence lifetime spectra of a diverse set of fluorescent**
154 **proteins across confocal systems and plant species.** (a) Emission spectra of transiently
155 expressed fluorescent proteins in *N. benthamiana*, measured with optimized settings on
156 Leica's TCS LSI, Stellaris 5, and Stellaris 8, show imaging system-dependent variations,
157 particularly in the red part of emission spectra compared to FPbase reference spectra. (b)

bioRxiv preprint doi: https://doi.org/10.64898/2026.03.13.711581; this version posted June 18, 2026. The copyright holder for this preprint (which was not certified by peer review) is the author/funder, who has granted bioRxiv a license to display the preprint in perpetuity. It is made available under a CC-BY-NC 4.0 International license.

158 Comparison of three selected fluorescent proteins emission spectra in *N. benthamiana*
159 (green) and potato (*Solanum tuberosum*, gray) reveals similar spectral profiles. (c)
160 Fluorescence lifetime of selected fluorescent proteins and chlorophyll, recorded on Stellaris 8
161 using white light laser excitation, highlighting clear separation of mKate2 signal from other
162 red spectra emission fluorescent proteins.

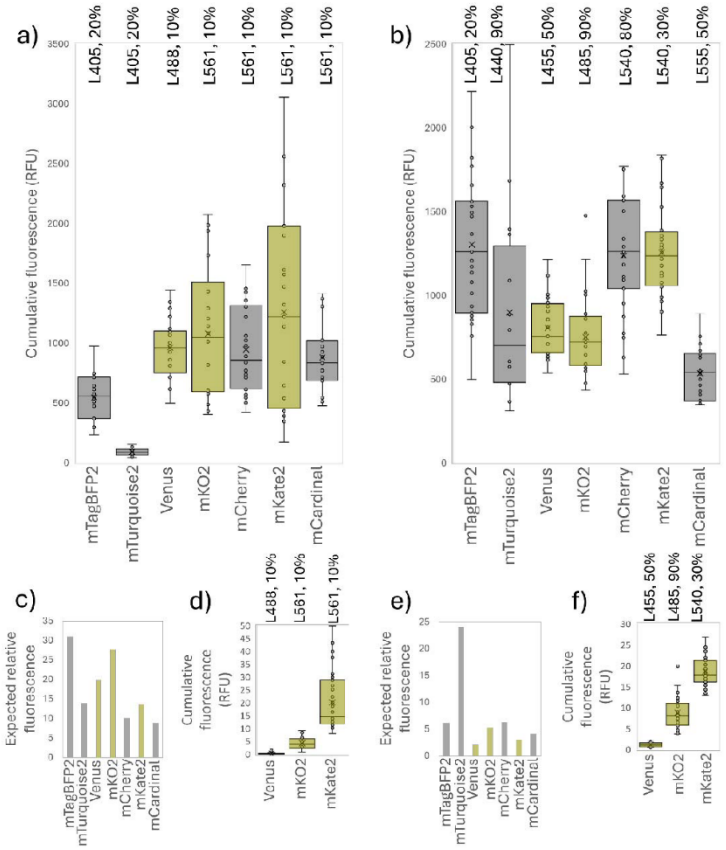
163 All selected fluorescent proteins, except mTurquoise2, show comparable 164 brightness using standard lasers in confocal system

165 Fluorescent protein brightness is determined not only by extinction coefficient and quantum
166 yield, but also by level of expression, maturation efficiency and pH stability (Cranfill et al.,
167 2016), with additional contributions from laser power and detector sensitivity. Maintaining
168 comparable brightness among spectrally overlapping proteins is essential for accurate
169 separation and broad quantification range: the dimmer fluorophore must remain detectable,
170 while the brighter should avoid oversaturation.

171 To assess fluorescent proteins' brightness, we measured cumulative brightness using
172 standard lasers setting (Stellaris 5) or a white light laser or 405 nm laser (Stellaris 8). We
173 limited emission detection to 640 nm to minimize chlorophyll interference. All fluorescent
174 proteins exhibited similar brightness except mTurquoise2 if excited with 405 nm laser, which
175 showed lower brightness compared to FPbase predictions (Figure 2a, b). However, excitation
176 with white light laser (440 nm) resulted in comparable brightness of mTurquoise2 with other
177 fluorescent proteins, although it was still much lower compared to FPbase predictions (Figure
178 2c, e). These results suggest that although valuable, FPbase predictions might not
179 necessarily reflect the achievable brightness *in planta*.

180 We selected Venus, mKO2 and mKate2 for additional analysis as their brightness was the
181 highest in *N. benthamiana* leaves (Figure 2a; highlighted in yellow in Figure 2). Stable
182 expression of Venus, mKO2, and mKate2 in potato produced fluorescence signals in leaves,
183 which were 100–500× weaker than in transient expression in *N. benthamiana* (see y-axis
184 values in Figure 2d, f versus Figure 2a, b), possibly due to silencing of the transgene
185 (Rajeevkumar et al., 2015).

bioRxiv preprint doi: https://doi.org/10.64898/2026.03.13.711581; this version posted June 18, 2026. The copyright holder for this preprint (which was not certified by peer review) is the author/funder, who has granted bioRxiv a license to display the preprint in perpetuity. It is made available under a CC-BY-NC 4.0 International license.



186

187 **Figure 2. Brightness comparison of fluorescent proteins in *N. benthamiana* and *S.***
188 ***tuberosum* leaves.** *mTagBFP2, mTurquoise2, Venus, mKO2, mCherry, mKate2,* and
189 *mCardinal* exhibit approximately comparable brightness across different excitation
190 conditions. All fluorescent proteins were fused to a nuclear localisation signal. (a) Cumulative
191 fluorescence intensity (RFU) of transiently expressed proteins in *N. benthamiana,* measured
192 using standard laser lines on the Leica Stellaris 5 microscope. (b) The same measurement
193 performed using the 405 nm or a white light laser on Stellaris 8, with excitation wavelengths
194 set just below each protein's emission peak. Fluorescent proteins are indicated below each
195 bar chart, while laser wavelengths and power settings are shown above. Detector gain was
196 kept at the minimum setting for all fluorescent proteins. For each condition, at least two
197 independent images were analysed. Mean fluorescence intensity per nucleus was plotted as
198 bar charts with overlaid points (each dot represents one nucleus). (c, e) Expected
199 fluorescence intensity based on FPbase.org data (excitation × brightness), shown for (c)
200 Stellaris 5 and (e) Stellaris 8, calculated for (a) and (d) standard laser lines, and (b) and (f)

bioRxiv preprint doi: https://doi.org/10.64898/2026.03.13.711581; this version posted June 18, 2026. The copyright holder for this preprint (which was not certified by peer review) is the author/funder, who has granted bioRxiv a license to display the preprint in perpetuity. It is made available under a CC-BY-NC 4.0 International license.

white light laser excitation. Among the tested fluorescent proteins, *Venus*, *mKO2* and *mKate2* were selected for stable transformation in potato (highlighted in yellow across all charts). (d, f) Brightness of fluorescent proteins measured in *S. tuberosum* (potato) leaves (d) using standard laser lines or (f) the white light laser, as described in panels (a□b). Brightness is shown for one transgenic line per fluorescent protein. Analysis of a second transgenic line gave similar results (results available on Zenodo: 10.5281/zenodo.19691651).

Spectrally overlapping fluorescent proteins can be distinguished using linear unmixing

Next, we evaluated the available linear unmixing approaches for separation of fluorescent proteins. Linear unmixing is a powerful method for resolving mixed spectral contributions within individual pixels (Zimmermann, 2005). Previous studies have applied this approach to separate two fluorescent proteins in plant leaves using Olympus and Zeiss systems (Mylle et al., 2013). These authors reported acquiring lambda scans of a combination of two selected fluorescent proteins followed by linear unmixing and its qualitative evaluation. Here, we acquired images by Leica's Stellaris 5 and applied two linear unmixing strategies. The first one was spectral unmixing, which processes xyλ(z) (lambda scan) images across the entire emission range with fixed wavelength steps. This method works by taking emission spectra (a lambda scan) of every single pixel and then mathematically calculating how much of each known fluorophore (e.g., 60% GFP, 40% Venus) is in each pixel. However, this process is time-consuming, as it requires the microscope to scan the entire emission spectrum for every pixel, typically in 5 or 10 nm steps. The second strategy was channel separation, which processes images obtained by standard acquisition in channels with defined, typically wider emission windows (xy(z) images), where the number of the detection channels must be equal to or greater than the number of fluorophores. This simpler and faster method uses standard channel images (e.g., a 'green' channel and an 'orange' channel) and calculates a correction matrix based on how much 'green' signal is known to bleed into the 'orange' channel (and vice-versa) to remove the crosstalk. To set up optimal image acquisition and analysis protocol, we co-expressed three fluorescent proteins: EGFP, Venus, and mKO2, selected for their strong spectral overlap and high brightness. Each protein was targeted to its own cellular compartment; EGFP was localized in the cytoplasm, Venus in chloroplasts (pt-Venus) and mKO2 in nuclei (mKO2-N7). We opted for nuclei and chloroplasts localisation to enable automated segmentation and thus robust quantification. We have previously developed a script for chloroplast segmentation and quantification (Lukan et al., 2023), which we have now adapted for nuclei segmentation and quantification, allowing parallel analysis of up to four different fluorescent proteins (https://github.com/NIB-SI/Nuclei-segmentation). Cytoplasmic fluorescent proteins can alternatively be quantified using mean or cumulative fluorescence across the entire field of view or the remaining part that was not segmented, which is also an available option in the MATLAB script. Apart from co-expression of these

bioRxiv preprint doi: https://doi.org/10.64898/2026.03.13.711581; this version posted June 18, 2026. The copyright holder for this preprint (which was not certified by peer review) is the author/funder, who has granted bioRxiv a license to display the preprint in perpetuity. It is made available under a CC-BY-NC 4.0 International license.

three fluorescent proteins, we transformed plants with each of the proteins separately for generation of experimentally determined reference spectra (for spectral unmixing) or reference channels (for channel separation).

We first tested the spectral unmixing approach. As the selected fluorescent proteins have emission peaks close together, the narrowest possible (5 nm) λ-steps for the Leica's system, were required in image acquisition. Reference spectra were derived from FPbase or acquired experimentally from single-object regions of interest (ROIs) in plants expressing individual fluorescent proteins (Figure 3). Figure 3a illustrates spectral overlap between fluorescent proteins in selected xyλ images: at 510 and 525 nm EGFP (cytoplasm) overlaps with Venus (chloroplasts) and mKO2 (nuclei); and at 560 nm Venus and mKO2 overlap. Using FPbase spectra as references (Figure 3b) resulted in incomplete separation, with residual signals in unintended compartments (arrows, Figure 3b). Improved separation was achieved using experimentally acquired reference spectra (Figure 3c). However, we still observed an insignificant crosstalk signal (Figure 3c, arrows). This is likely due to organelle movement during prolonged imaging, especially at higher magnifications, and reduced signal-to-noise ratio due to narrow λ-steps imaging (Zimmermann, 2005).

bioRxiv preprint doi: https://doi.org/10.64898/2026.03.13.711581; this version posted June 18, 2026. The copyright holder for this preprint (which was not certified by peer review) is the author/funder, who has granted bioRxiv a license to display the preprint in perpetuity. It is made available under a CC-BY-NC 4.0 International license.

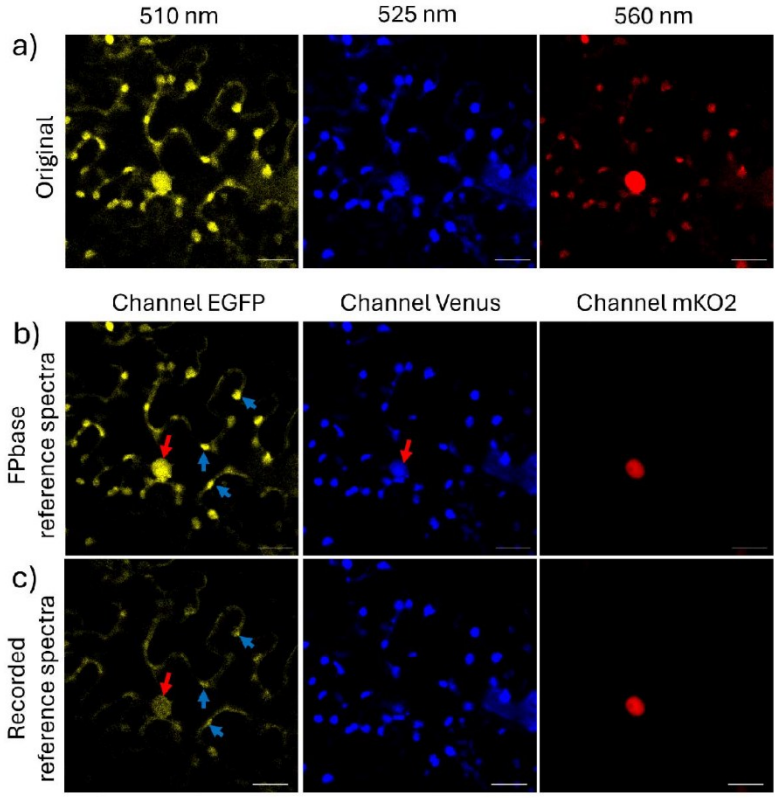


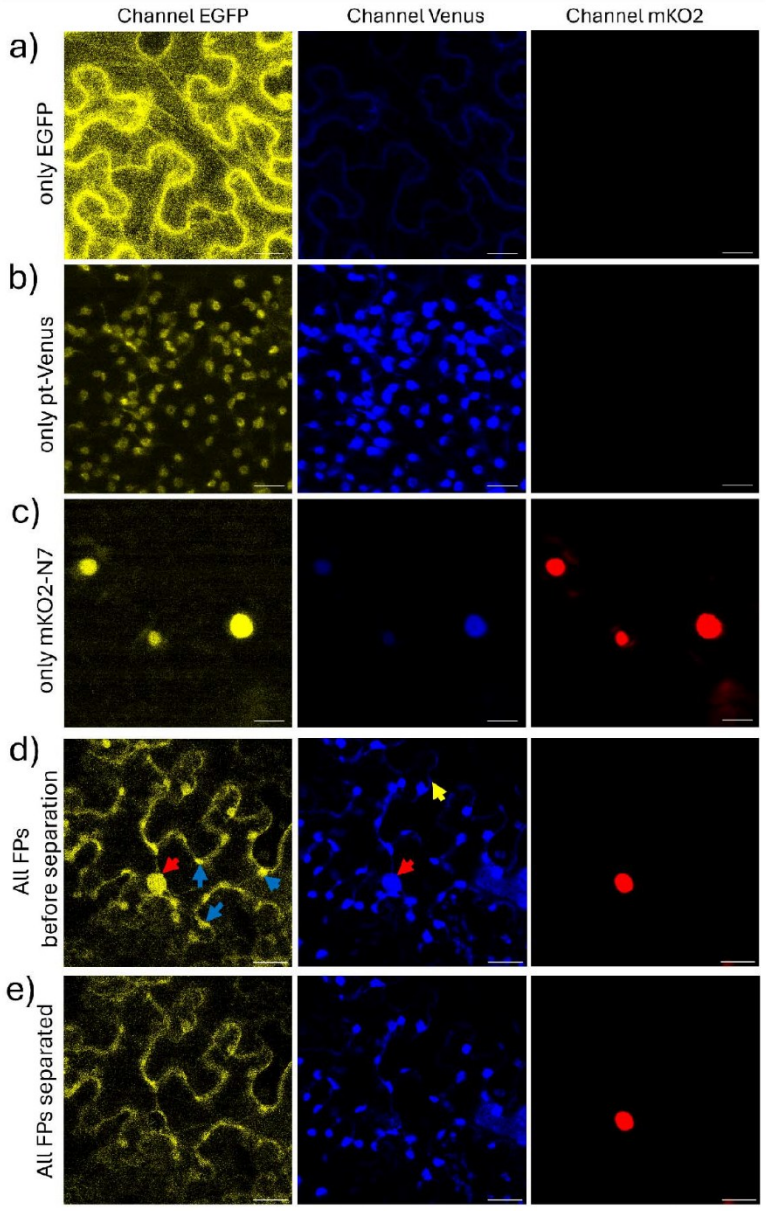
Figure 3: Accurate reference spectra are critical for effective spectral unmixing. (a) Selected images of an xyλ image show crosstalk between fluorescent proteins localized in different cellular compartments. From left to right: images taken at emission peak of EGFP (510 nm), Venus (525 nm) and mKO2 (560 nm). Spectral unmixing results using different reference spectra: (b) FPbase obtained reference spectra, and (c) experimentally recorded reference spectra. From left to right: images obtained after spectral unmixing showing EGFP, Venus and mKO2 channel. Examples of remaining crosstalk from mKO2 in the nucleus and Venus in the plastids after unmixing are pointed with red and blue arrows, respectively. Scale bar: 25 µm.

For unmixing of images obtained by standard acquisition channels (channel separation), reference channels were recorded from plants expressing single fluorescent proteins: (a) EGFP, (b) Venus, and (c) mKO2 (Figure 4). Experimental images were acquired from plants co-expressing all three proteins with the same acquisition settings as for reference channels. In all cases, imaging was performed in three channels with optimized emission windows for

bioRxiv preprint doi: https://doi.org/10.64898/2026.03.13.711581; this version posted June 18, 2026. The copyright holder for this preprint (which was not certified by peer review) is the author/funder, who has granted bioRxiv a license to display the preprint in perpetuity. It is made available under a CC-BY-NC 4.0 International license.

the selected fluorophores. Reference channels were then used to manually construct the crosstalk matrix, which was subsequently applied to the experimental images. This approach, which requires substantially shorter acquisition times and can also include channels excited with different lasers, produced results comparable to spectral unmixing using system-acquired reference spectra (Figure 4d□e vs. Figure 3). Quantitative analysis of residual crosstalk error across all unmixing approaches supported the qualitative observations (See Methods for quantification approach; results are presented in Table S1). The most effective separation across all acquired images was achieved using time-demanding spectral unmixing, followed by channel separation, both using experimentally obtained reference spectra. However, even when approximate spectra from FPbase were used, unmixing improved fluorophore separation compared to unprocessed images. For multiplexed fluorescent protein imaging, we therefore recommend channel separation as the preferred method, as its shorter acquisition time reduces motion artifacts and photobleaching while introducing only minimal residual crosstalk. While we used organelle-targeted fluorescent proteins for a robust quantification of unmixing accuracy, linear unmixing can also separate more than three overlapping and colocalized signals with comparable precision. As a proof of principle, we performed channel separation of five fluorescent proteins and chlorophyll (Figure 5). After channel separation, the remaining crosstalk (normalized to the unmixed signal in the main channel) was insignificant (2% for Venus signal in chlorophyll channel, 1% and 4% for chlorophyll signal in mCherry channel and mCardinal channel, respectively, 1% for mKO2 signal in the channels of chlorophyll, mCherry and mCardinal, 3% for mCherry signal in mCardinal channel and 2% for mCardinal signal in mCherry channel; Figure 5). All the remaining combinations of detected signal in other channels resulted in less than 1% of the remaining crosstalk. This demonstrates a significant improvement in signal separation compared to the crosstalk observed before separation (Table 4). However, any residual crosstalk should be taken into account when quantifying individual signals. In addition, crosstalk can be evaluated on a case-by-case basis by comparing subcellular localization at high magnification: strong pixel-wise spatial correlation between channels suggests persistent crosstalk, whereas distinct localization patterns indicate effective signal separation.

bioRxiv preprint doi: https://doi.org/10.64898/2026.03.13.711581; this version posted June 18, 2026. The copyright holder for this preprint (which was not certified by peer review) is the author/funder, who has granted bioRxiv a license to display the preprint in perpetuity. It is made available under a CC-BY-NC 4.0 International license.



299

bioRxiv preprint doi: https://doi.org/10.64898/2026.03.13.711581; this version posted June 18, 2026. The copyright holder for this preprint (which was not certified by peer review) is the author/funder, who has granted bioRxiv a license to display the preprint in perpetuity. It is made available under a CC-BY-NC 4.0 International license.

Figure 4: Channel separation produces results comparable to spectral unmixing. (a–c) Reference channels used to generate the unmixing matrix for individual fluorescent proteins: (a) EGFP, (b) pt-Venus, and (c) mKO2-N7. Input (d) and output (e) of channel separation for co-expressed EGFP, pt-Venus, and mKO2. Examples of crosstalk from mKO2 in the nucleus, Venus in the plastids and EGFP in the cytoplasm before unmixing are pointed with red, blue and yellow arrows, respectively. Scale bar: 25 µm.

Table S1: Quantification of successfulness of signal separation

Original or unmixed set of images	Crosstalk error estimate	Improvement of error compared to original image set (%)
Original set	2.29	0
Spectral unmixing using FPbase reference spectra	1.95	14.9
Channel separation using recorded reference images	1.89	17.5
Spectral unmixing using recorded reference spectra	1.80	21.2

bioRxiv preprint doi: https://doi.org/10.64898/2026.03.13.711581; this version posted June 18, 2026. The copyright holder for this preprint (which was not certified by peer review) is the author/funder, who has granted bioRxiv a license to display the preprint in perpetuity. It is made available under a CC-BY-NC 4.0 International license.

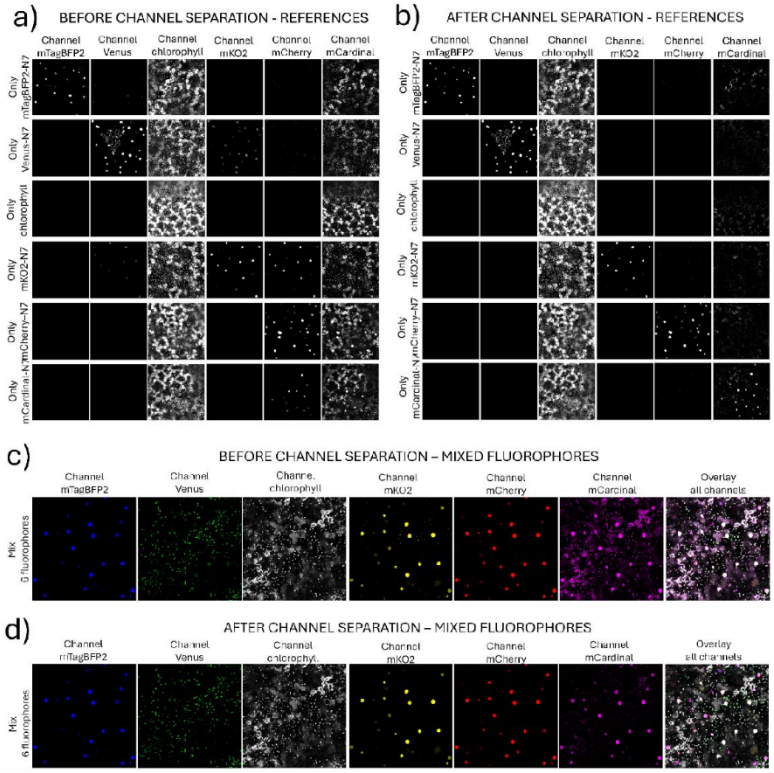


Figure 5: Channel separation enables separation of multiple overlapping fluorescent proteins and chlorophyll. (a) Reference channels of single fluorescent proteins with N7 localization signal for nuclei (mTagBFP2, Venus, mKO2, mCherry, and mCardinal), and chlorophyll channel were used to generate the crosstalk matrix. Images were acquired covering epidermis and mesophyll. (b) Reference channels after channel separation based on the crosstalk matrix produced from images in (a). Note a significant improvement after signal separation. (c-d) Coexpression of five fluorescent proteins (mTagBFP2, mKO2, mCherry and mCardinal in nuclei, and Venus in chloroplasts) and chlorophyll, before (c) and after (d) channel separation with crosstalk matrix calculated from (a). Images were acquired covering epidermis in a single plane. Full image diameter (instead of scale bar): 581 µm.

bioRxiv preprint doi: https://doi.org/10.64898/2026.03.13.711581; this version posted June 18, 2026. The copyright holder for this preprint (which was not certified by peer review) is the author/funder, who has granted bioRxiv a license to display the preprint in perpetuity. It is made available under a CC-BY-NC 4.0 International license.

Dye separation in practice: monitoring cell dynamics and distinguishing fluorescent proteins from autofluorescence

Segmenting nuclei in roots

Finally, we applied linear unmixing under realistic experimental conditions to demonstrate its potential for uncovering new biological insights. As shown earlier, fluorescent protein signals were markedly weaker in potato than in *N. benthamiana*, which limited detection due to a low signal-to-noise ratio. Plant roots are also highly autofluorescent, and in potato, root autofluorescence strongly overlaps with Venus emission, hindering automated nuclear segmentation (Figure 6). Image acquisition on the Stellaris 5 system followed by either spectral unmixing with 5 nm λ-steps or channel separation (Figure 6) increased the contrast between Venus-labelled nuclei and autofluorescent cell walls. Both approaches remarkably improved Venus detectability, enabling reliable automated nuclear segmentation and subsequent quantitative analysis (Figure S1).

bioRxiv preprint doi: https://doi.org/10.64898/2026.03.13.711581; this version posted June 18, 2026. The copyright holder for this preprint (which was not certified by peer review) is the author/funder, who has granted bioRxiv a license to display the preprint in perpetuity. It is made available under a CC-BY-NC 4.0 International license.

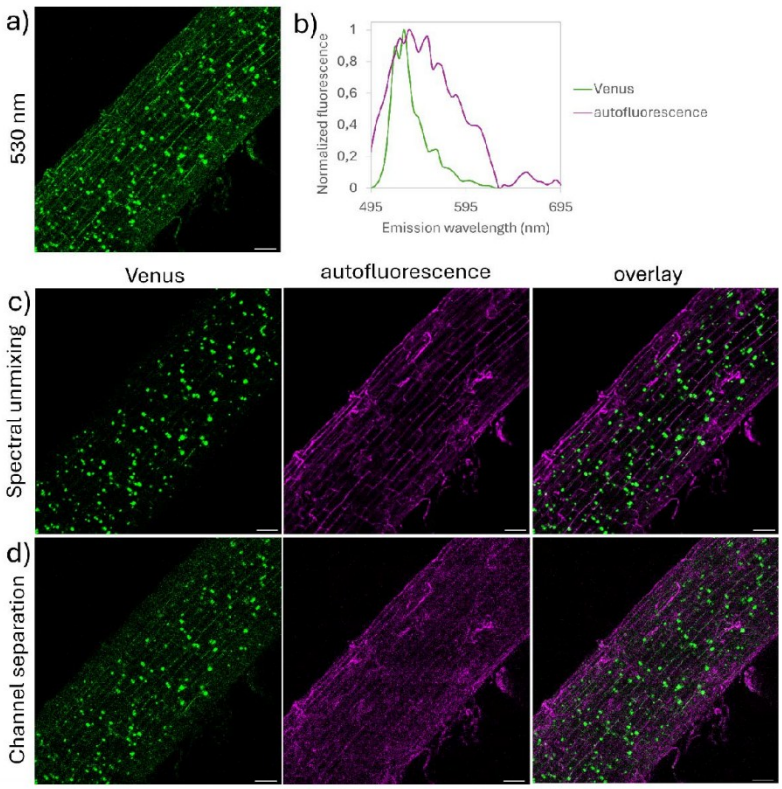


Figure 6: Spectral unmixing and channel separation enhance signal-to-noise ratio for fluorescent protein detection in plant roots. (a□b) Overlap of Venus-labelled nuclear emission (shown in green) with potato root autofluorescence (shown in purple). (c) Spectral unmixing of Venus and autofluorescence. (d) Channel separation of Venus and autofluorescence. From left to right: unmixed Venus, autofluorescence and overlay of both unmixed channels. Scale bar: 100 µm.

bioRxiv preprint doi: https://doi.org/10.64898/2026.03.13.711581; this version posted June 18, 2026. The copyright holder for this preprint (which was not certified by peer review) is the author/funder, who has granted bioRxiv a license to display the preprint in perpetuity. It is made available under a CC-BY-NC 4.0 International license.

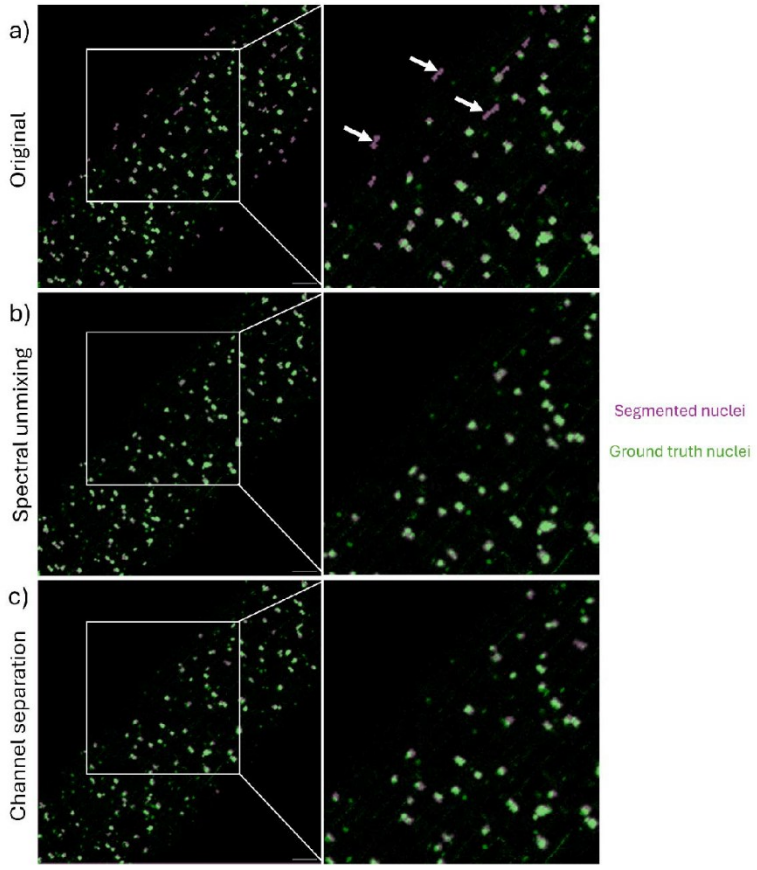


Figure S1: Spectral unmixing and channel separation enable correct segmentation of nuclei in plant root. Ground truth nuclei are marked in green, automatically segmented nuclei in purple. (a) Many nuclei were falsely segmented on image before unmixing (some instances pointed with arrows). Segmentation after (b) spectral unmixing and (c) channel separation is correct. Scale bar: 100 µm.

Separation of red fluorescent proteins from chlorophyll autofluorescence

Comparable to nuclear Venus fluorescence from potato root cell walls, nuclear mKate2 fluorescence could be clearly separated from chlorophyll autofluorescence in *N. benthamiana* leaves (Figure 7). In addition to spectral unmixing and channel separation

bioRxiv preprint doi: https://doi.org/10.64898/2026.03.13.711581; this version posted June 18, 2026. The copyright holder for this preprint (which was not certified by peer review) is the author/funder, who has granted bioRxiv a license to display the preprint in perpetuity. It is made available under a CC-BY-NC 4.0 International license.

353 described above, we evaluated a combined approach that exploits fluorescence lifetime
354 differences together with channel separation, using pulsed white-light laser excitation on the
355 Stellaris 8 system. Among the three methods, channel separation yielded the most effective
356 fluorophore distinction (Figure 7). Spectral unmixing performance was limited by sample
357 movement during long acquisition times (arrows in Figure 7 indicate nuclei appearing in the
358 chlorophyll channel). While the Tau gating lifetime-based approach also achieved satisfactory
359 signal separation, it resulted in an overall reduction of fluorescence intensity in both
360 channels, making this combined approach less effective than channel separation alone. Both
361 spectral unmixing and channel separation also enabled complete separation of mCardinal
362 and chlorophyll signals, despite their even larger emission overlap (Figure S2).

bioRxiv preprint doi: https://doi.org/10.64898/2026.03.13.711581; this version posted June 18, 2026. The copyright holder for this preprint (which was not certified by peer review) is the author/funder, who has granted bioRxiv a license to display the preprint in perpetuity. It is made available under a CC-BY-NC 4.0 International license.

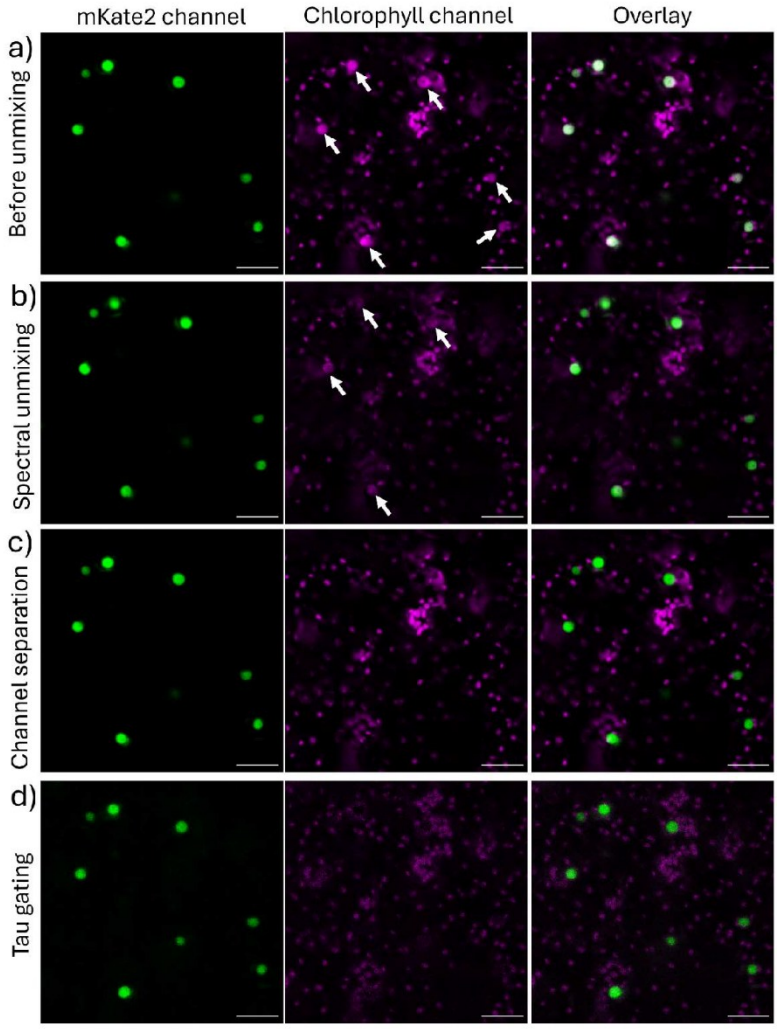


Figure 7: Chlorophyll autofluorescence can be unmixed from mKate2 based on spectral or lifetime properties. Arrows point to mKate2 crosstalk in the chlorophyll channel before and after unmixing. (a) Before unmixing, (b) spectral unmixing using recorded reference spectra, (c) channel separation of mKate2 and chlorophyll, (d) Tau gating followed by channel separation for unmixing. From left to right: mKate2, chlorophyll and overlay of both channels. Scale bar: 50 µm.

bioRxiv preprint doi: https://doi.org/10.64898/2026.03.13.711581; this version posted June 18, 2026. The copyright holder for this preprint (which was not certified by peer review) is the author/funder, who has granted bioRxiv a license to display the preprint in perpetuity. It is made available under a CC-BY-NC 4.0 International license.

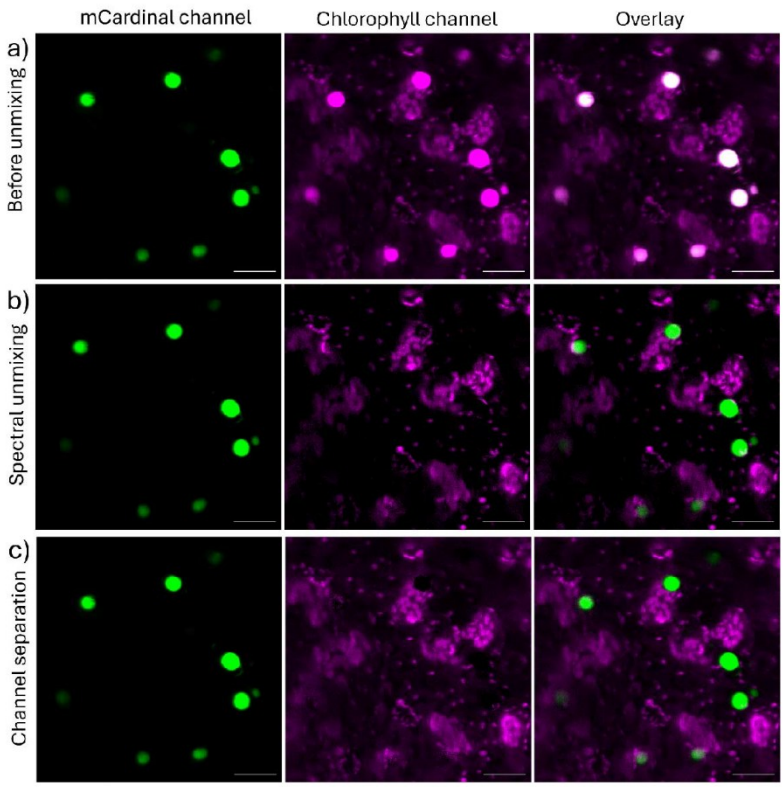


Figure S2: Chlorophyll autofluorescence can be unmixed from mCardinal based on emission spectra. (a) Before unmixing, (b) spectral unmixing using recorded reference spectra, (c) channel separation of mCardinal and chlorophyll. From left to right: mCardinal, chlorophyll and overlay of both channels. Scale bar: 50 µm.

Channel separation in live cell imaging

Channel separation can be effectively applied to study organelle dynamics and protein relocalization. As shown in Figures 3b□c and 6b, long acquisitions required for spectral unmixing are prone to disruption by organelle movement and dynamic changes in protein localisation. To overcome these limitations, we recommend simultaneous rather than sequential imaging of overlapping fluorophores, followed by channel separation. This approach enables faster acquisition and thus even real-time tracking of cellular dynamics.

bioRxiv preprint doi: https://doi.org/10.64898/2026.03.13.711581; this version posted June 18, 2026. The copyright holder for this preprint (which was not certified by peer review) is the author/funder, who has granted bioRxiv a license to display the preprint in perpetuity. It is made available under a CC-BY-NC 4.0 International license.

Using co-expression of strongly overlapping fluorescent proteins, pt-Venus and mKO2-N7 located in the plastids and nuclei, respectively, in *N. benthamiana* cells infected with GFP-tagged PVY (Lukan et al., 2023), where GFP localized to the cytoplasm and nuclei of infected cells, we demonstrated that channel separation supports the visualization of rapid and dynamic intracellular processes (Figure 8, Movie 1, Movie S1). Besides faster acquisition, channel separation offers greater flexibility, as it can incorporate fluorescent proteins excited by different laser lines and does not require exact reference spectra, which are strongly system dependent. However, successful application of this method requires reference images of individually expressed fluorescent proteins with comparable brightness in the experimental samples, in order to ensure sufficient signal and avoid signal saturation.

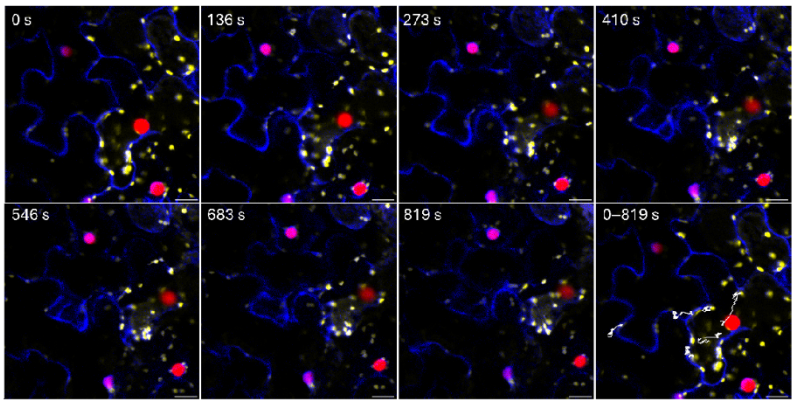


Figure 8: Capturing cell dynamics in PVY-infected cells of *N. benthamiana*. Channel separation enables distinction of cytoplasmic (blue, PVY-GFP) and organellar (yellow, chloroplasts tagged with pt-Venus, and red, nuclei tagged with mKO2-N7) movements in infected cells. Bottom right: tracked movement of selected plastids through time course aligned to the first image (0 s). Scale bar: 25 µm.

Conclusion

We compared different approaches for separating fluorescent proteins with overlapping excitation and emission spectra in plant leaves. Both spectral unmixing and channel separation effectively distinguished fluorophores, with spectral unmixing achieving the highest accuracy when exact reference spectra were available. However, its application was limited by long acquisition times and motion artifacts, especially at higher magnifications. Channel separation, in contrast, provided comparable separation accuracy with substantially faster acquisition and greater flexibility, allowing the use of multiple laser lines or fluorescence lifetimes. While fluorescence lifetime-based unmixing offered partial improvements, it resulted in lower overall signal intensity.

bioRxiv preprint doi: https://doi.org/10.64898/2026.03.13.711581; this version posted June 18, 2026. The copyright holder for this preprint (which was not certified by peer review) is the author/funder, who has granted bioRxiv a license to display the preprint in perpetuity. It is made available under a CC-BY-NC 4.0 International license.

Overall, our results demonstrate that channel separation offers the best balance between accuracy, speed and robustness and provide a practical framework for optimizing multiplexed fluorescent imaging in plant systems. We showed that five fluorescent proteins and chlorophyll can be separated with insignificant crosstalk. This practical framework would be especially valuable when combining multiple fluorescent protein-based transcriptional reporters in the same plant to follow precise spatiotemporally linked processes, such as different hormonal signalling pathways. Moreover, fluorescent protein multiplexing can prove useful when combining new fluorescent proteins with the existent genetically encoded biosensors which rely on fluorescent proteins with special features (such as fast-maturing Venus in markers of protein degradation (Larrieu et al., 2015; Mir et al., 2016; Song et al., 2021)), e.g. to follow proposed consecutive steps in signalling cascades. However, this approach has limitation for applications requiring high precision, such as colocalization studies, and cannot be used within the same excitation/emission range of ratiometric biosensors such as FRET-based biosensors or roGFP and HyPer and biosensors with normalization channel (Belousov et al., 2006; Hanson et al., 2004; Miyawaki et al., 1997). In such cases, we recommend using non-overlapping fluorophores, such as a combination of mTagBFP2, Venus, and mKate2 or mCardinal, or targeting overlapping fluorophores to different subcellular compartments. To promote reproducibility, we provide MATLAB scripts for nuclear segmentation and signal quantification.

Finally, although databases such as FPbase provide valuable reference data on fluorescent protein brightness and emission spectra, these values may not accurately represent achievable brightness *in planta* or the detected emission profiles. The latter are influenced primarily by the specific confocal system and acquisition settings rather than by the plant tissue itself.

Materials and methods

Plant Material and Growth Conditions

NahG-Désirée potato plants were obtained from the Leibniz Institute of Plant Biochemistry, Halle, Germany. Désirée, *NahG*-Désirée and newly transformed potato plants were maintained in stem node tissue culture as previously described by Baebler et al. (2009). Two weeks after node segmentation in MS30 agar medium, the plants were transferred to soil and cultivated in a growth chamber under controlled environmental conditions □ 22 °C in the light and 19 °C in the dark, at a relative humidity of 55%, with 120 µmol/m^2/s radiation for potato (35% white, 5% deep-red and 10% far-red LED lights; PSI, Brno, Czechia) with 16 h photoperiod. *N. benthamiana* were grown from seeds sown to soil and grown as potato

bioRxiv preprint doi: https://doi.org/10.64898/2026.03.13.711581; this version posted June 18, 2026. The copyright holder for this preprint (which was not certified by peer review) is the author/funder, who has granted bioRxiv a license to display the preprint in perpetuity. It is made available under a CC-BY-NC 4.0 International license.

446 plants but with 80 µmol/m^2/s radiation (20% white, 3% deep-red and 3% far-red LED lights;
447 PSI, Brno, Czechia). Three to five weeks old, soiled potato and *N. benthamiana* plants were
448 used for the experiments.

449 **Cloning and Vector Construction**

450 Fluorescent protein coding sequences and localization signals were obtained from various
451 sources. N7 localization signal together with mTurquoise2, Venus, and mKate2 (plasmids
452 pHG128, pHG132, and pHG154, respectively) were kindly provided by Hassan Ghareeb
453 (Ghareeb et al., 2016). mTagBFP2 (plasmid pJL1-mTagBFP2; Addgene #102638; (Stark et
454 al., 2018)), mKO2 (plasmid pTU-A-005; Addgene #124412; (Santos-Moreno & Schaerli,
455 2019)), mCardinal (plasmid mCardinal-pBAD; Addgene #54800; (Chu et al., 2014)) , and
456 miRFP713 (plasmid pmiRFP713-N1; Addgene #136559; (Matlashov et al., 2020)) were
457 obtained from Addgene. The plastid transit peptide was amplified from pt-roGFP plasmid
458 kindly provided by Jacob O. Brunkard (Stonebloom et al., 2012), and the H2B nuclear
459 localization signal from the H2B-RFP plasmid kindly provided by Jim Haseloff and Fernán
460 Federici (University of Cambridge, UK).

461 Fluorescent protein and localization signal coding sequences were assembled through PCR
462 (Table S2) using Phusion® High-Fidelity DNA Polymerase (New England Biolabs, Ipswich,
463 MA, USA) with primers listed in Table S3. PCR products were cloned into the pENTR/D-
464 TOPO vector (Thermo Fisher Scientific, MA, USA) following the manufacturer's instructions.
465 Constructs were then recombined into binary destination vectors (pB7WG2, pK7WG2, or
466 pH7WG2; VIB Vector Vault, Belgium) via LR reaction (Thermo Fisher Scientific, MA, USA).
467 Chemically competent *E. coli* were transformed with the constructs with heat shock. After
468 growth on selection, plasmids were isolated from transformed *E. coli* colonies using the
469 GenElute™ Plasmid Miniprep Kit (Merck, Vienna, Austria). Sequencing was performed by
470 GATC Biotech using commercial M13 forward and reverse primers (Thermo Fisher Scientific,
471 MA, USA). Finally, constructs were introduced into *Agrobacterium tumefaciens* strains
472 GV3101 and LBA4404 via electroporation for transient or stable transformation of *N.*
473 *benthamiana* and potato as explained below.

474 **Transient transformation**

475 For transient transformation, *Agrobacterium tumefaciens* strain GV3101 carrying
476 pB7WG2_Venus-N7, pB7WG2_mTurquoise2-N7, pB7WG2_mCherry-N7, pB7WG2_mKate2-
477 N7, pK7WG2_mKO2-N7, pK7WG2_miRFP713-N7, pK7WG2_mCardinal-N7,
478 pK7WG2_mTagBFP2-N7, pH7WG2_Venus, pH7WG2_pt-Venus, and pH7WG2_H2B-Venus
479 and strain LBA4404 carrying pB7WG2_Venus-N7, pB7WG2_mTurquoise2-N7,
480 pB7WG2_mCherry-N7, pK7WG2_mKate2-N7, pK7WG2_mKO2-N7, pK7WG2_mCardinal-

bioRxiv preprint doi: https://doi.org/10.64898/2026.03.13.711581; this version posted June 18, 2026. The copyright holder for this preprint (which was not certified by peer review) is the author/funder, who has granted bioRxiv a license to display the preprint in perpetuity. It is made available under a CC-BY-NC 4.0 International license.

N7, pK7WG2_mTagBFP2-N7, pH7WG2_Venus, pH7WG2_pt-Venus, and pH7WG2_H2B-Venus were grown overnight at 28 °C with shaking at 200 rpm. After 18 h, cultures were centrifuged, and the pellet was resuspended in infiltration buffer containing 10 mM MES, 10 mM $MgCl_2$ and 0.15 mM acetosyringone to an OD_{600} 0.3–0.5. For signal comparison, the OD_{600} of Agrobacteria suspensions was adjusted to ensure a maximum difference of 0.05. The suspension was incubated at room temperature with gentle shaking (about 20 rpm) for 2–4 h prior agroinfiltration. Three- to five-week-old *N. benthamiana* were used for transient transformation. For comparison of fluorescent protein brightness only GV3101 strain was used.

Virus inoculation

On the day of agroinfiltration, four weeks old *N. benthamiana* were first inoculated with PVY-N605(123)-GFP (Lukan et al., 2023) as previously described (Milavec et al., 2008). Briefly, systemic leaves of *N. clevelandii* plants inoculated with PVY-N605(123)-GFP were homogenized in PBS, pH 7.6 (4 ml of buffer per 1 g of infected tissue). The homogenized solution was gently rubbed on the *N. benthamiana* leaf surface sprinkled with carborundum and washed after 10 min.

Stable transformation

Stable transformations of potato plants cv. Désirée or *NahG*-Désirée with fluorescent protein constructs (pK7WG2_mKate2, pK7WG2_mKO2, and pB7WG2_Venus) were carried out as described in Lukan et al. (2023). Transgenic lines were screened for construct expression using confocal microscopy.

Confocal microscopy

Confocal imaging was performed using a Leica TCS LSI system with a PMT detector or Leica Stellaris 5 and Stellaris 8 systems with three HyD S detectors. All images were acquired with Plan APO 20×/0.75 NA objectives using LAS X software (Leica Microsystems, Wetzlar, Germany). Exact imaging settings are available in .lif files, image Properties (.lif files are available on Zenodo:10.5281/zenodo.19691651). To enable cross-comparison with other laser scanning confocal systems, we provide the then-current maximum laser powers measured by our service provider: Leica TCS LSI: 405 nm – 2.6 mW, 488 nm – 5.8 mW, 532 nm – 7.0 mW, 635 nm – 2.4 mW. Stellaris 5: 405 nm – 48 mW, 488 nm – 59 mW, 561 nm – 165 mW, 638 nm – 159 mW. Stellaris 8: 405 nm – 50 mW, 488 nm – 20 mW, WLL 5 mW. To enable cross-comparison of fluorescent protein excitability primarily based on laser intensity, we performed brightness imaging using 20 nm–wide emission windows and the same

bioRxiv preprint doi: https://doi.org/10.64898/2026.03.13.711581; this version posted June 18, 2026. The copyright holder for this preprint (which was not certified by peer review) is the author/funder, who has granted bioRxiv a license to display the preprint in perpetuity. It is made available under a CC-BY-NC 4.0 International license.

514 detector, whose sensitivity was kept constant across different lasers within the same confocal
515 system.

516 *Emission Spectra and Brightness Measurements*

517 Emission spectra were measured in xyλ scanning mode (λ scan) with 5□nm wide steps and
518 5 nm apart on leaves of transiently transformed *N. benthamiana* plants and stably
519 transformed potato plants. Excitation was performed using 405, 488 or 532 nm lasers (TCS
520 LSI), 405, 488, or 561□nm lasers (Stellaris 5) and 405□nm or a white light laser with
521 wavelength selected just below the emission range (Stellaris 8).

522 *Linear unmixing: Spectral unmixing approach*

523 For spectral unmixing, xyλ images were acquired with steps 5□nm wide and 5 nm apart.
524 Experimental and reference spectra were acquired with identical λ-steps to ensure accurate
525 spectral matching. Imaging was performed on Stellaris 5 using 488 nm laser.

526 *Linear unmixing: Channel separation approach*

527 For channel separation, images were acquired in multi-channel mode, with each fluorophore
528 captured in its own channel. Detectors gain and emission windows were optimized to
529 balance fluorophore brightness and minimize bleed-through (Table 1, Table 2), ensuring
530 effective separation with minimal signal loss. For separation of mKate2 and chlorophyll based
531 on their fluorescence lifetime, Tau gating was applied at 1.5 ns.

532 **Table 1: Optimal confocal settings for Channel separation imaging of 4 fluorophores**

Fluorophore	Excitation laser (nm) and laser power	Emission window (nm)	Detector gain
EGFP	488. 5%	497–515	70
Venus	488. 5%	515–547	50
mKO2	561. 2%	572–623	2
Chlorophyll	488. 5%	663–740	50

533

534 **Table 2: Optimal confocal settings for Channel separation imaging of 6 fluorophores**

Fluorophore	Excitation laser (nm) and laser power	Emission window (nm)	Detector gain
mTagBFP2	405. 42%	425–470	2
Venus	488. 2%	515–520	2

bioRxiv preprint doi: https://doi.org/10.64898/2026.03.13.711581; this version posted June 18, 2026. The copyright holder for this preprint (which was not certified by peer review) is the author/funder, who has granted bioRxiv a license to display the preprint in perpetuity. It is made available under a CC-BY-NC 4.0 International license.

Chlorophyll	488. 2%	670–730	2
mKO2	WLL 540. 2%	550–570	2
mCherry	WLL 590. 2.5%	595–635	2
mCardinal	WLL 640. 2%	645–700	2

535 WLL, white light laser.

536 **Data analyses**

537 All results of image analyses have been deposited on Zenodo: 10.5281/zenodo.19691651.

538 *Emission and Tau spectra analysis*

539 Average emission and Tau spectra were determined from 15–30 manually selected nuclei
540 across 2–3 micrographs. Chlorophyll autofluorescence was measured in non-transformed *N.*
541 *benthamiana* by analysing the entire field of view. Average emission and Tau spectra across
542 all nuclei were exported from LAS X (Figure 1).

543 *Brightness analysis*

544 Fluorescent protein brightness was quantified as cumulative fluorescence from manually
545 selected nuclei in xyλ images, measured from 5 nm above the laser wavelength (Stellaris 5)
546 or from the beginning of the emission range (Stellaris 8) up to 640 nm to exclude chlorophyll
547 interference (Figure 2). Brightness was determined on 15–30 manually selected nuclei
548 across 2–3 micrographs. Expected relative fluorescence (Figure 2) was calculated from data
549 available at FPbase.org: achievable brightness = brightness × excitation strength at used
550 laser wavelength.

551 *Linear unmixing: Spectral unmixing approach*

552 Spectral unmixing was used to separate fluorophores excited by the same laser with
553 overlapping emission spectra. Spectral unmixing was performed on xyλ images using *LAS X*
554 *Dye Separation* module, *Spectral Unmixing* tool. Reference spectra were obtained from
555 FPbase.org or acquired on plants expressing single fluorescent protein and used by the LAS
556 X Spectral Unmixing tool to mathematically assign emission contributions to individual
557 fluorophores.

558 *Linear unmixing: Channel separation approach*

559 Channel separation was used to separate fluorophores with overlapping emission, with
560 excitation from the same or different laser lines using *LAS X Dye Separation, Channel Dye*

bioRxiv preprint doi: https://doi.org/10.64898/2026.03.13.711581; this version posted June 18, 2026. The copyright holder for this preprint (which was not certified by peer review) is the author/funder, who has granted bioRxiv a license to display the preprint in perpetuity. It is made available under a CC-BY-NC 4.0 International license.

Separation tool. Channel separation was performed using the *LAS X Dye Separation* module with the *Automatic Dye Separation* tool in *manual* mode. Reference images of single fluorescent proteins were used to calculate a crosstalk matrix (Table 3), with the following assignments: Dye 1 – EGFP (cytoplasm), Dye 2 – Venus (plastids), Dye 3 – chlorophyll, and Dye 4 – mKO2 (nuclei). Channels were defined as Ch1 – primarily EGFP, Ch2 – primarily Venus, Ch3 – primarily chlorophyll, and Ch4 – primarily mKO2. Crosstalk matrix was determined on images acquired on plants expressing single fluorescent protein, normalized to its main channel. More specifically, the brightest object with least chlorophyll bleed-through for each fluorescent protein was manually selected, and its pixel intensities across individual channels were used to build the matrix. Average pixel intensities across individual channels were normalized to the brightest channel of the corresponding fluorescent protein. The matrix was corrected for chlorophyll contributions, which were present in Ch3 for all dyes, by assigning a value of 0 for Dye 1, 2, and 4. This corrected matrix was then applied to unmix images acquired in multichannel mode.

Table 3: Matrix used for unmixing of 4 fluorophores

	Ch1	Ch2	Ch3	Ch4
Dye 1	1.00	0.16	0.00	0.00
Dye 2	0.41	1.00	0.00	0.00
Dye 3	0.00	0.00	1.00	0.00
Dye 4	0.34	0.17	0.00	1.00

For separation of six fluorophores, new reference and experimental images containing individual fluorophores were acquired and crosstalk matrix (Table 4) was calculated based on the signal in the nuclei (fluorescent proteins with N7 nuclear localization marker) or within a large portion of image (chlorophyll). Dye 1 – mTagBFP2, Dye 2 – Venus, Dye 3 – chlorophyll, Dye 4 – mKO2, Dye 5 – mCherry, Dye 6 – mCardinal; Ch1 – primarily mTagBFP2, Ch2 – primarily Venus, Ch3 – primarily chlorophyll, Ch4 – primarily mKO2, Ch5 – primarily mCherry, Ch6 – primarily mCardinal. The matrix was not corrected for chlorophyll contributions. This crosstalk matrix was applied to unmix images of separate (Figure 5b) and mixed (Figure 5d) fluorophores.

Table 4: Matrix used for unmixing of 6 fluorophores

	Ch1	Ch2	Ch3	Ch4	Ch5	Ch6
Dye 1	1.00	0.02	0.03	0.00	0.00	0.00
Dye 2	0.00	1.00	0.13	0.08	0.01	0.02
Dye 3	0.00	0.00	1.00	0.00	0.00	0.35
Dye 4	0.00	0.06	0.18	1.00	0.45	0.15
Dye 5	0.00	0.00	0.17	0.01	1.00	0.56
Dye 6	0.00	0.00	0.41	0.00	0.23	1.00

bioRxiv preprint doi: https://doi.org/10.64898/2026.03.13.711581; this version posted June 18, 2026. The copyright holder for this preprint (which was not certified by peer review) is the author/funder, who has granted bioRxiv a license to display the preprint in perpetuity. It is made available under a CC-BY-NC 4.0 International license.

586

587 *Segmentation followed by estimation of error after linear unmixing*

588 Residual crosstalk after channel separation or spectral unmixing was quantified using
589 histogram areas of segmented objects, with each fluorescent protein localized to a distinct
590 cellular compartment. The segmentation and histograms were acquired using MATLAB script
591 (https://github.com/NIB-SI/Nuclei-segmentation). The parameters used in the script to
592 achieve appropriate segmentation are listed on GitHub, Case 1 (https://github.com/NIB-
593 SI/Nuclei-segmentation).

594 Crosstalk error was quantified as error = $\mathrm{sqrt}(((\mu_1-\mu_{teor1})/\sigma_1)^2+ (\mu_2-\mu_{teor2})/\sigma_2)^2)$, where μ is an
595 average value of histogram area for unmixed signal of the segmented FP in a channel with
596 the residual crosstalk and σ is standard deviation of histogram area for unmixed signal of the
597 segmented FP in the same channel. E.g. crosstalk error of mKO2 was calculated using the
598 average value of histogram area in segmented nuclei in Venus (μ_1), and EGFP (μ_2), channel,
599 and standard deviation in the segmented nuclei in corresponding channels. μ_{teor} equals 0 as
600 theoretical remaining crosstalk after unmixing equals 0. Fifteen images were used for
601 quantification of crosstalk error. Error was estimated for each cellular compartment
602 (containing one fluorescent protein) separately and an average error calculated for all three
603 fluorescent proteins is presented in Table S1.

604 *Nuclei segmentation in images with root autofluorescence*

605 Automated segmentation of nuclei in root was performed using the provided MATLAB script
606 using the parameters listed on GitHub, Case 2 (https://github.com/NIB-SI/Nuclei-
607 segmentation).

608 *Plastid tracking*

609 For visualization and to distinguish plastid movements from sample drift, we used a MATLAB
610 tracking tool (Track2, custom script). Time-lapse confocal stacks were split into individual
611 frames in FIJI (ImageJ) and imported into Track2. A stable nucleus was tracked first to
612 estimate in-plane stage drift (x–y), which was subtracted from all frames for drift correction.
613 We then tracked multiple plastids. Track coordinates were exported to Excel for plotting, and
614 tracks were overlaid on the first confocal frame for visualization.

615

bioRxiv preprint doi: https://doi.org/10.64898/2026.03.13.711581; this version posted June 18, 2026. The copyright holder for this preprint (which was not certified by peer review) is the author/funder, who has granted bioRxiv a license to display the preprint in perpetuity. It is made available under a CC-BY-NC 4.0 International license.

Acknowledgements

We thank Tjaša Mahkovec Povalej for her help with experimental work and Miha Tome for reading and commenting on the draft. Potato plants were obtained from the Leibniz Institute of Plant Biochemistry, Halle, Germany (cv. Désirée). This research was funded by the Slovenian Research and Innovation Agency (research core funding No. P4-0165 and P4-0463, projects J4-1777, J4-60073, J4-70169 and ARIS program for young researchers).

References

Baebler, Š., Krečič-Stres, H., Rotter, A., Kogovšek, P., Cankar, K., Kok, E. J., Gruden, K., Kovač, M., Žel, J., Pompe-Novak, M., & Ravnikar, M. (2009). PVYNTN elicits a diverse gene expression response in different potato genotypes in the first 12 h after inoculation. *Molecular Plant Pathology*, *10*(2), 263–275. https://doi.org/10.1111/j.1364-3703.2008.00530.x

Brunoud, G., Wells, D. M., Oliva, M., Larrieu, A., Mirabet, V., Burrow, A. H., Beeckman, T., Kepinski, S., Traas, J., Bennett, M. J., & Vernoux, T. (2012). A novel sensor to map auxin response and distribution at high spatio-temporal resolution. *Nature 2012 482:7383*, *482*(7383), 103–106. https://doi.org/10.1038/nature10791

Chu, J., Haynes, R. D., Corbel, S. Y., Li, P., González-González, E., Burg, J. S., Ataie, N. J., Lam, A. J., Cranfill, P. J., Baird, M. A., Davidson, M. W., Ng, H. L., Garcia, K. C., Contag, C. H., Shen, K., Blau, H. M., & Lin, M. Z. (2014). Non-invasive intravital imaging of cellular differentiation with a bright red-excitable fluorescent protein. *Nature Methods*, *11*(5), 572–578. https://doi.org/10.1038/NMETH.2888

Cranfill, P. J., Sell, B. R., Baird, M. A., Allen, J. R., Lavagnino, Z., De Gruiter, H. M., Kremers, G. J., Davidson, M. W., Ustione, A., & Piston, D. W. (2016). Quantitative assessment of fluorescent proteins. *Nature Methods 2016 13:7*, *13*(7), 557–562. https://doi.org/10.1038/nmeth.3891

Day, R. N., & Davidson, M. W. (2009). The fluorescent protein palette: tools for cellular imaging. *Chemical Society Reviews*, *38*(10), 2921. https://doi.org/10.1039/B901966A

Donaldson, L. (2020). Autofluorescence in Plants. *Molecules*, *25*(10). https://doi.org/10.3390/MOLECULES25102393

Ghareeb, H., Laukamm, S., & Lipka, V. (2016). COLORFUL-Circuit: A Platform for Rapid Multigene Assembly, Delivery, and Expression in Plants. *Frontiers in Plant Science 7*, 246. https://doi.org/10.3389/fpls.2016.00246

Lambert, T. J. (2019). FPbase: a community-editable fluorescent protein database. *Nature Methods 2019 16:4*, *16*(4), 277–278. https://doi.org/10.1038/s41592-019-0352-8

Larrieu, A., Champion, A., Legrand, J., Lavenus, J., Mast, D., Brunoud, G., Oh, J., Guyomarc'H, S., Pizot, M., Farmer, E. E., Turnbull, C., Vernoux, T., Bennett, M. J., & Laplaze, L. (2015). A fluorescent hormone biosensor reveals the dynamics of jasmonate signalling in plants. *Nature Communications*, *6*(1), 1–9. https://doi.org/10.1038/ncomms7043

bioRxiv preprint doi: https://doi.org/10.64898/2026.03.13.711581; this version posted June 18, 2026. The copyright holder for this preprint (which was not certified by peer review) is the author/funder, who has granted bioRxiv a license to display the preprint in perpetuity. It is made available under a CC-BY-NC 4.0 International license.

653 Lukan, T., & Coll, A. (2022). Intertwined Roles of Reactive Oxygen Species and Salicylic Acid Signaling
654 Are Crucial for the Plant Response to Biotic Stress. *International Journal of Molecular Sciences*,
655 *23*(10), 5568. https://doi.org/10.3390/IJMS23105568

656 Lukan, T., Županič, A., Mahkovec Povalej, T., Brunkard, J. O., Kmetič, M., Juteršek, M., Baebler, Š., &
657 Gruden, K. (2023). Chloroplast redox state changes mark cell-to-cell signaling in the
658 hypersensitive response. *New Phytologist*, *237*(2), 548–562. https://doi.org/10.1111/nph.18425

659 Matlashov, M. E., Shcherbakova, D. M., Alvelid, J., Baloban, M., Pennacchietti, F., Shemetov, A. A.,
660 Testa, I., & Verkhusha, V. V. (2020). A set of monomeric near-infrared fluorescent proteins for
661 multicolor imaging across scales. *Nature Communications*, *11*(1).
662 https://doi.org/10.1038/S41467-019-13897-6

663 Milavec, M., Gruden, K., Ravnikar, M., & Kovač, M. (2008). Peroxidases in the early responses of
664 different potato cultivars to infection by Potato virus YNTN. *Plant Pathology*, *57*(5), 861–869.
665 https://doi.org/10.1111/J.1365-3059.2008.01833.X

666 Mir, R., Aranda, L. Z., Biaocchi, T., Luo, A., Sylvester, A. W., & Rasmussen, C. G. (2016). A DII Domain-
667 Based Auxin Reporter Uncovers Low Auxin Signaling during Telophase and Early G1. *Plant*
668 *Physiology*, *173*(1), 863. https://doi.org/10.1104/PP.16.01454

669 Mylle, E., Codreanu, M. C., Boruc, J., & Russinova, E. (2013). Emission spectra profiling of fluorescent
670 proteins in living plant cells. *Plant Methods*, *9*(1), 1–8. https://doi.org/10.1186/1746-4811-9-10

671 Rajeevkumar, S., Anunanthini, P., & Sathishkumar, R. (2015). Epigenetic silencing in transgenic plants.
672 *Frontiers in Plant Science*, *6*(September), 152056. https://doi.org/10.3389/FPLS.2015.00693

673 Rigoulot, S. B., Schimel, T. M., Lee, J. H., Sears, R. G., Brabazon, H., Layton, J. S., Li, L., Meier, K. A.,
674 Poindexter, M. R., Schmid, M. J., Seaberry, E. M., Brabazon, J. W., Madajian, J. A., Finander, M. J.,
675 DiBenedetto, J., Occhialini, A., Lenaghan, S. C., & Stewart, C. N. (2021). Imaging of multiple
676 fluorescent proteins in canopies enables synthetic biology in plants. *Plant Biotechnology*
677 *Journal*, *19*(4), 830. https://doi.org/10.1111/PBI.13510

678 Santos-Moreno, J., & Schaerli, Y. (2019). A Framework for the Modular and Combinatorial Assembly
679 of Synthetic Gene Circuits. *ACS Synthetic Biology*, *8*(7), 1691–1697.
680 https://doi.org/10.1021/ACSSYNBIO.9B00174

681 Shu, X., Royant, A., Lin, M. Z., Aguilera, T. A., Lev-Ram, V., Steinbach, P. A., & Tsien, R. Y. (2009).
682 Mammalian expression of infrared fluorescent proteins engineered from a bacterial
683 phytochrome. *Science (New York, N.Y.)*, *324*(5928), 807.
684 https://doi.org/10.1126/SCIENCE.1168683

685 Stark, J. C., Huang, A., Nguyen, P. Q., Dubner, R. S., Hsu, K. J., Ferrante, T. C., Anderson, M.,
686 Kanapskyte, A., Mucha, Q., Packett, J. S., Patel, P., Patel, R., Qaq, D., Zondor, T., Burke, J.,
687 Martinez, T., Miller-Berry, A., Puppala, A., Reichert, K., … Jewett, M. C. (2018). BioBits^{TM} Bright: A
688 fluorescent synthetic biology education kit. *Science Advances*, *4*(8).
689 https://doi.org/10.1126/SCIADV.AAT5107

690 Stonebloom, S., Brunkard, J. O., Cheung, A. C., Jiang, K., Feldman, L., & Zambryski, P. (2012). Redox
691 States of Plastids and Mitochondria Differentially Regulate Intercellular Transport via
692 Plasmodesmata. *Plant Physiology*, *158*(1), 190–199. https://doi.org/10.1104/PP.111.186130

bioRxiv preprint doi: https://doi.org/10.64898/2026.03.13.711581; this version posted June 18, 2026. The copyright holder for this preprint (which was not certified by peer review) is the author/funder, who has granted bioRxiv a license to display the preprint in perpetuity. It is made available under a CC-BY-NC 4.0 International license.

693 Xiao, H., Li, M., Ohad, N., & Hao, G. F. (2025). Genetically encoded biosensors for spatiotemporal
694 monitoring of plant proteins in growth and stress responses. *Advanced Agrochem*, *4*(3), 177–
695 187. https://doi.org/10.1016/J.AAC.2025.03.002

696 Zhang, H., Zhao, Y., & Zhu, J. K. (2020). Thriving under Stress: How Plants Balance Growth and the
697 Stress Response. *Developmental Cell*, *55*(5), 529–543.
698 https://doi.org/10.1016/J.DEVCEL.2020.10.012

699 Zhang, H., Zhu, J., Gong, Z., & Zhu, J. K. (2021). Abiotic stress responses in plants. *Nature Reviews*
700 *Genetics 2021 23:2*, *23*(2), 104–119. https://doi.org/10.1038/s41576-021-00413-0

701 Zimmermann, T. (2005). Spectral imaging and linear unmixing in light microscopy. *Advances in*
702 *Biochemical Engineering/Biotechnology*, *95*, 245–265. https://doi.org/10.1007/B102216

703

Chapter 3

Discussion

Biosensors, including genetically encoded biosensors, became indispensable tools in biological research. Especially genetically encoded biosensors that rely on fluorescent proteins, enable insights into spatiotemporal dynamics *in vivo* at whole organism, tissue, cell and subcellular level. Considering novel insights into plant immunity, biosensors are key to research the quantity of the involved molecules or their spatiotemporal coordination. With that, they inform and complement omics analyses by contextualizing the results and highlight critical time points and spatial context. Their time-series data can also infer parameters for mathematical models, detect emergent behaviours (thresholds, crosstalk between the modules, feedback loops) and validate them.

In our experiments, we used genetically encoded biosensors in potato leaves and followed responses to herbivore and mechanical wounding. Wounding often precedes or occurs concurrently with pathogen infection, making it impossible to study the infection process independently of wounding. Single-cell sequencing is increasingly used to investigate various plant-pathogen systems, with the goal of identifying cell-specific responses based on cell type or distance from the infected tissue. However, in plants, single-cell approaches require protoplasting—the removal of cell walls—which itself triggers a response similar to wounding (Delannoy et al., 2023). As a result, early wounding-related gene responses are often masked in the data, appearing in both mock treatments and negative controls. Although studies suggest that relatively few genes are affected in this way (Delannoy et al., 2023; Zhu et al., 2023), there remains a need for complementary tools to study wound responses. Genetically encoded biosensors offer one such approach, allowing *in vivo* imaging without the destruction of the tissue under study. Response to wounding is known to be governed by JA, so we selected biosensors to track JA signalling.

Plant vegetative tissues are scarce in proteins and thus nitrogen content. While these tissues represent the only protein source for herbivores, they largely rely on digestive proteinases in their guts. However, in defence against herbivores, plants produce proteinase inhibitors (Martinez et al., 2016). We therefore exploited a promoter of the proteinase inhibitor multicystatin (MC), which is upregulated upon CPB infestation and *coi1*-dependent (Petek et al., 2014) and used it as a sensor. In tomato, *MC* showed high induction in roots following methyl jasmonate (MeJA) spraying of the leaves, even to relatively low MeJA concentrations, already 1 hpt (Fujimoto et al., 2011), and was along with some other proteinase inhibitors of tomato better marker of MeJA response compared to JA-biosynthesis genes (Fujimoto et al., 2011). MC functions as a proteinase inhibitor with multiple cystatin inhibitory domains that was shown to strongly inhibit endogenous cysteine proteinases of the papain family (Popovič & Brzin, 2007) and cysteine proteinases which are abundant in herbivores' guts (Gruden et al., 2003, 2004; Murdock et al., 1987; Orr et al., 1994). Potato MC protein is also present in tubers in a very stable crystalline form and solubilizes at acidic pH (Nissen et al., 2009). After wounding, the MC protein content is induced in leaves to up to 2% of the soluble protein fraction (Walsh & Strickland, 1993). Our results with *MC::EYFP* after MeJA application and mechanical and herbivore wounding confirmed that *MC* expression can be used as a marker of JA-dependent gene activity in potato locally and systemically.

Beside a transcriptional reporter of JA-dependent gene expression *MC::EYFP*, we also employed another two genetically encoded biosensors, direct reporter of JA signalling that is based on JAZ degron sequence which binds JA-Ile, AtJas9-Venus-N7 (Larrieu et al., 2015), and a bacterial transcriptional reporter of SA, Acinetobacter ADPWH_*lux* (Huang et al., 2005, 2006). Before our work on *MC::EYFP* and AtJas9-Venus-N7 sensors, biosensors were already implemented and used in potato plants, namely aequorin to track Ca^{2+} responses in different sampled tissues upon treatments with DAMPs and PAMPs (Moroz & Tanaka, 2020), chl-roGFP2 to track redox changes in the chloroplasts upon abiotic stresses on the level of whole plants (Hipsch et al., 2021) and upon PVY infection where imaging was performed on sampled leaves (Lukan et al., 2023), and *DR5rev::3xVenus-N7* and *CycB1;1::GUS* to track Aux signalling and cell division in stem cuttings that formed adventitious roots (Joshi et al., 2016). Our work thus extended the use of biosensors in potato to three novel ones. We prepared protocols to track the JA sensors on intact plants, which enabled us to follow plant response to wounding *in vivo* and in a spatiotemporal manner, thus confirming our first hypothesis. In fact, the need for imaging of intact plants arose from the fact that we did not observe any *MC::EYFP* response when the smaller portion of the leaf was sampled or when leaf was detached from plant and the petiole was immersed in water. The imaging of *MC::EYFP* required covering sufficient portion of the leaf where we predicted the occurrence of its signal, therefore the imaging was performed as tilescan, merging neighbouring fields of view. On the other hand, imaging of AtJas9-Venus-N7 required gentle handling of plants and imaging without mounting the leaf. Low signal-to-noise ratio of both JA biosensors was complemented by increasing the confocal pinhole diameter to maximum and thus extending the obtained signal from thicker portion of the tissue. The comparison of spatial response between inducible *MC::EYFP* and strongly constitutively expressed AtJas9-Venus-N7 revealed their similarity, indicating that the presence of the biosensors did not perturb the system, as previously demonstrated for ABA biosensors (Isoda et al., 2020). However, we observed relatively long lag in the response of transcriptional reporter, which results from additional steps in fluorophore formation, including protein maturation, which is temperature dependent and thus slower in plants compared to mammalian cells (Balleza et al., 2018). While JA was followed by biosensors *in planta*, tracking SA levels with Acinetobacter ADPWH_*lux* was not possible following infiltration of potato leaves with the bacterial biosensor. Therefore, we adapted the protocol by Defraia et al., 2008, for tracking of SA levels in potato plant leaf homogenates. While the JA sensors used are limited in terms of *in planta* calibration due to the unknown penetration of potential calibrating solutions, this limitation was overcome by using Acinetobacter ADPWH_*lux* in homogenized tissue. All three sensors and the corresponding protocols can now be used over a range of research areas that include JA and SA signalling.

The *MC::EYFP* and AtJas9-Venus-N7 sensors were used to track two stages in the JA signalling cascade following herbivory attack and mechanical wounding of potato leaves. The literature so far distinguished the responses between these two types of wounding, as it reported that herbivore's saliva and the microbes present in it can cause inhibition of JA-dependent response through triggering SA-dependent response (Chung et al., 2013), leaving plant more susceptible to herbivory attack (Consales et al., 2012; Wang et al., 2017). It was also reported that oral secretions can induce ERF branch of JA signalling, which opposes MYC2 branch that triggers anti-herbivore defence (Verhage et al., 2011). Therefore, we expected that the responses of both sensors would differ in action followed herbivore compared to mechanical wounding. The responses observed following both types of wounding were largely comparable, particularly between wounds caused by CPB larval probing and those produced by piercing the leaf with a sterile needle. However, *MC::EYFP*

activity was weaker in cells surrounding CPB bite wounds. Therefore, the second hypothesis was partially rejected.

Moreover, we continuously observed that JA-dependent gene expression was inhibited in cells closest to the wound in both, herbivory and mechanically applied wounds, although JA-Ile dependent AtJas9-Venus-N7 degradation was active there. Responses to both types of wounding in this region were surprisingly comparable, especially between needle and probing wounds, while in case of bite wounds the region without JA-dependent gene expression was wider. The reason for this might lie in differences in applied mechanical forces during wounding, amount of produced DAMPs or content of microbiota in insect saliva. While such spatial response has not been previously described in this context, similar patterns of JA-dependent gene expression have been noted after mechanical wounding in Arabidopsis, such as *JAZ10* and *LOX2* in cotyledon leaf (Farmer et al., 2014; Gasperini et al., 2015) or *OPR3* in leaves, especially following high (but not low) concentration of JA application (Body et al., 2019). In search for the mechanism of *MC::EYFP* non-activation in cells closest to the wound, we used Acinetobacter ADPWH_*lux* to check for an increase of SA in wound proximity. This observation was confirmed by introducing *MC::EYFP* into SA-depleted *NahG* lines and by treating the *MC::EYFP* sensor in nontransgenic background with JA and SA analogue, INA. Following *MC::YFP* sensor over 7 days post wounding revealed that its activity in cells around the wound was transiently inhibited in majority of cells surrounding the wound, and permanently inhibited in 2–3 cells wide band right at the wound edge. These cells lost chlorophyll fluorescence and showed increased autofluorescence in cell walls, probably due to formation of the lignin-rich secondary cell wall. We propose that in this band of cells, within the first two days after wounding, SA-JA crosstalk occurs with the final aim to select the cells which then form a secondary cell wall, supposedly to limit water and nutrient loss and to prevent microbial infection at the wounded site. This is in accordance with results showing that herbivory activity on *N. attenuata* leaves caused reduced maximal efficiency of PSII (Fv/Fm) in cells proximal to the wound edge and that this effect was reduced in transgenics with silenced *LOX* that contain lower levels of JA (Nabity et al., 2013).

Spatial antagonism between SA and JA was first time observed in ETI following *P. syringae* pv. tomato DC3000 carrying AvrRpt2 effector infection of Arabidopsis leaves through spatially distinct expression of SA-dependent *PR1* and JA-dependent *VSP1* (Betsuyaku et al., 2018). This phenomenon was also observed for TFs WRKY70 and WRKY11, of which the first was expressed in SA-dependent HR zone and the latter in JA-dependent surrounding tissue in hemibiotrophic *F. oxysporum* infection of Arabidopsis root (Calabria et al., 2025). Considering SA-JA antagonism, JA mutants showed enhanced SA and callose deposition after wounding (Lewandowska et al., 2024). JA-dependent expression upon wounding of Arabidopsis leaves was shown for DHS1, an enzyme of lignin biosynthesis (McConn et al., 1997). Although not spatially resolved, some reports have already suggested involvement of SA-dependent gene expression in response to wounding: a transient increase of SA in the wounded leaves (Ang et al. 2024; Ogawa et al. 2010), and *PR1* transcript was detected in both, local and systemic leaves after wounding by puncturing the leaves (Myers et al., 2023) in wild type, but not in *npr1* (SA perception) mutants. Our results suggest that these unresolved dependencies between SA and JA are spatially regulated, and that spatial SA-JA antagonism is established in response to wounding.

Spatial separation of processes supports a balance between defence against pathogens and pests with opposing strategies: biotrophic microbes and viruses on one side and necrotrophic fungi and herbivores on the other. Moreover, another balance is needed between defence and growth. Spatially confined activation of defence thus conserves

resources. Interestingly, it has been shown that response to wounding relies on its extent, thus being limited (and localized) as in our and above-mentioned cases or reaching systemic response when larger veins are wounded (Farmer et al., 2013) as these are required for systemic spread of the signal (Salvador-Recatalà, Tjallingii & Farmer 2014; Farmer et al. 2020; Farmer, Gasperini & Acosta 2014; Gao & Farmer 2023). Larger damage indicates more intensive insect pressure, making investment into systemic defence economic.

Compared to omics analyses, a limitation of biosensors lies in the necessity to monitor a limited number of analytes, focusing on the most informative ones, due to constraints in discriminating fluorescent proteins during imaging. To address this issue, the third aim of our work was to research the possibilities of multiplexing sensors within the same organism. Specifically, we hypothesized that we could discriminate between sensors employing different fluorescent proteins, even if their emission spectra overlap. With this, we could expand the number of analytes we follow. For example, we could correlate multiple pathways spatiotemporally, e.g. SA and JA-dependent gene expression and corresponding redox state in different cellular organelles, as the expression analysis revealed that redox-related enzymes correlate with JA-dependent gene expression. Moreover, we could test other possible hypotheses for the observed SA-JA spatial antagonism at cell-level resolution, such as that Ca^{2+} influx signatures differ at different regions in wound proximity (Bellandi et al., 2022; Nakai et al., 2001), or that the expression of the two MAPK kinases, StMKK6 and StMKK3, correlates with SA and JA region, respectively, or show distinct phosphorylation states in these two regions (Lazar et al., 2014; Seitz & Krysan, 2020). Besides that, we could examine the possibility of NPR1-MYC2 interaction in the *MC::EYFP* attenuation zone as a possible crosstalk hub (Nomoto et al., 2021).

While multiplexing enables us to follow multiple targets within the same tissue or a cell, it is subjected to crosstalk of excitation and emission ranges of the fluorophores. This problem can undermine accurate distinction of the followed biological targets. Key determinants in successful unmixing are comparable brightness of overlapping fluorescent proteins and high signal-to-noise ratio (SNR).

Comparable brightness can be expected while using comparably bright fluorescent proteins and similarly expressed targets, e.g. promoters of similar strength. When comparable brightness of the selected targets cannot be achieved, e.g. due to large differences in expression, it is recommended to use spectrally nonoverlapping fluorescent proteins to enable their distinction. On the other hand, fluorescent proteins of lower brightness can be used to follow highly expressed targets, such as proteins produced during virus multiplication. As candidates for unmixing, we selected a palette of fluorescent proteins previously published for their brightness and monomeric quality (Cranfill et al., 2016) and transiently expressed them in *N. benthamiana* and three of the brightest were also stably expressed in potato. We showed that mTagBFP2, Venus, mKO2, mCherry, mKate2 and mCardinal show comparable brightness, while mTurquoise2 was much weaker than expected from FPbase data (Lambert, 2019).

SNR depends on more than absolute brightness. Increased SNR can also be achieved by concatenation of more than one fluorescent protein, such as 3xVenus (Steiner et al., 2020) or tdTomato (Nagano et al., 2020) and its localization in a smaller compartment, such as nucleus. Optimizing SNR to minimize background fluorescence (autofluorescence) or crosstalk can also be achieved by adjusting laser scan speed, reducing PMT voltage (detector gain), and applying line or frame averaging. For applications where high axial resolution is not critical, such as tissue-level imaging, increasing the pinhole beyond 1 Airy unit can further enhance signal detection (Deagle et al., 2017; Jonkman et al., 2020). Indeed, the latter approach enabled imaging of *MC::EYFP* as it strongly increased SNR.

As a proof of principle, we assessed the possibility of unmixing three spectrally overlapping fluorescent proteins, EGFP, Venus and mKO2, which can all be excited by the same standard laserline at 488 nm. They were expressed in distinct cellular compartments to qualitatively and, by using the segmentation script, also quantitatively measure the unmixing efficiency. Spectral unmixing, which relies on high-resolution lambda scans, provided the most precise signal separation but required long acquisition times and was therefore more sensitive to organelle movement and noise. In contrast, channel separation—using standard multichannel images and experimentally derived reference spectra—offered comparable separation with much shorter acquisition times, minimizing motion artifacts and photobleaching. Because the latter are frequently more important than the higher spectral precision of a slow lambda scan while achieving comparable fluorophore separation, we recommend channel separation as the most efficient and reliable method.

Chapter 4

Conclusions

A deep understanding of plant responses underlies the development of stress-tolerant and disease-resistant cultivars. In the context of emerging insights into plant immunity, biosensors are crucial for investigating the abundance of key molecules and their spatiotemporal dynamics. They complement omics analyses by providing contextual information that highlights critical time points and spatial patterns. Moreover, time-series data obtained from biosensors can inform and parameterize mathematical models, reveal emergent behaviours, such as signalling thresholds, pathway crosstalk, and feedback loops, and serve to validate model predictions.

In this study, we focused on JA-responsive genetically encoded biosensors to monitor responses to mechanical and herbivore-induced wounding in potato leaves. By combining these biosensors with precise leaf sectioning and subsequent quantification of SA levels, we identified two distinct regions in the vicinity of wounds: one located at the wound edge, where both JA and SA accumulate and JA-dependent gene expression is suppressed, and another, situated a few cells away, where JA-dependent gene expression is active. These spatially defined hormonal patterns are accompanied by two distinct cellular outcomes near the wound — one promoting wound healing, localized cell death, and protection against biotrophic invasion, and the other supporting the production of defensive compounds, such as proteinase inhibitors, that counteract necrotrophs and herbivores. Interestingly, this wounding response mirrors the hypersensitive response previously described in plant–pathogen interactions.

Because processes, including the response to wounding, involve multiple interacting hormonal pathways, employing multiple biosensors simultaneously is desirable to capture their precise coordination. Accurate discrimination between different reporters, such as fluorescent proteins, is essential to achieve this. By multiplexing fluorescent protein–based biosensors and applying linear unmixing to resolve overlapping signals, it becomes possible to monitor a larger number of analytes concurrently and to correlate multiple signalling pathways in space and time. In this study, we show that at least three spectrally overlapping proteins excited with the same laserline can be successfully unmixed using linear unmixing. This work, therefore, paves the way to multiplexing biosensors and thus identifying the occurrence of important steps in the cascades as well as crosstalk hubs between different signalling pathways and their spatiotemporal coordination.

Appendix A

Supplementary Material of Included Publications

A.1 Supplementary Material for Publication 2.2

All supplementary material is available at https://academic.oup.com/pcp/advance-article/doi/10.1093/pcp/pcaf120/8262811#supplementary-data (Accessed December 23, 2025). All raw files were deposited to Zenodo, DOI: 10.5281/zenodo.16875337.

A.2 Supplementary Material for Publication 2.3

All raw files were deposited to Zenodo, DOI: 10.5281/zenodo.19691651. The code was deposited to GitHub: https://github.com/NIB-SI/Nuclei-segmentation (Accessed December 23, 2025).

Appendix B

Permission for Reproduction of Included Publications

B.1 Permission for Reproduction of Publication 2.1

life

MDPI

Review

Biosensors: A Sneak Peek into Plant Cell's Immunity

Valentina Levak [1,2,*], Tjaša Lukan [1], Kristina Gruden [1] and Anna Coll [1]

[1] National Institute of Biology, Večna pot 111, 1000 Ljubljana, Slovenia;tjasa.lukan@nib.si (T.L.); kristina.gruden@nib.si (K.G.); anna.coll@nib.si (A.C.)
[2] Jožef Stefan International Postgraduate School, Jamova cesta 39, 1000 Ljubljana, Slovenia
* Correspondence: valentina.levak@nib.si

Abstract: Biosensors are indispensable tools to understand a plant's immunity as its spatiotemporal dimension is key in withstanding complex plant immune signaling. The diversity of genetically encoded biosensors in plants is expanding, covering new analytes with ever higher sensitivity and robustness, but their assortment is limited in some respects, such as their use in following biotic stress response, employing more than one biosensor in the same chassis, and their implementation into crops. In this review, we focused on the available biosensors that encompass these aspects. We show that in vivo imaging of calcium and reactive oxygen species is satisfactorily covered with the available genetically encoded biosensors, while on the other hand they are still underrepresented when it comes to imaging of the main three hormonal players in the immune response: salicylic acid, ethylene and jasmonic acid. Following more than one analyte in the same chassis, upon one or more conditions, has so far been possible by using the most advanced genetically encoded biosensors in plants which allow the monitoring of calcium and the two main hormonal pathways involved in plant development, auxin and cytokinin. These kinds of biosensor are also the most evolved in crops. In the last section, we examine the challenges in the use of biosensors and demonstrate some strategies to overcome them.

Keywords: genetically encoded biosensors; live spatiotemporal imaging; crops; plant immune response; multiparameter imaging; biotic stress

check for updates

Citation: Levak, V.; Lukan, T.; Gruden, K.; Coll, A. Biosensors: A Sneak Peek into Plant Cell's Immunity. *Life* **2021**, *11*, 209. https://doi.org/10.3390/life11030209

Academic Editors: Pasquale Stano, Stéphane D. Lemaire and Paul P. South

Received: 27 January 2021
Accepted: 3 March 2021
Published: 7 March 2021

Publisher's Note: MDPI stays neutral with regard to jurisdictional claims in published maps and institutional affiliations.

Copyright: © 2021 by the authors. Licensee MDPI, Basel, Switzerland. This article is an open access article distributed under the terms and conditions of the Creative Commons Attribution (CC BY) license (https://creativecommons.org/licenses/by/4.0/).

1. Biosensors: Exploiting Molecular Hubs to Better Understand the Processes

A biosensor is a sensitive device that detects an analyte or event in a living organism and consequently produces a measurable output [1]. Thus, it consists of two functional parts: detector and reporter [2]. The detector domain must be specific and sensitive to enable detection of the biological concentration of analytes or events. The biosensor as a whole should enable detection with high signal to noise ratio (SNR), high spatiotemporal resolution on the organelle level, enable fast response, and must be functional in different cellular conditions (low pH, different redox states). Besides, it should not interfere with cellular processes and should not be toxic to the cells. Although each of available biosensors has its own limitations and cannot meet all of the abovementioned requirements, they are vital to obtain an insight into cellular events.

According to their mechanism of action, they can be separated into direct and indirect biosensors. Typical direct biosensors report protein activity upon ligand binding. Usually, they consist of two protein domains, one serving as a ligand receptor while the other can sense structural changes upon ligand binding and report it by measurable output. This is the mode of action of one of the first known biosensors named Cameleon, which is still widely used to measure Ca^{2+} concentration (Figure 1). It is translated as a single peptide chain, with two fluorescent proteins on each side, which are either blue and green or cyan and yellow, linked by calmodulin (CaM) and the M13 domain. When the concentration of Ca^{2+} in the cellular compartment increases, Ca^{2+} binds to CaM, which twists around the M13 domain and thereupon the two fluorescent proteins are close enough to enable

B.2 Permission for Reproduction of Publication 2.2

PCP
PLANT & CELL PHYSIOLOGY

Jasmonic acid and salicylic acid interact to determine spatial regulation of gene expression responses in potato leaf to herbivory by Colorado potato beetle and mechanical wounding

Valentina Levak[1,2,*], Tjaša Mahkovec Povalej[1], Karmen Pogačar[1,2], Katja Stare[1], Maja Zagorščak[1], Tim Hawkins[3], Joanne Robson[3], David Dobnik[1], Tjaša Lukan[1,†] and Kristina Gruden[1,†,*]

[1]Department of Biotechnology and Systems Biology, National Institute of Slovenia, Večna pot 121, 1000 Ljubljana, Slovenia, [2]Jožef Stefan International Postgraduate School, Jamova 39, 1000 Ljubljana, Slovenia, [3]Department of Biosciences, Durham University, South Rd, Durham DH1 3LE, UK

*Corresponding authors: Valentina Levak, E-mail, valentina.levak@nib.si; Kristina Gruden, E-mail, kristina.gruden@nib.si
†Shared last authorship.

Received 19 June 2025; Accepted 22 September 2025

Downloaded from https://academic.oup.com/pcp/advance-article/doi/10.1093/pcp/pcaf120/8262811 by National and University Library Ljubljana user on 11 December 2025

Regular Paper

Abstract

We investigated the spatial dynamics of potato (*Solanum tuberosum*) responses to herbivory and mechanical wounding. We first followed the spatiotemporal response of jasmonic acid (JA) signaling, known to be involved in the response. We generated two potato sensor lines: a JAZ degradation sensor and a downstream multicystatin (MC) transcriptional reporter. Both sensors revealed concentric, locally restricted responses on wounded leaves. Notably, JA-dependent gene expression was absent in cells immediately adjacent to the wound, whereas JAZ degradation spread continuously outward from the wound site. This pattern occurred after both herbivore attack and mechanical injury by the needle. To probe the mechanism, a salicylic acid (SA) reporter showed SA accumulation near the wound. Introducing the MC reporter into SA-depleted *NahG* plants produced a uniform spread of MC expression, confirming that SA attenuates the JA response in proximal cells. Together, these results show that a locally distinct, spatiotemporal SA–JA crosstalk shapes wound responses in potato, extending principles known from pathogen–plant interactions to herbivory and mechanical damage.

Keywords: Colorado potato beetle • herbivore • hormonal crosstalk • jasmonic acid • potato • salicylic acid • wounding

Introduction

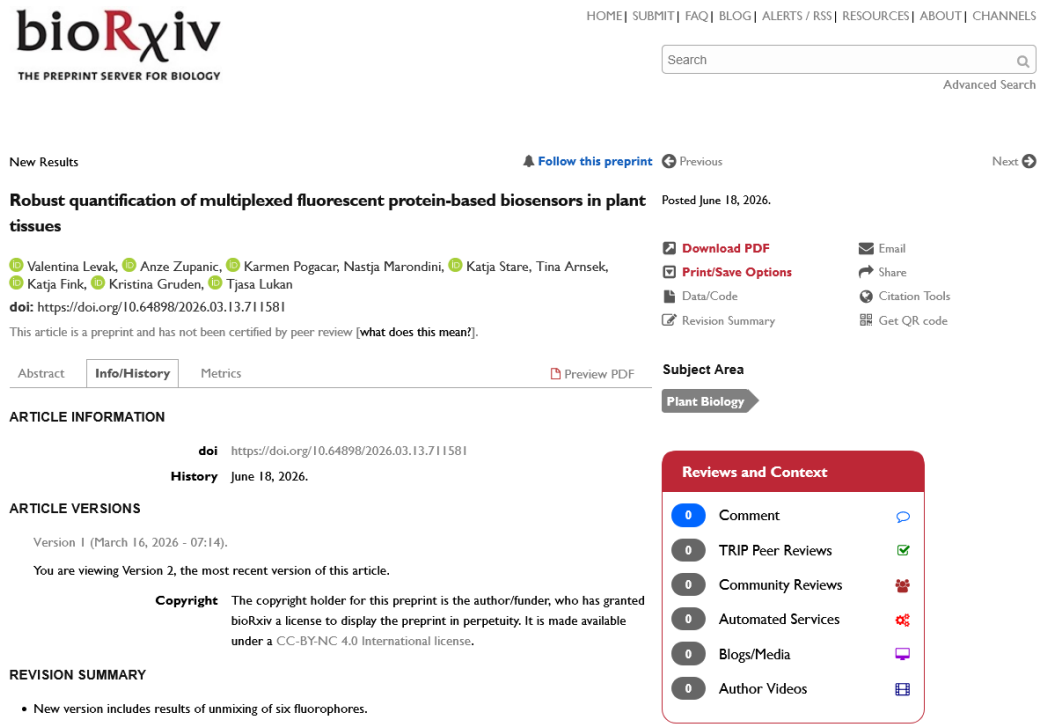
Plants rely on two interconnected arms of innate immunity to perceive and respond to pathogen attack (Jones et al. 2024). Pattern-triggered immunity uses cell-surface pattern-recognition receptors to detect microbe-associated molecular patterns, host-derived damage-associated molecular patterns, and herbivore-associated molecular patterns (Hou et al. 2019). Effector-triggered immunity (ETI) employs disease-resistance (R) proteins to recognize effector molecules delivered by pathogens and herbivores (Nguyen et al. 2021). Invasion by necrotrophic pathogens and herbivore infestation typically causes wounding and initiates cascades of biochemical and cellular signals, including calcium fluxes, phytohormone signaling, and reactive oxygen species production.

Jasmonic acid (JA) is a central phytohormone in wound responses. Its biosynthesis begins within minutes via 13-lipoxygenase (13-LOX)-mediated oxidation of plastid fatty acids and does not require *de novo* transcription or translation (Chung et al. 2008, Glauser et al. 2008, Chauvin et al. 2013, Kimberlin et al. 2022). Subsequent steps yield 12-oxo-phytodienoic acid, which is transported to peroxisomes and converted to JA. JA then enters the cytosol, where JAR1 conjugates it to isoleucine (JA–Ile), the most bioactive JA derivative. JA–Ile promotes assembly of the SCF^{COI1} complex with JAZ transcriptional repressors, triggering proteasomal degradation of JAZ within minutes and releasing transcriptional activators such as MYC2/3/4 (Chini et al. 2007, Fernández-Calvo et al. 2011, Larrieu et al. 2015). These can then drive JA-dependent gene expression. JA-dependent transcription is temporally tuned. In *Arabidopsis*, transcripts encoding JA biosynthesis regulators (e.g. MYC2, ORA47, MYB75, JAZs) rise about 15 min after JA treatment, followed by downregulation of primary metabolism and salicylic acid (SA)-pathway regulators (e.g. WRKY transcription factors) about 30 min after, and upregulation of JA biosynthetic genes and defense proteins (e.g. LOX, AOC, AOS, JAR1, VSP1/2) by 1 h after JA treatment (Koo et al. 2009, Hickman et al. 2017).

Plant defense—including responses to wounding—is coordinated not only by JA but also by other signaling pathways that can be activated independently and intersect at distinct

© The Author(s) 2025. Published by Oxford University Press on behalf of the Japanese Society of Plant Physiologists.
This is an Open Access article distributed under the terms of the Creative Commons Attribution-NonCommercial License (https://creativecommons.org/licenses/by-nc/4.0/), which permits non-commercial re-use, distribution, and reproduction in any medium, provided the original work is properly cited. For commercial re-use, please contact reprints@oup.com for reprints and translation rights for reprints. All other permissions can be obtained through our RightsLink service via the Permissions link on the article page on our site—for further information please contact journals.permissions@oup.com.

B.3 Permission for Reproduction of Publication 2.3



bioRxiv
THE PREPRINT SERVER FOR BIOLOGY

HOME | SUBMIT | FAQ | BLOG | ALERTS / RSS | RESOURCES | ABOUT | CHANNELS

Search
Advanced Search

New Results | Follow this preprint | Previous | Next

Robust quantification of multiplexed fluorescent protein-based biosensors in plant tissues

Valentina Levak, Anze Zupanic, Karmen Pogacar, Nastja Marondini, Katja Stare, Tina Arnsek, Katja Fink, Kristina Gruden, Tjasa Lukan

doi: https://doi.org/10.64898/2026.03.13.711581

This article is a preprint and has not been certified by peer review [what does this mean?].

Abstract | Info/History | Metrics | Preview PDF

ARTICLE INFORMATION

doi https://doi.org/10.64898/2026.03.13.711581
History June 18, 2026.

ARTICLE VERSIONS

Version 1 (March 16, 2026 - 07:14).

You are viewing Version 2, the most recent version of this article.

Copyright The copyright holder for this preprint is the author/funder, who has granted bioRxiv a license to display the preprint in perpetuity. It is made available under a CC-BY-NC 4.0 International license.

REVISION SUMMARY

- New version includes results of unmixing of six fluorophores.

Posted June 18, 2026.

Download PDF | Email
Print/Save Options | Share
Data/Code | Citation Tools
Revision Summary | Get QR code

Subject Area

Plant Biology

Reviews and Context

0 Comment
0 TRIP Peer Reviews
0 Community Reviews
0 Automated Services
0 Blogs/Media
0 Author Videos

References

Aderem, A. (2005). Systems Biology: Its Practice and Challenges. Cell, 121(4), 511–513. https://doi.org/10.1016/j.cell.2005.04.020

Altpeter, F., Springer, N. M., Bartley, L. E., Blechl, A. E., Brutnell, T. P., Citovsky, V., Conrad, L. J., Gelvin, S. B., Jackson, D. P., Kausch, A. P., Lemaux, P. G., Medford, J. I., Orozco-Cárdenas, M. L., Tricoli, D. M., Van Eck, J., Voytas, D. F., Walbot, V., Wang, K., Zhang, Z. J., & Neal Stewart, C. (2016). Advancing Crop Transformation in the Era of Genome Editing. The Plant Cell, 28(7), 1510. https://doi.org/10.1105/TPC.16.00196

Andres, J., Schmunk, L. J., Grau-Enguix, F., Braguy, J., Samodelov, S. L., Blomeier, T., Ochoa-Fernandez, R., Weber, W., Al-Babili, S., Alabadí, D., Blázquez, M. A., & Zurbriggen, M. D. (2024). Ratiometric Gibberellin Biosensors for the Analysis of Signaling Dynamics and Metabolism in Plant Protoplasts. The Plant Journal, 118(4), 927–939. https://doi.org/10.1111/TPJ.16725

Ang, M. C. Y., Saju, J. M., Porter, T. K., Mohaideen, S., Sarangapani, S., Khong, D. T., Wang, S., Cui, J., Loh, S. I., Singh, G. P., Chua, N. H., Strano, M. S., & Sarojam, R. (2024). Decoding Early Stress Signaling Waves in Living Plants Using Nanosensor Multiplexing. Nature Communications, 15(1), 1–17. https://doi.org/10.1038/s41467-024-47082-1

Balleza, E., Kim, J. M., & Cluzel, P. (2018). Systematic Characterization of Maturation Time of Fluorescent Proteins in Living Cells. Nature Methods, 15(1), 51. https://doi.org/10.1038/NMETH.4509

Bari, R., & Jones, J. D. G. (2009). Role of plant hormones in plant defence responses. Plant Molecular Biology, 69(4), 473–488. https://doi.org/10.1007/S11103-008-9435-0

Bartoli, C., & Roux, F. (2017). Genome-Wide Association Studies in Plant Pathosystems: Toward an Ecological Genomics Approach. Frontiers in Plant Science, 8, 262323. https://doi.org/10.3389/FPLS.2017.00763

Bellandi, A., Papp, D., Breakspear, A., Joyce, J., Johnston, M. G., de Keijzer, J., Raven, E. C., Ohtsu, M., Vincent, T. R., Miller, A. J., Sanders, D., Hogenhout, S. A., Morris, R. J., & Faulkner, C. (2022). Diffusion and Bulk Flow of Amino Acids Mediate Calcium Waves in Plants. Science Advances, 8(42), eabo6693. https://doi.org/10.1126/sciadv.abo6693

Beneloujaephajri, E., Costa, A., L'Haridon, F., Métraux, J.-P., & Binda, M. (2013). Production of Reactive Oxygen Species and Wound-Induced Resistance in Arabidopsis thaliana against Botrytis cinerea Are Preceded and Depend on a Burst of Calcium. BMC Plant Biology, 13(1), 160. https://doi.org/10.1186/1471-2229-13-160

Bernoux, M., Zetzsche, H., & Stuttmann, J. (2022). Connecting the Dots Between Cell Surface- and Intracellular-Triggered Immune Pathways in Plants. Current Opinion in Plant Biology, 69, 102276. https://doi.org/10.1016/J.PBI.2022.102276

Betsuyaku, S., Katou, S., Takebayashi, Y., Sakakibara, H., Nomura, N., & Fukuda, H. (2018). Salicylic Acid and Jasmonic Acid Pathways are Activated in Spatially Different Domains around the Infection Site during Effector-Triggered Immunity in Arabidopsis thaliana. Plant and Cell Physiology, 59(1), 8–16. https://doi.org/10.1093/pcp/pcx181

Body, M. J. A., Dave, D. F., Coffman, C. M., Paret, T. Y., Koo, A. J., Cocroft, R. B., & Appel, H. M. (2019). Use of Yellow Fluorescent Protein Fluorescence to Track OPR3 Expression in Arabidopsis Thaliana Responses to Insect Herbivory. Frontiers in Plant Science, 10, 1586. https://doi.org/10.3389/FPLS.2019.01586

Brunoud, G., Wells, D. M., Oliva, M., Larrieu, A., Mirabet, V., Burrow, A. H., Beeckman, T., Kepinski, S., Traas, J., Bennett, M. J., & Vernoux, T. (2012). A Novel Sensor to Map Auxin Response and Distribution at High Spatio-Temporal Resolution. Nature, 482(7383), 103–106. https://doi.org/10.1038/nature10791

Calabria, J., Wang, L., Rast-Somssich, M. I., Chen, H.-W., Watt, M., Persson, S., Andersen, T. G., Idnurm, A., & Somssich, M. (2025). Resolving Spatially Distinct Phytohormone Response Zones in Arabidopsis thaliana Roots Colonized by Fusarium oxysporum. Journal of Experimental Botany, 76(7), 2022–2034. https://doi.org/10.1093/JXB/ERAE516

Chauvin, A., Caldelari, D., Wolfender, J., & Farmer, E. E. (2013). Four 13-lipoxygenases Contribute to Rapid Jasmonate Synthesis in Wounded Arabidopsis thaliana Leaves: A Role for Lipoxygenase 6 in Responses to Long-Distance Wound Signals. New Phytologist, 197(2), 566–575. https://doi.org/10.1111/nph.12029

Chini, A., Fonseca, S., Fernández, G., Adie, B., Chico, J. M., Lorenzo, O., García-Casado, G., López-Vidriero, I., Lozano, F. M., Ponce, M. R., Micol, J. L., & Solano, R. (2007). The JAZ Family of Repressors is the Missing Link in Jasmonate Signalling. Nature, 448(7154), 666–671. https://doi.org/10.1038/nature06006

Chung, H. S., Koo, A. J. K., Gao, X., Jayanty, S., Thines, B., Jones, A. D., & Howe, G. A. (2008). Regulation and Function of Arabidopsis JASMONATE ZIM-Domain Genes in Response to Wounding and Herbivory. Plant Physiology, 146(3), 964. https://doi.org/10.1104/PP.107.115691

Chung, S. H., Rosa, C., Scully, E. D., Peiffer, M., Tooker, J. F., Hoover, K., Luthe, D. S., & Felton, G. W. (2013). Herbivore Exploits Orally Secreted Bacteria to Suppress Plant Defenses. Proceedings of the National Academy of Sciences of the United States of America, 110(39), 15728–15733. https://doi.org/10.1073/pnas.1308867110

Consales, F., Schweizer, F., Erb, M., Gouhier-Darimont, C., Bodenhausen, N., Bruessow, F., Sobhy, I., & Reymond, P. (2012). Insect Oral Secretions Suppress Wound-Induced Responses in Arabidopsis. Journal of Experimental Botany, 63(2), 727–737. https://doi.org/10.1093/JXB/ERR308

Corwin, J. A., & Kliebenstein, D. J. (2017). Quantitative Resistance: More Than Just Perception of a Pathogen. The Plant Cell, 29(4), 655–665. https://doi.org/10.1105/TPC.16.00915

Cranfill, P. J., Sell, B. R., Baird, M. A., Allen, J. R., Lavagnino, Z., De Gruiter, H. M., Kremers, G. J., Davidson, M. W., Ustione, A., & Piston, D. W. (2016). Quantitative Assessment of Fluorescent Proteins. Nature Methods, 13(7), 557–562. https://doi.org/10.1038/nmeth.3891

Cui, F., Brosché, M., Sipari, N., Tang, S., & Overmyer, K. (2013). Regulation of ABA Dependent Wound Induced Spreading Cell Death by MYB108. New Phytologist, 200(3), 634–640. https://doi.org/10.1111/NPH.12456

Cui, F., Wu, W., Wang, K., Zhang, Y., Hu, Z., Brosché, M., Liu, S., & Overmyer, K. (2019). Cell Death Regulation but not Abscisic Acid Signaling is Required for Enhanced Immunity to Botrytis in Arabidopsis Cuticle-Permeable Mutants. Journal of Experimental Botany, 70(20), 5971–5984. https://doi.org/10.1093/JXB/ERZ345

Dangl, J. L., & Jones, J. D. G. (2001). Plant Pathogens and Integrated Defence Responses to Infection. Nature, 411(6839), 826–833. https://doi.org/10.1038/35081161

Defraia, C. T., Schmelz, E. A., & Mou, Z. (2008). A Rapid Biosensor-Based Method for Quantification of Free and Glucose-Conjugated Salicylic Acid. Plant Methods, 4(1), 28. https://doi.org/10.1186/1746-4811-4-28

Delannoy, E., Batardiere, B., Pateyron, S., Soubigou-Taconnat, L., Chiquet, J., Colcombet, J., & Lang, J. (2023). Cell Specialization and Coordination in Arabidopsis leaves upon Pathogenic Attack Revealed by scRNA-seq. Plant Communications, 4(5), 100676. https://doi.org/10.1016/J.XPLC.2023.100676

Delplace, F., Huard-Chauveau, C., Dubiella, U., Khafif, M., Alvarez, E., Langin, G., Roux, F., Peyraud, R., & Roby, D. (2020). Robustness of Plant Quantitative Disease Resistance is Provided by a Decentralized Immune Network. Proceedings of the National Academy of Sciences of the United States of America, 117(30), 18099–18109. https://doi.org/10.1073/PNAS.2000078117

Donaldson, L. (2020). Autofluorescence in Plants. Molecules, 25(10), 2393. https://doi.org/10.3390/MOLECULES25102393

Doughari, J. H. (2015). An Overview of Plant Immunity. Journal of Plant Pathology & Microbiology, 6(11), 1–11. https://doi.org/10.4172/2157-7471.1000322

Farmer, E. E., Gao, Y. Q., Lenzoni, G., Wolfender, J. L., & Wu, Q. (2020). Wound- and Mechanostimulated Electrical Signals Control Hormone Responses. New Phytologist, 227(4), 1037–1050. https://doi.org/10.1111/NPH.16646

Farmer, E. E., Gasperini, D., & Acosta, I. F. (2014). The Squeeze Cell Hypothesis for the Activation of Jasmonate Synthesis in Response to Wounding. New Phytologist, 204, 282–288.

Farmer, E., Mousavi, S., & Lenglet, A. (2013). Leaf Numbering for Experiments on Long Distance Signalling in Arabidopsis. Protocol Exchange. https://doi.org/10.1038/PROTEX.2013.071

Fujimoto, T., Tomitaka, Y., Abe, H., Tsuda, S., Futai, K., & Mizukubo, T. (2011). Expression Profile of Jasmonic Acid-Induced Genes and the Induced Resistance against the Root-Knot Nematode (Meloidogyne incognita) in Tomato Plants (Solanum lycopersicum) after Foliar Treatment with Methyl Jasmonate. Journal of Plant Physiology, 168(10), 1084–1097. https://doi.org/10.1016/j.jplph.2010.12.002

Gasperini, D., Chauvin, A., Acosta, I. F., Kurenda, A., Stolz, S., Chételat, A., Wolfender, J. L., & Farmer, E. E. (2015). Axial and Radial Oxylipin Transport. Plant Physiology, 169(3), 2244–2254. https://doi.org/10.1104/PP.15.01104

Ghareeb, H., El-Sayed, M., Pound, M., Tetyuk, O., Hanika, K., Herrfurth, C., Feussner, I., & Lipka, V. (2020). Quantitative Hormone Signaling Output Analyses of Arabidopsis thaliana Interactions With Virulent and Avirulent Hyaloperonospora arabidopsidis Isolates at Single-Cell Resolution. Frontiers in Plant Science, 11, 603693. https://doi.org/10.3389/FPLS.2020.603693

Glauser, G., Grata, E., Dubugnon, L., Rudaz, S., Farmer, E. E., & Wolfender, J.-L. (2008). Spatial and Temporal Dynamics of Jasmonate Synthesis and Accumulation in Arabidopsis in Response to Wounding. Journal of Biological Chemistry, 283(24), 16400–16407. https://doi.org/10.1074/jbc.M801760200

Griffiths, J., Rizza, A., Tang, B., Frommer, W. B., & Jones, A. M. (2024). GIBBERELLIN PERCEPTION SENSOR 2 Reveals Genesis and Role of Cellular GA Dynamics in Light-Regulated Hypocotyl Growth. The Plant Cell, 36(10), 4426–4441. https://doi.org/10.1093/PLCELL/KOAE198

Gruden, K., Kuipers, A. G. J., Gunčar, G., Slapar, N., Štrukelj, B., & Jongsma, M. A. (2004). Molecular Basis of Colorado Potato Beetle Adaptation to Potato Plant Defence at the Level of Digestive Cysteine Proteinases. Insect Biochemistry and Molecular Biology, 34(4), 365–375. https://doi.org/10.1016/J.IBMB.2004.01.003

Gruden, K., Popovič, T., Cimerman, N., Križaj, I., & Štrukelj, B. (2003). Diverse Enzymatic Specificities of Digestive Proteases, 'Intestains', Enable Colorado Potato Beetle Larvae to Counteract the Potato Defence Mechanism. Biological Chemistry, 384(2), 305–310. https://doi.org/10.1515/BC.2003.034

Hander, T., Fernández-Fernández, Á. D., Kumpf, R. P., Willems, P., Schatowitz, H., Rombaut, D., Staes, A., Nolf, J., Pottie, R., Yao, P., Gonçalves, A., Pavie, B., Boller, T., Gevaert, K., Van Breusegem, F., Bartels, S., & Stael, S. (2019). Damage on Plants Activates Ca^{2+}-Dependent Metacaspases for Release of Immunomodulatory Peptides. Science, 363(6433), eaar7486. https://doi.org/10.1126/SCIENCE.AAR7486

Herud-Sikimić, O., Stiel, A. C., Kolb, M., Shanmugaratnam, S., Berendzen, K. W., Feldhaus, C., Höcker, B., & Jürgens, G. (2021). A Biosensor for the Direct Visualization of Auxin. Nature, 592(7856), 768–772. https://doi.org/10.1038/s41586-021-03425-2

Hickman, R., Van Verk, M. C., Van Dijken, A. J. H., Mendes, M. P., Vroegop-Vos, I. A., Caarls, L., Steenbergen, M., Van der Nagel, I., Wesselink, G. J., Jironkin, A., Talbot, A., Rhodes, J., De Vries, M., Schuurink, R. C., Denby, K., Pieterse, C. M. J., & Van Wees, S. C. M. (2017). Architecture and Dynamics of the Jasmonic Acid Gene Regulatory Network. The Plant Cell, 29(9), 2086–2105. https://doi.org/10.1105/TPC.16.00958

Hipsch, M., Lampl, N., Zelinger, E., Barda, O., Waiger, D., & Rosenwasser, S. (2021a). Sensing Stress Responses in Potato with Whole-Plant Redox Imaging. Plant Physiology, 187(2), 618. https://doi.org/10.1093/PLPHYS/KIAB159

Hoermayer, L., Montesinos, J. C., Marhava, P., Benková, E., Yoshida, S., & Friml, J. (2020). Wounding-Induced Changes in Cellular Pressure and Localized Auxin

Signalling Spatially Coordinate Restorative Divisions in Roots. Proceedings of the National Academy of Sciences of the United States of America, 117(26), 15322–15331. https://doi.org/10.1073/PNAS.2003346117

Hou, S., Liu, Z., Shen, H., & Wu, D. (2019). Damage-Associated Molecular Pattern-Triggered Immunity in Plants. Frontiers in Plant Science, 10, 646. https://doi.org/10.3389/FPLS.2019.00646

Howe, G. A., & Schaller, A. (2008). Direct Defenses in Plants and Their Induction by Wounding and Insect Herbivores. Induced Plant Resistance to Herbivory, 7–29. https://doi.org/10.1007/978-1-4020-8182-8_1

Huang, S., Zhang, X., & Fernando, W. G. D. (2020). Directing Trophic Divergence in Plant-Pathogen Interactions: Antagonistic Phytohormones With NO Doubt? Frontiers in Plant Science, 11, 600063. https://doi.org/10.3389/FPLS.2020.600063

Huang, W. E., Huang, L., Preston, G. M., Naylor, M., Carr, J. P., Li, Y., Singer, A. C., Whiteley, A. S., & Wang, H. (2006). Quantitative In Situ Assay of Salicylic Acid in Tobacco Leaves Using a Genetically Modified Biosensor Strain of Acinetobacter sp. ADP1. The Plant Journal, 46(6), 1073–1083. https://doi.org/10.1111/J.1365-313X.2006.02758.X

Huang, W. E., Wang, H., Zheng, H., Huang, L., Singer, A. C., Thompson, I., & Whiteley, A. S. (2005). Chromosomally Located Gene Fusions Constructed in Acinetobacter sp. ADP1 for the Detection of Salicylate. Environmental Microbiology, 7(9), 1339–1348. https://doi.org/10.1111/J.1462-5822.2005.00821.X

Inzé, D., & Nelissen, H. (2022). The Translatability of Genetic Networks from Model to Crop Species: Lessons from the Past and Perspectives for the Future. New Phytologist, 236(1), 43–48. https://doi.org/10.1111/NPH.18364

Isoda, R., Yoshinari, A., Ishikawa, Y., Sadoine, M., Simon, R., Frommer, W. B., & Nakamura, M. (2020). Sensors for the Quantification, Localization and Analysis of the Dynamics of Plant Hormones. The Plant Journal, 105(2), 542. https://doi.org/10.1111/TPJ.15096

Jacob, P., Hige, J., & Dangl, J. L. (2023). Is Localized Acquired Resistance the Mechanism for Effector-Triggered Disease Resistance in Plants? Nature Plants, 9(8), 1184–1190. https://doi.org/10.1038/s41477-023-01466-1

Jedličková, V., Naghani, S. E., & Robert, H. S. (2022). On the Trail of Auxin: Reporters and Sensors. The Plant Cell, 34(9), 3200–3213. https://doi.org/10.1093/PLCELL/KOAC179

Jones, A. M., Danielson, J. Å. H., Manojkumar, S. N., Lanquar, V., Grossmann, G., & Frommer, W. B. (2014). Abscisic Acid Dynamics in Roots Detected with Genetically Encoded FRET Sensors. eLife, 3(3), e01741. https://doi.org/10.7554/ELIFE.01741

Jones, J. D. G., & Dangl, J. L. (2006). The Plant Immune System. Nature, 444(7117), 323–329. https://doi.org/10.1038/nature05286

Jones, J. D. G., Staskawicz, B. J., & Dangl, J. L. (2024). The Plant Immune System: From Discovery to Deployment. Cell, 187(9), 2095–2116. https://doi.org/10.1016/J.CELL.2024.03.045

Joshi, M., Fogelman, E., Belausov, E., & Ginzberg, I. (2016). Potato Root System Development and Factors that Determine Its Architecture. Journal of Plant Physiology, 205, 113–123. https://doi.org/10.1016/J.JPLPH.2016.08.014

Khakhar, A., Leydon, A. R., Lemmex, A. C., Klavins, E., & Nemhauser, J. L. (2018). Synthetic Hormone-Responsive Transcription Factors Can Monitor and Reprogram Plant Development. eLife, 7, e34702. https://doi.org/10.7554/ELIFE.34702

Kimberlin, A. N., Holtsclaw, R. E., Zhang, T., Mulaudzi, T., & Koo, A. J. (2022). On the Initiation of Jasmonate Biosynthesis in Wounded Leaves. Plant Physiology, 189(4), 1925–1942. https://doi.org/10.1093/plphys/kiac163

Koo, A. J. K., Gao, X., Daniel Jones, A., & Howe, G. A. (2009). A Rapid Wound Signal Activates the Systemic Synthesis of Bioactive Jasmonates in Arabidopsis. The Plant Journal, 59(6), 974–986. https://doi.org/10.1111/J.1365-313X.2009.03924.X

Lambert, T. J. (2019). FPbase: A Community-Editable Fluorescent Protein Database. Nature Methods, 16(4), 277–278. https://doi.org/10.1038/s41592-019-0352-8

Larrieu, A., Champion, A., Legrand, J., Lavenus, J., Mast, D., Brunoud, G., Oh, J., Guyomarc'H, S., Pizot, M., Farmer, E. E., Turnbull, C., Vernoux, T., Bennett, M. J., & Laplaze, L. (2015). A Fluorescent Hormone Biosensor Reveals the Dynamics of Jasmonate Signalling in Plants. Nature Communications, 6(1), 1–9. https://doi.org/10.1038/ncomms7043

Lazar, A., Coll, A., Dobnik, D., Baebler, Š., Bedina-Zavec, A., Žel, J., & Gruden, K. (2014). Involvement of Potato (Solanum tuberosum L.) MKK6 in Response to Potato virus Y. PLOS ONE, 9(8), e104553. https://doi.org/10.1371/JOURNAL.PONE.0104553

Leiwe, M. N., Fujimoto, S., Baba, T., Moriyasu, D., Saha, B., Sakaguchi, R., Inagaki, S., & Imai, T. (2022). Automated Neuronal Reconstruction with Super-Multicolour Tetbow Labelling and Threshold-Based Clustering of Colour Hues. Nature Communications, 15, 5279. https://doi.org/10.1038/s41467-024-49455-y

Lewandowska, M., Zienkiewicz, K., Zienkiewicz, A., Kelly, A., König, S., Feussner, K., Kunst, L., & Feussner, I. (2024). Wounding Triggers Wax Biosynthesis in Arabidopsis Leaves in an Abscisic Acid–Dependent and Jasmonoyl-Isoleucine-Dependent Manner. Plant and Cell Physiology, 65(6), 928–938. https://doi.org/10.1093/PCP/PCAD137

L'Haridon, F., Besson-Bard, A., Binda, M., Serrano, M., Abou-Mansour, E., Balet, F., Schoonbeek, H. J., Hess, S., Mir, R., Léon, J., Lamotte, O., & Métraux, J. P. (2011). A Permeable Cuticle Is Associated with the Release of Reactive Oxygen Species and Induction of Innate Immunity. PLOS Pathogens, 7(7), e1002148. https://doi.org/10.1371/JOURNAL.PPAT.1002148

Liu, H., & Timko, M. P. (2021). Jasmonic Acid Signaling and Molecular Crosstalk with Other Phytohormones. International Journal of Molecular Sciences, 22(6), 2914. https://doi.org/10.3390/IJMS22062914

Lu, Y., & Tsuda, K. (2021). Intimate Association of PRR- and NLR-Mediated Signaling in Plant Immunity. Molecular Plant-Microbe Interactions, 34(1), 3–14. https://doi.org/10.1094/MPMI-08-20-0239-IA

Lukan, T. (2018). Spatiotemporal Study of Potato Hypersensitive Response-Conferred Resistance to Potato Virus Y: Doctoral Dissertation. https://plus-legacy.cobiss.net/cobiss/si/sl/bib/4691023

Lukan, T., Pompe-Novak, M., Baebler, Š., Tušek-Žnidarič, M., Kladnik, A., Križnik, M., Blejec, A., Zagorščak, M., Stare, K., Dušak, B., Coll, A., Pollmann, S., Morgiewicz, K., Hennig, J., & Gruden, K. (2020). Precision Transcriptomics of Viral Foci Reveals the Spatial Regulation of Immune-Signaling Genes and Identifies RBOHD as an Important Player in the Incompatible Interaction Between Potato Virus Y and Potato. The Plant Journal, 104(3), 645–661. https://doi.org/10.1111/tpj.14953

Lukan, T., Županič, A., Mahkovec Povalej, T., Brunkard, J. O., Kmetič, M., Juteršek, M., Baebler, Š., & Gruden, K. (2023). Chloroplast Redox State Changes Mark Cell-to-Cell Signaling in the Hypersensitive Response. New Phytologist, 237(2), 548–562. https://doi.org/10.1111/nph.18425

Mahkovec Povalej, T. (2020). Optimizacija priprave senzorskih rastlin krompirja za raziskave imunske signalizacije: magistrsko delo. https://plus-legacy.cobiss.net/cobiss/si/sl/bib/26619907

Marhava, P., Hoermayer, L., Yoshida, S., Marhavý, P., Benková, E., & Friml, J. (2019). Re-activation of Stem Cell Pathways for Pattern Restoration in Plant Wound Healing. Cell, 177(4), 957-969.e13. https://doi.org/10.1016/J.CELL.2019.04.015

Marhavý, P., Kurenda, A., Siddique, S., Tendon, V. D., Zhou, F., Holbein, J., Hasan, M. S., Grundler, F. M., Farmer, E. E., & Geldner, N. (2019). Single-Cell Damage Elicits Regional, Nematode-Restricting Ethylene Responses in Roots. The EMBO Journal, 38(10), e100972. https://doi.org/10.15252/EMBJ.2018100972

Martinez, M., Santamaria, M. E., Diaz-Mendoza, M., Arnaiz, A., Carrillo, L., & Ortego, F. (2016). Phytocystatins: Defense Proteins against Phytophagous Insects and Acari. International Journal of Molecular Sciences, 17(10), 1747. https://doi.org/10.3390/IJMS17101747

McConn, M., Creelman, R. A., Bell, E., Mullet, J. E., & Browse, J. (1997). Jasmonate is Essential for Insect Defense in Arabidopsis. Proceedings of the National Academy of Sciences of the United States of America, 94(10), 5473–5477. https://doi.org/10.1073/PNAS.94.10.5473

Morel, J.-B., & Dangl, J. L. (1997). The Hypersensitive Response and the Induction of Cell Death in Plants. Cell Death & Differentiation, 4(8), 671–683. https://doi.org/10.1038/sj.cdd.4400309

Moroz, N., & Tanaka, K. (2020). FlgII-28 Is a Major Flagellin-Derived Defense Elicitor in Potato. Molecular Plant-Microbe Interactions, 33(2), 247–255. https://doi.org/10.1094/MPMI-06-19-0164-R

Murdock, L. L., Brookhart, G., Dunn, P. E., Foard, D. E., Kelley, S., Kitch, L., Shade, R. E., Shukle, R. H., & Wolfson, J. L. (1987). Cysteine Digestive Proteinases in Coleoptera. Comparative Biochemistry and Physiology -- Part B: Comparative Biochemistry, 87(4), 783–787. https://doi.org/10.1016/0305-0491(87)90388-9

Myers, R. J., Fichman, Y., Zandalinas, S. I., & Mittler, R. (2023). Jasmonic Acid and Salicylic Acid Modulate Systemic Reactive Oxygen Species Signaling during Stress Responses. Plant Physiology, 191(2), 862–873. https://doi.org/10.1093/PLPHYS/KIAC449

Mylle, E., Codreanu, M. C., Boruc, J., & Russinova, E. (2013). Emission Spectra Profiling of Fluorescent Proteins in Living Plant Cells. Plant Methods, 9(1), 1–8. https://doi.org/10.1186/1746-4811-9-10

Nabity, P. D., Zavala, J. A., & Delucia, E. H. (2013). Herbivore Induction of Jasmonic Acid and Chemical Defences Reduce Photosynthesis in Nicotiana attenuata. Journal of Experimental Botany, 64(2), 694. https://doi.org/10.1093/JXB/ERS364

Nagano, M., Ueda, H., Fukao, Y., Kawai-Yamada, M., & Hara-Nishimura, I. (2020). Generation of Arabidopsis Lines with a Red Fluorescent Marker for Endoplasmic Reticulum Using a Tail-Anchored Protein Cytochrome b5 -B. Plant Signaling & Behavior, 15(9), 1790196. https://doi.org/10.1080/15592324.2020.1790196

Nakai, J., Ohkura, M., & Imoto, K. (2001). A High Signal-to-Noise Ca^{2+} Probe Composed of a Single Green Fluorescent Protein. Nature Biotechnology, 19(2), 137–141. https://doi.org/10.1038/84397

Ngou, B. P. M., Ahn, H. K., Ding, P., & Jones, J. D. G. (2021). Mutual Potentiation of Plant Immunity by Cell-Surface and Intracellular Receptors. Nature, 592(7852), 110–115. https://doi.org/10.1038/s41586-021-03315-7

Ngou, B. P. M., Ding, P., & Jones, J. D. G. (2022). Thirty Years of Resistance: Zig-Zag through the Plant Immune System. The Plant Cell, 34(5), 1447–1478. https://doi.org/10.1093/PLCELL/KOAC041

Nissen, M. S., Kumar, G. N. M., Youn, B., Knowles, D. B., Lam, K. S., Ballinger, W. J., Knowles, N. R., & Kang, C. (2009). Characterization of Solanum tuberosum Multicystatin and Its Structural Comparison with Other Cystatins. Plant Cell, 21(3), 861–875. https://doi.org/10.1105/tpc.108.064717

Nomoto, M., Skelly, M. J., Itaya, T., Mori, T., Suzuki, T., Matsushita, T., Tokizawa, M., Kuwata, K., Mori, H., Yamamoto, Y. Y., Higashiyama, T., Tsukagoshi, H., Spoel, S. H., & Tada, Y. (2021). Suppression of MYC Transcription Activators by the Immune Cofactor NPR1 Fine-Tunes Plant Immune Responses. Cell Reports, 37(11), 110125. https://doi.org/10.1016/J.CELREP.2021.110125

Ogawa, T., Ara, T., Aoki, K., Suzuki, H., & Shibata, D. (2010). Transient Increase in Salicylic Acid and Its Glucose Conjugates after Wounding in Arabidopsis Leaves. Plant Biotechnology, 27, 205–209. https://doi.org/10.5511/plantbiotechnology.27.205

Orr, G. L., Strickland, J. A., & Walsh, T. A. (1994). Inhibition of Diabrotica Larval Growth by a Multicystatin from Potato Tubers. Journal of Insect Physiology, 40(10), 893–900. https://doi.org/10.1016/0022-1910(94)90023-X

Petek, M., Rotter, A., Kogovšek, P., Baebler, Š., Mithöfer, A., & Gruden, K. (2014). Potato Virus Y Infection Hinders Potato Defence Response and Renders Plants More Vulnerable to Colorado Potato Beetle Attack. Molecular Ecology, 23(21), 5378–5391. https://doi.org/10.1111/mec.12932

Popovič, T., & Brzin, J. (2007). Purification and Characterization of Two Cysteine Proteinases from Potato Leaves and the Mode of Their Inhibition with Endogenous Inhibitors. Croatica Chemica Acta, 80(1), 45–52.

Prasad, A., Sedlářová, M., Balukova, A., Rác, M., & Pospíšil, P. (2020). Reactive Oxygen Species as a Response to Wounding: In Vivo Imaging in Arabidopsis thaliana. Frontiers in Plant Science, 10, 1660. https://doi.org/10.3389/fpls.2019.01660

Pruitt, R. N., Locci, F., Wanke, F., Zhang, L., Saile, S. C., Joe, A., Karelina, D., Hua, C., Fröhlich, K., Wan, W. L., Hu, M., Rao, S., Stolze, S. C., Harzen, A., Gust, A. A., Harter, K., Joosten, M. H. A. J., Thomma, B. P. H. J., Zhou, J. M., Parker, J. E., Nürnberger, T. (2021). The EDS1–PAD4–ADR1 Node Mediates Arabidopsis Pattern-Triggered Immunity. Nature, 598(7881), 495–499. https://doi.org/10.1038/s41586-021-03829-0

Reddy, M. S. S., Dinkins, R. D., & Collins, G. B. (2003). Gene Silencing in Transgenic Soybean Plants Transformed via Particle Bombardment. Plant Cell Reports, 21(7), 676–683. https://doi.org/10.1007/S00299-002-0567-4

Resentini, F., Grenzi, M., Ancora, D., Cademartori, M., Luoni, L., Franco, M., Bassi, A., Bonza, M. C., & Costa, A. (2021). Simultaneous Imaging of ER and Cytosolic Ca^{2+} Dynamics Reveals Long-Distance ER Ca^{2+} Waves in Plants. Plant Physiology, 187(2), 603–617. https://doi.org/10.1093/PLPHYS/KIAB251

Ross, B. T., Zidack, N. K., & Flenniken, M. L. (2021). Extreme Resistance to Viruses in Potato and Soybean. Frontiers in Plant Science, 12, 658981. https://doi.org/10.3389/FPLS.2021.658981

Rowe, J., Grangé-Guermente, M., Exposito-Rodriguez, M., Wimalasekera, R., Lenz, M. O., Shetty, K. N., Cutler, S. R., & Jones, A. M. (2023). Next-Generation ABACUS Biosensors Reveal Cellular ABA Dynamics Driving Root Growth at Low Aerial Humidity. Nature Plants, 9(7), 1103. https://doi.org/10.1038/S41477-023-01447-4

Sabatini, S., Beis, D., Wolkenfelt, H., Murfett, J., Guilfoyle, T., Malamy, J., Benfey, P., Leyser, O., Bechtold, N., Weisbeek, P., & Scheres, B. (1999). An Auxin-Dependent Distal Organizer of Pattern and Polarity in the Arabidopsis Root. Cell, 99(5), 463–472. https://doi.org/10.1016/S0092-8674(00)81535-4

Sadanandom, A., & Napier, R. M. (2010). Biosensors in Plants. Current Opinion in Plant Biology, 13(6), 736–743. https://doi.org/10.1016/J.PBI.2010.08.010

Salguero-Linares, J., Serrano, I., Ruiz-Solani, N., Salas-Gómez, M., Phukan, U. J., González, V. M., Bernardo-Faura, M., Valls, M., Rengel, D., & Coll, N. S. (2022). Robust Transcriptional Indicators of Immune Cell Death Revealed by Spatiotemporal Transcriptome Analyses. Molecular Plant, 15(6), 1059–1075. https://doi.org/10.1016/j.molp.2022.04.010

Salvador-Recatalà, V., Tjallingii, W. F., & Farmer, E. E. (2014). Real-time, In Vivo Intracellular Recordings of Caterpillar-Induced Depolarization Waves in Sieve Elements Using Aphid Electrodes. New Phytologist, 203(2), 674–684. https://doi.org/10.1111/nph.12807

Seitz, K., & Krysan, P. J. (2020). Expanding the Toolkit of Fluorescent Biosensors for Studying Mitogen Activated Protein Kinases in Plants. International Journal of Molecular Sciences, 21(15), 5350. https://doi.org/10.3390/IJMS21155350

Serra, O., & Geldner, N. (2022). The Making of Suberin. New Phytologist, 235(3), 848–866. https://doi.org/10.1111/NPH.18202

Shi, B., Felipo-Benavent, A., Cerutti, G., Galvan-Ampudia, C., Jilli, L., Brunoud, G., Mutterer, J., Vallet, E., Sakvarelidze-Achard, L., Davière, J. M., Navarro-Galiano, A., Walia, A., Lazary, S., Legrand, J., Weinstain, R., Jones, A. M., Prat, S., Achard, P., & Vernoux, T. (2024). A Quantitative Gibberellin Signaling Biosensor Reveals a Role

for Gibberellins in Internode Specification at the Shoot Apical Meristem. Nature Communications, 15(1), 3895. https://doi.org/10.1038/s41467-024-48116-4

Sözen, C., Schenk, S. T., Boudsocq, M., Chardin, C., Almeida-Trapp, M., Krapp, A., Hirt, H., Mithöfer, A., & Colcombet, J. (2020). Wounding and Insect Feeding Trigger Two Independent MAPK Pathways with Distinct Regulation and Kinetics. The Plant Cell, 32(6), 1988–2003. https://doi.org/10.1105/TPC.19.00917

Steiner, E., Israeli, A., Gupta, R., Shwartz, I., Nir, I., Leibman-Markus, M., Tal, L., Farber, M., Amsalem, Z., Ori, N., Müller, B., & Bar, M. (2020). Characterization of the Cytokinin Sensor TCSv2 in Arabidopsis and Tomato. Plant Methods, 16(1), 152. https://doi.org/10.1186/S13007-020-00694-2

Tang, D., Wang, G., & Zhou, J. M. (2017). Receptor Kinases in Plant-Pathogen Interactions: More Than Pattern Recognition. The Plant Cell, 29(4), 618. https://doi.org/10.1105/TPC.16.00891

Tena, G., Boudsocq, M., & Sheen, J. (2011). Protein kinase signaling networks in plant innate immunity. Current Opinion in Plant Biology, 14(5), 519–529. https://doi.org/10.1016/J.PBI.2011.05.006

Thomma, B. P. H. J., Nürnberger, T., & Joosten, M. H. A. J. (2011). Of PAMPs and Effectors: The Blurred PTI-ETI Dichotomy. The Plant Cell, 23(1), 4–15. https://doi.org/10.1105/TPC.110.082602

Tian, H., Wu, Z., Chen, S., Ao, K., Huang, W., Yaghmaiean, H., Sun, T., Xu, F., Zhang, Y., Wang, S., Li, X., & Zhang, Y. (2021). Activation of TIR Signalling Boosts Pattern-Triggered Immunity. Nature, 598(7881), 500–503. https://doi.org/10.1038/s41586-021-03987-1

Toyota, M., Spencer, D., Sawai-Toyota, S., Jiaqi, W., Zhang, T., Koo, A. J., Howe, G. A., & Gilroy, S. (2018). Glutamate Triggers Long-Distance, Calcium-Based Plant Defense Signaling. Science, 361(6407), 1112–1115. https://doi.org/10.1126/SCIENCE.AAT7744

Tsuda, K., & Katagiri, F. (2010). Comparing Signaling Mechanisms Engaged in Pattern-Triggered and Effector-Triggered Immunity. Current Opinion in Plant Biology, 13(4), 459–465. https://doi.org/10.1016/J.PBI.2010.04.006

Tsuda, K., Sato, M., Stoddard, T., Glazebrook, J., & Katagiri, F. (2009). Network Properties of Robust Immunity in Plants. PLOS Genetics, 5(12), e1000772. https://doi.org/10.1371/JOURNAL.PGEN.1000772

Uauy, C., Nelissen, H., Chan, R. L., Napier, J. A., Seung, D., Liu, L., & McKim, S. M. (2025). Challenges of Translating Arabidopsis Insights into Crops. The Plant Cell, 37(5), 59. https://doi.org/10.1093/PLCELL/KOAF059

Van Der Biezen, E. A., & Jones, J. D. G. (1998). Plant Disease-Resistance Proteins and the Gene-for-Gene Concept. Trends in Biochemical Sciences, 23(12), 454–456. https://doi.org/10.1016/S0968-0004(98)01311-5

Van der Does, D., Leon-Reyes, A., Koornneef, A., Van Verk, M. C., Rodenburg, N., Pauwels, L., Goossens, A., Körbes, A. P., Memelink, J., Ritsema, T., Van Wees, S. C. M., & Pieterse, C. M. J. (2013). Salicylic Acid Suppresses Jasmonic Acid Signaling Downstream of SCFCOI1-JAZ by Targeting GCC Promoter Motifs via Transcription

Factor ORA59. The Plant Cell, 25(2), 744–761. https://doi.org/10.1105/tpc.112.108548

Van Der Hoorn, R. A. L., & Kamoun, S. (2008). From Guard to Decoy: A New Model for Perception of Plant Pathogen Effectors. The Plant Cell, 20(8), 2009. https://doi.org/10.1105/TPC.108.060194

Vega-Muñoz, I., Duran-Flores, D., Fernández-Fernández, Á. D., Heyman, J., Ritter, A., & Stael, S. (2020). Breaking Bad News: Dynamic Molecular Mechanisms of Wound Response in Plants. Frontiers in Plant Science, 11, 610445. https://doi.org/10.3389/FPLS.2020.610445

Verhage, A., Vlaardingerbroek, I., Raaymakers, C., Van Dam, N. M., Dicke, M., Van Wees, S. C. M., & Pieterse, C. M. J. (2011). Rewiring of the Jasmonate Signaling Pathway in Arabidopsis during Insect Herbivory. Frontiers in Plant Science, 2, 47. https://doi.org/10.3389/FPLS.2011.00047

Vernoux, T., Brunoud, G., Farcot, E., Morin, V., Van Den Daele, H., Legrand, J., Oliva, M., Das, P., Larrieu, A., Wells, D., Guédon, Y., Armitage, L., Picard, F., Guyomarc'H, S., Cellier, C., Parry, G., Koumproglou, R., Doonan, J. H., Estelle, M., Godin, C., Kepinski, S., Bennett, M., De Veylder, L., Traas, J. (2011). The Auxin Signalling Network Translates Dynamic Input into Robust Patterning at the Shoot Apex. Molecular Systems Biology, 7, 508. https://doi.org/10.1038/MSB.2011.39

Vincent, T. R., Canham, J., Toyota, M., Avramova, M., Mugford, S. T., Gilroy, S., Miller, A. J., Hogenhout, S., & Sanders, D. (2017). Real-time In Vivo Recording of Arabidopsis Calcium Signals During Insect Feeding Using a Fluorescent Biosensor. J. Vis. Exp, 126, 56142. https://doi.org/10.3791/56142

Waadt, R., Hitomi, K., Nishimura, N., Hitomi, C., Adams, S. R., Getzoff, E. D., & Schroeder, J. I. (2014). FRET-Based Reporters for the Direct Visualization of Abscisic Acid Concentration Changes and Distribution in Arabidopsis. eLife, 3(3), e01739. https://doi.org/10.7554/ELIFE.01739

Walia, A., Waadt, R., & Jones, A. M. (2018). Genetically Encoded Biosensors in Plants: Pathways to Discovery. Annual Review of Plant Biology, 69, 497–524. https://doi.org/10.1146/ANNUREV-ARPLANT-042817-040104

Walsh, T. A., & Strickland, J. A. (1993). Proteolysis of the 85-Kilodalton Crystalline Cysteine Proteinase lnhibitor from Potato Releases Functional Cystatin Domains. Plant Physiology, 103, 1227–1234. https://doi.org/10.1104/pp.103.4.1227

Wang, J., Peiffer, M., Hoover, K., Rosa, C., Zeng, R., & Felton, G. W. (2017). Helicoverpa zea Gut-Associated Bacteria Indirectly Induce Defenses in Tomato by Triggering a Salivary Elicitor(s). New Phytologist, 214(3), 1294–1306. https://doi.org/10.1111/NPH.14429

Wiesel, L., Davis, J. L., Milne, L., Redondo Fernandez, V., Herold, M. B., Middlefell Williams, J., Morris, J., Hedley, P. E., Harrower, B., Newton, A. C., Birch, P. R. J., Gilroy, E. M., & Hein, I. (2015). A Transcriptional Reference Map of Defence Hormone Responses in Potato. Scientific Reports, 5, 1–12. https://doi.org/10.1038/srep15229

Yang, W., Zhai, H., Wu, F., Deng, L., Chao, Y., Meng, X., Chen, Q., Liu, C., Bie, X., Sun, C., Yu, Y., Zhang, X., Zhang, X., Chang, Z., Xue, M., Zhao, Y., Meng, X., Li, B., Zhang, X., Zhang, D., Zhao, X., Gao, C., Li, J., Li, C. (2024). Peptide REF1 Is a Local

Wound Signal Promoting Plant Regeneration. Cell, 187(12), 3038. https://doi.org/10.1016/J.CELL.2024.04.040

Yuan, M., Jiang, Z., Bi, G., Nomura, K., Liu, M., Wang, Y., Cai, B., Zhou, J. M., He, S. Y., & Xin, X. F. (2021). Pattern-Recognition Receptors Are Required for NLR-Mediated Plant Immunity. Nature, 592(7852), 105–109. https://doi.org/10.1038/s41586-021-03316-6

Yuan, M., Ngou, B. P. M., Ding, P., & Xin, X. F. (2021). PTI-ETI Crosstalk: An Integrative View of Plant Immunity. Current Opinion in Plant Biology, 62, 102030. https://doi.org/10.1016/J.PBI.2021.102030

Yue, R., & Dutta, A. (2022). Computational Systems Biology in Disease Modeling and Control, Review and Perspectives. Npj Systems Biology and Applications, 8(1), 1–16. https://doi.org/10.1038/s41540-022-00247-4

Zhai, Q., Deng, L., & Li, C. (2020). Mediator Subunit MED25: At the Nexus of Jasmonate Signaling. Current Opinion in Plant Biology, 57, 78–86. https://doi.org/10.1016/J.PBI.2020.06.006

Zhang, G., Zhao, F., Chen, L., Pan, Y., Sun, L., Bao, N., Zhang, T., Cui, C. X., Qiu, Z., Zhang, Y., Yang, L., & Xu, L. (2019). Jasmonate-Mediated Wound Signalling Promotes Plant Regeneration. Nature Plants, 5(5), 491–497. https://doi.org/10.1038/s41477-019-0408-x

Zhou, F., Emonet, A., Dénervaud Tendon, V., Marhavy, P., Wu, D., Lahaye, T., & Geldner, N. (2020). Co-incidence of Damage and Microbial Patterns Controls Localized Immune Responses in Roots. Cell, 180(3), 440–453.e18. https://doi.org/10.1016/j.cell.2020.01.013

Zhu, J., Lolle, S., Tang, A., Guel, B., Kvitko, B., Cole, B., & Coaker, G. (2023). Single-Cell Profiling of Arabidopsis Leaves to Pseudomonas syringae Infection. Cell Reports, 42(7), 112676. https://doi.org/10.1016/j.celrep.2023.112676

Zimmermann, T. (2005). Spectral Imaging and Linear Unmixing in Light Microscopy. Advances in Biochemical Engineering/Biotechnology, 95, 245–265. https://doi.org/10.1007/B102216

Zürcher, E., Tavor-Deslex, D., Lituiev, D., Enkerli, K., Tarr, P. T., & Müller, B. (2013). A Robust and Sensitive Synthetic Sensor to Monitor the Transcriptional Output of the Cytokinin Signaling Network In Planta. Plant Physiology, 161(3), 1066–1075. https://doi.org/10.1104/PP.112.211763

Bibliography

Publications Related to the Thesis

Journal Articles

Levak, V., Lukan, T., Gruden, K., Coll Rius, A. (2021). Biosensors : a sneak peek into plant cell's immunity. Life. 3, 209, 1-18. https://doi.org/10.3390/life11030209.

Levak, V., Mahkovec Povalej, T., Pogačar, K., Stare, K., Zagorščak, M., Hawkins, T., Robson, J., Dobnik, D., Lukan, T., Gruden, K. (2025). Jasmonic acid and salicylic acid interact to determine spatial regulation of gene expression responses in potato leaf to herbivory by Colorado potato beetle and mechanical wounding. Plant and Cell Physiology, pcaf120. https://doi.org/10.1093/pcp/pcaf120

Levak, V., Županič, A., Pogačar, K., Marondini, N., Stare, K., Arnšek, T., Fink, K., Gruden, K., Lukan, T. (2026) Robust quantification of multiplexed fluorescent protein-based biosensors in plant tissues. bioRxiv, 2026/711581; accepted in The Plant Journal, 19 June 2026.

Biography

Valentina Levak was born on December 2, 1994, in Brežice, Slovenia. She completed her primary and secondary education in Brežice. In 2013, she enrolled in the Biochemistry program at the Faculty of Chemistry and Chemical Technology, University of Ljubljana. She conducted her bachelor's and master's research at the National Institute of Biology, Department of Biotechnology and Systems Biology, under the mentorship of Prof. Dr. Kristina Gruden, and continued her research at the doctoral level under the same mentorship, with co-mentorship from Assist. Prof. Dr. Tjaša Lukan. Her research experience includes molecular cloning, Agrobacterium-mediated stable and transient plant transformation, work with tissue cultures, luciferase, beta-glucuronidase and fluorescent protein-based gene reporter assays, and confocal and transmission electron microscopy.

During her graduate study, she presented her research with a poster at 3rd FEBS workshop: Plant organellar signaling (2021), The 45th FEBS Congress (2021), Plants in changing environment: International conference of the Slovenian society of plant biology (2022), and Botanical microscopy meeting 2023, or with a talk at The 2023 Jasmonate meeting, Annular general meeting of Slovenian society of plant biology (2023), 17th Multinational congress on microscopy (2025), and 6th Slovene microscopy symposium (2026). She also attended some workshops, SPS Summer school 2025: Advanced plant imaging – From super-resolution to fluorescence lifetime imaging microscopy, and RMS Electron microscopy spring school 2025.